

AFRL-RX-TY-TR-2008-4565



CHARACTERIZATION OF REAEROSOLIZATION IN AN EFFORT TO IMPROVE SAMPLING OF AIRBORNE VIRUSES

Lindsey Riemenschneider

**Department of Environmental Engineering Sciences
University of Florida
Gainesville, FL 32611**

APRIL 2008

Interim Report for 1 March 2007 – 30 April 2008

**DISTRIBUTION STATEMENT A: Approved for public release;
distribution unlimited.**

**AIRBASE TECHNOLOGIES DIVISION
MATERIALS AND MANUFACTURING DIRECTORATE
AIR FORCE RESEARCH LABORATORY
AIR FORCE MATERIEL COMMAND
139 BARNES DRIVE, SUITE 2
TYNDALL AIR FORCE BASE, FL 32403-5323**

NOTICE AND SIGNATURE PAGE

Using Government drawings, specifications, or other data included in this document for any purpose other than Government procurement does not in any way obligate the U.S. Government. The fact that the Government formulated or supplied the drawings, specifications, or other data does not license the holder or any other person or corporation; or convey any rights or permission to manufacture, use, or sell any patented invention that may relate to them.

This report was cleared for public release by the Air Force Research Laboratory, Materials and Manufacturing Directorate, Airbase Technologies Division, Public Affairs and is available to the general public, including foreign nationals. Copies may be obtained from the Defense Technical Information Center (DTIC) (<http://www.dtic.mil>).

REPORT NUMBER AFRL-RX-TY-TR-2008-4565 HAS BEEN REVIEWED AND IS APPROVED FOR PUBLICATION IN ACCORDANCE WITH ASSIGNED DISTRIBUTION STATEMENT.

//signature//
JOSEPH D. WANDER, Ph.D.
Work Unit Manager

//signature//
DANIEL M. SAUCER, Major, USAF
Chief, Airbase Sciences Branch

//signature//
ALBERT N. RHODES, Ph.D.
Acting Chief, Airbase Technologies Division

This report is published in the interest of scientific and technical information exchange, and its publication does not constitute the Government's approval or disapproval of its ideas or findings.

REPORT DOCUMENTATION PAGE					<i>Form Approved OMB No. 0704-0188</i>	
<small>The public reporting burden for this collection of information is estimated to average 1 hour per response, including the time for reviewing instructions, searching existing data sources, gathering and maintaining the data needed, and completing and reviewing the collection of information. Send comments regarding this burden estimate or any other aspect of this collection of information, including suggestions for reducing the burden, to Department of Defense, Washington Headquarters Services, Directorate for Information Operations and Reports (0704-0188), 1215 Jefferson Davis Highway, Suite 1204, Arlington, VA 22202-4302. Respondents should be aware that notwithstanding any other provision of law, no person shall be subject to any penalty for failing to comply with a collection of information if it does not display a currently valid OMB control number.</small>						
PLEASE DO NOT RETURN YOUR FORM TO THE ABOVE ADDRESS.						
1. REPORT DATE (DD-MM-YYYY)		2. REPORT TYPE			3. DATES COVERED (From - To)	
4. TITLE AND SUBTITLE				5a. CONTRACT NUMBER		
				5b. GRANT NUMBER		
				5c. PROGRAM ELEMENT NUMBER		
6. AUTHOR(S)				5d. PROJECT NUMBER		
				5e. TASK NUMBER		
				5f. WORK UNIT NUMBER		
7. PERFORMING ORGANIZATION NAME(S) AND ADDRESS(ES)					8. PERFORMING ORGANIZATION REPORT NUMBER	
9. SPONSORING/MONITORING AGENCY NAME(S) AND ADDRESS(ES)					10. SPONSOR/MONITOR'S ACRONYM(S)	
					11. SPONSOR/MONITOR'S REPORT NUMBER(S)	
12. DISTRIBUTION/AVAILABILITY STATEMENT						
13. SUPPLEMENTARY NOTES						
14. ABSTRACT						
15. SUBJECT TERMS						
16. SECURITY CLASSIFICATION OF:			17. LIMITATION OF ABSTRACT	18. NUMBER OF PAGES	19a. NAME OF RESPONSIBLE PERSON	
a. REPORT	b. ABSTRACT	c. THIS PAGE			19b. TELEPHONE NUMBER (Include area code)	

PREFACE

This technical report is a reprint of the thesis submitted to the Graduate School of the University of Florida in partial fulfillment of the requirements for the Masters degree in Engineering by Lindsey Riemenschneider. Because it is reproduced intact formatting within the document might vary somewhat from standards used in AFRL technical reports.

This report describes work accomplished between 1 March 2007 and 30 April 2008 at the University of Florida, Department of Environmental Engineering Sciences, Gainesville, FL 32611 with partial support from U.S. Air Force Research Laboratory Contract No. FA8560-06-C-5913.

CHARACTERIZATION OF REAEROSOLIZATION IN AN EFFORT TO IMPROVE
SAMPLING OF AIRBORNE VIRUSES
APRIL 30, 2008

By

LINDSEY RIEMENSCHNEIDER

A THESIS PRESENTED TO THE GRADUATE SCHOOL
OF THE UNIVERSITY OF FLORIDA IN PARTIAL FULFILLMENT
OF THE REQUIREMENTS FOR THE DEGREE OF
MASTER OF ENGINEERING

UNIVERSITY OF FLORIDA

2008

© 2008 Lindsey Riemenschneider

To my family and friends

ACKNOWLEDGMENTS

I would like to thank my family and friends for all of their support, encouragement, and understanding. I would also like to thank Dr. Wu for his patience, dependability, and generosity and for serving as an inspiration on how to interact with others. I would also like to express my gratitude to Dr. Lundgren for always providing so many ideas along with a smile to help improve both my project and my mood. I am also very grateful to have Dr. Wander for his encouragement and willingness to provide tremendous help, along with the many ideas and suggestions he provided. I also feel very fortunate and proud to belong to my research group and thank each of my lab mates, past and present, for all of their kindness, assistance, and hard work. It has truly been a pleasure to work along side all of them every day for the past two years.

I would also like to recognize the sources of financial support which helped me get through graduate school: Camp Dresser McKee for the CDM Fellowship; the UF Environmental Engineering Department for Teaching and Research Assistantships; and the US Air Force (Project No. FA8650-06-C-5913) for the research project.

TABLE OF CONTENTS

	<u>page</u>
ACKNOWLEDGMENTS	4
LIST OF TABLES	8
LIST OF FIGURES	9
LIST OF ABBREVIATIONS.....	12
ABSTRACT.....	13
 CHAPTER	
1 INTRODUCTION	15
Introduction.....	15
Bioaerosol Sampling Methodologies.....	15
Bioaerosol Amplification Unit	16
Description of Technology	17
Conceptual Implementation of In-line Bioaerosol Amplification Device	20
Reaerosolization	22
Objective.....	28
2 EXPERIMENTAL METHODOLOGY.....	30
Reaerosolization with PSL	31
Reaerosolization with MS2.....	32
Effect of Surface Tension and Viscosity on Reaerosolization	35
Reaerosolization with BioSampler	36
3 RESULTS	37
Reaerosolization with PSL	37
Reaerosolization with MS2.....	38
Effect of Surface Tension and Viscosity on Reaerosolization	43
Reaerosolization with BioSampler	45
4 DISCUSSION.....	47
Reaerosolization with PSL	47
Reaerosolization with MS2.....	50
Effect of Surface Tension and Viscosity on Reaerosolization	54
Reaerosolization with BioSampler	55
5 CONCLUSION.....	58

APPENDIX

A	BIOAEROSOL AMPLIFICATION UNIT INFORMATION	60
	Bioaerosol Amplification Unit Design	60
	Experimental Methodology	61
	Inert Particle Amplification	62
	Physical Collection Challenge.....	64
	Viable Collection Challenge.....	65
	Preliminary Results.....	66
B	REAEROSOLIZATION WITH PSL DATA SETS	68
	Test 1: 03/07/2008a	68
	Test 2: 03/07/2008b.....	69
	Test 3: 04/02/2008	70
C	REAEROSOLIZATION WITH MS2 DATA SETS	71
	Flow Rate: 3 Lpm	71
	Test 1: 03/15/2007a	71
	Test 2: 03/15/2007b	72
	Summary of 3 Lpm.....	73
	Flow Rate: 6 Lpm	74
	Test 1: 03/15/2007	74
	Summary of 6 Lpm.....	75
	Flow Rate: 9 Lpm	76
	Test 1: 02/14/2008a	76
	Test 2: 02/14/2008b	77
	Test 3: 03/15/2007	78
	Summary of 9 Lpm.....	79
	Flow Rate: 12.5 Lpm	80
	Test 1: 01/24/2008.....	80
	Test 2: 01/28/2008.....	81
	Test 3: 02/09/2008.....	82
	Summary of 12.5 Lpm.....	83
	Flow Rate: 15 Lpm	84
	Test 1: 02/17/2008a	84
	Test 2: 02/17/2008b	85
	Summary of 15 Lpm.....	86
	Mode Size of MS2 Experiments.....	87
D	EFFECT OF SURFACE TENSION AND VISCOSITY DATA SETS.....	88
	Effect of Surface Tension	88
	Test 1: 03/21/2008a	88
	Test 2: 03/21/2008b	89
	Test 3: 03/24/2008.....	90

Summary of Surface Tension	91
Effect of Viscosity	92
Test 1: 03/31/2008.....	92
Test 2: 04/02/2008a	93
Test 3: 04/02/2008b.....	94
Summary of Viscosity	95
E REAEROSOLIZATION WITH BIOSAMPLER DATA SETS	96
Test 1: 03/15/2008.....	96
Test 2: 03/19/2008a	97
Test 3: 03/19/2008b.....	98
Summary of BioSampler	99
LIST OF REFERENCES	100
BIOGRAPHICAL SKETCH	103

LIST OF TABLES

<u>Table</u>	<u>page</u>
1-1 Nomenclature for mass transfer of particles between bubbles and liquid	23
2-1 Summary of tests and corresponding purpose to characterize viral reaerosolization from impingers.....	30
2-2 Experimental matrix to determine the effect of flow rate and concentration on reaerosolization	33
3-1 Percent of PSL particles reaerosolized	37
3-2 Comparison of mode sizes for PSL particles under different experimental conditions	45
4-1 Comparison of reaerosolization for bacteria-sized particles to that for virus-sized particles	48
4-2 Estimated droplet volume generated from impinger	50
4-3 Comparison of present work to past research on reaerosolization from AGI-30 Impinger and BioSampler	56
A-1 Summary of tests and corresponding purpose to evaluate BAU	62
A-2 Preliminary results from viral aerosol sampling using BAU	67

LIST OF FIGURES

<u>Figure</u>	<u>page</u>
1-1 Bioaerosol amplification conceptual schematic.....	21
1-2 Coefficients of mass transfer due to inertia and diffusion for transfer of particles from bubbles to surrounding liquid.....	24
1-3 Coefficients of mass transfer due to inertia and diffusion for transfer of particles from liquid to bubbles.....	25
2-1 Reaerosolization experimental setup.	31
2-2 The BioSampler.	36
3-1 Reaerosolization as a function of impinger concentration for PSL particles at 12.5 Lpm.	38
3-2 Size distribution of reaerosolized particles as a function of flow rate at an impinger collection liquid concentration of 1×10^2 PFU/mL.	39
3-3 Size distribution of reaerosolized particles as a function of collection liquid concentration at a flow rate of 9 Lpm.	40
3-4 Reaerosolization as a function of flow and impinger concentration for MS2 viral particles.	41
3-5 Comparison of the reaerosolization of PSL at 12.5 Lpm with and without soap present.	44
3-6 Comparison of the reaerosolization of PSL at 12.5 Lpm with and without oil present.	44
3-7 Comparison of the reaerosolization of PSL at 12.5 Lpm from impinger and BioSampler.	46
4-1 Baseline at 12.5 Lpm from impinger with oil and without oil present.	55
A-1 BAU prototype schematic.....	61
A-2 Experimental setup for inert particle amplification.	62
A-3 Experimental setup for physical collection efficiency testing.	64
B-1 Size distribution and average concentration of PSL at 12.5 Lpm (03/07/08a).....	68
B-2 Size distribution and average concentration of PSL at 12.5 Lpm (03/07/08b).....	69
B-3 Size distribution and average concentration of PSL at 12.5 Lpm (04/02/08).....	70

C-1	Size distribution and adjusted avg concentration of MS2 at 3 Lpm (03/15/07a).	71
C-2	Size distribution and adjusted avg concentration of MS2 at 3 Lpm (03/15/07b).	72
C-3	Summary of adjusted average concentration of MS2 at 3 Lpm.	73
C-4	Size distribution and adjusted avg concentration of MS2 at 6 Lpm (03/15/07).	74
C-5	Summary of adjusted average concentration of MS2 at 6 Lpm.	75
C-6	Size distribution and adjusted avg concentration of MS2 at 9 Lpm (02/14/08a).	76
C-7	Size distribution and adjusted avg concentration of MS2 at 9 Lpm (02/14/08b).	77
C-8	Size distribution and adjusted avg concentration of MS2 at 9 Lpm (03/15/07).	78
C-9	Summary of adjusted average concentration of MS2 at 9 Lpm.	79
C-10	Size distribution and adjusted avg concentration of MS2 at 12.5 Lpm (01/24/07).	80
C-11	Size distribution and adjusted avg concentration of MS2 at 12.5 Lpm (01/28/07).	81
C-12	Size distribution and adjusted avg concentration of MS2 at 12.5 Lpm (02/09/07).	82
C-13	Summary of adjusted average concentration of MS2 at 12.5 Lpm.	83
C-14	Size distribution and adjusted avg concentration of MS2 at 15 Lpm (02/17/08a).	84
C-15	Size distribution and adjusted avg concentration of MS2 at 15 Lpm (02/17/08b).	85
C-16	Summary of adjusted average concentration of MS2 at 15 Lpm.	86
C-17	Average mode size as a function of flow and impinger concentration for MS2 viral particles.	87
D-1	Size distribution and adjusted avg concentration of PSL at 12.5 Lpm (03/21/08a).	88
D-2	Size distribution and adjusted avg concentration of PSL at 12.5 Lpm (03/21/08b).	89
D-3	Size distribution and adjusted avg concentration of PSL at 12.5 Lpm (03/21/08b).	90
D-4	Summary of adjusted average concentration of PSL at 12.5 Lpm.	91
D-5	Size distribution and adjusted avg concentration of PSL at 12.5 Lpm (03/31/08).	92
D-6	Size distribution and adjusted avg concentration of PSL at 12.5 Lpm (04/02/08a).	93
D-7	Size distribution and adjusted avg concentration of PSL at 12.5 Lpm (04/02/08b).	94
D-8	Summary of adjusted average concentration of PSL at 12.5 Lpm.	95

E-1	Size distribution and adjusted avg concentration of PSL at 12.5 Lpm (03/15/08).	96
E-2	Size distribution and adjusted avg concentration of PSL at 12.5 Lpm (03/19/08a).	97
E-3	Size distribution and adjusted avg concentration of PSL at 12.5 Lpm (03/19/08b).	98
E-4	Summary of adjusted average concentration of PSL at 12.5 Lpm.	99

LIST OF ABBREVIATIONS

BAU	Bioaerosol Amplification Unit
SMPS	Scanning Mobility Particle Sizer
PSL	Polystyrene Latex
nm	Nanometer
μm	Micrometer
AGI	Ace Glass, Inc.
ppm	Parts per million
PFU	Plaque forming unit
cP	Centipoise

Abstract of Thesis Presented to the Graduate School
of the University of Florida in Partial Fulfillment of the
Requirements for the Degree of Master of Engineering

CHARACTERIZATION OF REAEROSOLIZATION IN AN EFFORT TO IMPROVE
SAMPLING OF AIRBORNE VIRUSES

By

Lindsey Riemenschneider

August 2008

Chair: Chang-Yu Wu

Major: Environmental Engineering Sciences

Airborne virus outbreaks, including the influenza pandemic of 1918, the recent SARS pandemic, and the anticipated H5N1 outbreaks, plus the perceived threat of bioterrorism have led to heightened concern about the prevalence and potential effects of airborne viruses. However, current bioaerosol sampling methods are unable to effectively sample airborne viruses (typically 20 to 300 nanometers). To address this problem, a novel Bioaerosol Amplification Unit has been designed and constructed to increase the size of the virus particles by condensational growth, thereby enhancing sampling recovery. In order to evaluate the Bioaerosol Amplification Unit, reaerosolization of viral particles from the impinger needs to be investigated to assess its impact on the capability of the new device.

Reaerosolization as a function of flow rate and impinger collection liquid concentration has been characterized. An impinger containing a known concentration of particles (MS2 bacteriophage or polystyrene latex particles) was operated at various flow rates with sterile air, and a scanning mobility particle sizer was used to determine the reaerosolization rates. Results indicate that reaerosolization increases as flow rate increases, due to the additional energy introduced to the system. However, increased concentration does not necessarily lead to an increase in reaerosolization for virus particles. Rather, reaerosolization increases as

concentration increases until it reaches a concentration of approximately 10^6 PFU/mL, at which point reaerosolization begins to decrease. The phenomenon likely results from the aggregation of viral particles or the increase of surface tension or viscosity at high concentrations. Adjusting the surface tension by adding soap and increasing viscosity by adding a layer of heavy white mineral oil decreased reaerosolization. In summary, reaerosolization from an impinger could compromise the improved collection capability of the new BAU and is a major mode of loss in airborne virus sampling with impingers in certain scenarios, but reaerosolization can be minimized by sampling over shorter periods of time.

CHAPTER 1 INTRODUCTION

Introduction

The perceived threat of bioterrorism and airborne virus outbreaks, including historical epidemics of influenza and more recent occurrences of SARS and various strains of influenza, have led to heightened concern about the prevalence and potential effects of airborne viruses. Although there is increased attention to these potentially deadly microorganisms, current bioaerosol sampling methods are unable to effectively sample airborne viruses, which are typically in the 20–300 nanometer range (Madigan et al. 2003). Sampling efficiency of current bioaerosol sampling methods is less than 10% for the most challenging sizes of 30–100 nm (Hogan et al. 2005), a significant concern with respect to the common size of a virus. If sampling methodologies do not provide accurate results, the discrepancy between measured and actual virus concentrations could potentially lead to disastrous decision errors because the infectivity of viruses is measured as a minimum threshold.

Bioaerosol Sampling Methodologies

Bioaerosol sampling methods must physically collect the bioaerosols to subject them to viability analysis. The viability determines the infectivity of the particular air stream and provides critical health effect information. Therefore, the challenge in bioaerosol sampling is to have a system that provides high physical collection efficiency while maintaining high viable collection efficiency, such that viable organisms are not inactivated during the collection process. A typical sampling system for airborne viruses utilizes an impactor, liquid impinger, or filter (Tseng and Li 2005). Liquid impingement is often an advantageous choice, as the method lends itself nicely to viral enumeration techniques (Terzieva et al. 1996; Hogan et al. 2005). As previously mentioned, recent experiments with liquid impingers, including an AGI-30 impinger,

a BioSampler, and a frit bubbler, demonstrated that less than 10% of particles in the 30–100 nm range were collected (Hogan et al. 2005). Collection efficiency is highly dependent on particle size for the impingement methods. Collection efficiency increased with increasing particle size for particles greater than 100 nm due to the increased inertia (Hogan et al. 2005). On the other end of the spectrum, the collection efficiency of particles less than 30 nm increased as particle size decreased, likely due to increased diffusion. The particles in the 30–100 nm range had neither sufficient inertia nor sufficient diffusion to be collected well in the impinger. Reponen et al. (2001) report that the 50% cutpoint for the AGI-30 is 0.31 μm , at least ten times larger than viruses on the lower end of the viral size range.

Along with particle size, other characteristics of the airborne virus affect physical collection efficiency. Specifically, the hydrophobicity of the particle plays a significant role. Viruses are classified as enveloped if a lipid layer surrounds the nucleocapsid (Madigan et al. 2003). The presence of a lipid layer generally indicates that a virus will be hydrophobic, while the absence conversely indicates a hydrophilic nature (Vidaver et al. 1973; Madigan et al. 2003; Tseng and Li 2005). Comparison of collection efficiency in several different bioaerosol samplers for four different bacteriophages indicated that hydrophilic viruses are collected 10–100 times better than hydrophobic viruses (Tseng and Li 2005). This issue makes sampling hydrophobic viruses even more challenging than simply the issue of particle size, and these viral characteristics are important considerations for airborne virus sampling methodology.

Bioaerosol Amplification Unit

In review, airborne virus sampling is limited by the extremely small size of viruses as well as certain particle characteristics such as hydrophobicity. To address the limitations due to size, a novel device known as the Bioaerosol Amplification Unit (BAU) has recently been designed

and constructed to grow the ultrafine virus particles by condensational amplification, thus enhancing sampling recovery in impingers and improving the accuracy of measured results. The term amplification to describe the effective increase in particle size is consistent with other work in this field (Vonnegut 1954; Hering and Stolzenburg 2005). Particle amplification by condensational growth is an established method that has been previously applied to many inert ultrafine particles (Okuyama et al. 1984; Sioutas and Koutrakis 1996; Sioutas et al. 1999; Demokritou et al. 2002; Hering and Stolzenburg 2005). The ubiquitous condensation nuclei counter is a well known application of condensational growth to improve sampling and detection (Hinds 1999). Although the commercially available condensation nuclei counter is highly suitable for determining physical counts of aerosols, the unit lacks that necessary ability to provide viability information important for bioaerosol characterization.

The use of condensational growth to amplify bioaerosols for improved physical collection is a new application of a proven technology. By implementing the BAU prior to the selected bioaerosol sampling method, the effective particle size and subsequent collection efficiency of airborne viruses should increase significantly, as found in other research evaluating the use of condensational growth on inert particles (Okuyama et al. 1984; Sioutas and Koutrakis 1996; Demokritou et al. 2002).

Description of Technology

This novel bioaerosol collection method has been developed and disclosed through the University of Florida Office of Technology Licensing (oral disclosure UF#12430, Provisional Patent Application 60/956,316 filed 8/16/07). The main function of the device is to amplify the size of ultrafine bioaerosols, so as to make the particle size sufficiently large ($>1.0\ \mu\text{m}$) to be collected efficiently using standard bioaerosol collection techniques. The device employs condensational deposition onto the ultrafine particle to the extent that the particle has a new

effective diameter that is large enough for high sampling efficiency. This is accomplished by using an established process in which a supersaturated vapor–air mixture condenses onto condensation nuclei, which continue to grow until a vapor–liquid equilibrium is reached (Hinds 1999; Wu and Biswas 1998; Friedlander 2003). Condensation nuclei can be in either solid or liquid phase and serve primarily as a host for the saturated vapor. In the case of ultrafine bioaerosols such as viruses, individual or clusters of airborne viruses can serve as condensation nuclei in the presence of supersaturated water vapor, initiating water condensation on the virus particle surface. Provided sufficient time and appropriate conditions, the virus or other bioaerosol is capable of growing to micron-sized droplets and then can be collected efficiently using standard sampling techniques.

To successfully apply this concept specifically to viruses will require a substantial amount of amplification in the BAU. As discussed previously, Hogan et al. (2005) reported less than 10% collection efficiency for 30-nm particles in the AGI-30. Lin et al. (1997) reported approximately 70% collection efficiency during 30 minutes of sampling for 0.51-μm PSL in the AGI-30. That amount increased to nearly 90% collection efficiency for 1.02-μm PSL particles in the AGI-30 impinger for 30 minutes of sampling or less (Lin et al. 1997). Therefore, amplifying particle size from the lower end of the viral particle size range (30 nm) to 1 μm would increase collection efficiency from less than 10% to almost 90%. The time required to achieve this by the condensational amplification process can be estimated using Equation 1-1 (Hinds 1999).

$$\frac{d(d_p)}{dt} = \frac{4D_v M}{R\rho_p d_p} \left(\frac{p_\infty}{T_\infty} - \frac{p_d}{T_d} \right) \quad (1-1)$$

The equation describes the rate of particle growth, where d_p is particle size (amplified from 0.03 μm to 1.0 μm) and t is time to be calculated. D_v is the diffusion coefficient of the vapor

(2.35×10^{-5} m²/s at 15°C), M is the molecular weight of the liquid (18 g/gmole), ρ_p is the liquid density (1 g/cm³), and T_∞ is the surrounding temperature in the condensation chamber (15°C). p_d is the partial pressure of the vapor at the particle surface, assumed to be equal to saturation vapor pressure at 15°C (0.017 atm), calculated using Equation 1-2 (Hinds 1999). T_d is the temperature at the particle surface. p_∞ is the partial pressure of vapor in the surrounding air, which will be equal to the vapor pressure in the saturation chamber (0.072 atm at 40°C) as calculated by Equation 1-2.

$$p_s = \exp\left(16.7 - \frac{4060}{T - 37}\right) kPa \quad (1-2)$$

For simplicity, this estimate will not account for the effect on T_d due to the release of latent heat of vaporization during condensation. Equation 1-1 can be simplified and integrated to solve for the time required to grow the particle to the desired level under specific conditions. Equation 1-3 is the result.

$$\left(d_{p,t}^2 - d_{p,0}^2\right) = \frac{8D_v M}{R\rho_p} \left(\frac{p_\infty - p_d}{T_\infty}\right) t \quad (1-3)$$

An estimate indicates that the time for a 30-nm particle to grow to 1.0 μm in the condenser under such conditions would be 1.2×10^{-4} seconds, indicating that the amplification process is nearly instantaneous if the proper conditions are provided in the BAU.

Using the condensational amplification process, Okuyama et al. (1984) found that ZnCl₂ aerosols in the 0.005- to 0.05-μm range were all amplified to larger than 0.3 μm, sufficient for detection by contemporary optical techniques. Similarly, Sioutas and Koutrakis (1996) were able to sufficiently amplify 0.05-μm inert particles to achieve 89.3% collection efficiency in a virtual impactor with a 50% cut size of 1.4 μm. The virtual impactor operated at 8 Lpm and had

an acceleration nozzle diameter of 0.16 cm and a collection nozzle diameter of 0.24 cm. Their system used a water bath at 50°C followed by a cooling tube with a thermoelectric cooler at 8°C to obtain such results. Residence time in the saturator was approximately 10 seconds, while residence time was less than 1 second in the condenser. Demokritou et al. (2002) used the condensational amplification method for high-volume collection of ultrafine inert particles for inhalation studies. With a saturator temperature of 34°C and a condenser temperature of 16°C, the research team was able to collect 91% of all the ultrafine particles in a system with a 50% cut size of 1.0 μm , suggesting that nearly all of the ultrafine particles were grown to supermicron sizes. The system still maintained 88% collection in similar conditions (saturator at 33°C and condenser at 15°C) but with a 50% cut size of 1.8 μm . The fact that this method achieved nearly identical collection efficiencies regardless of the two different cut size values indicates that the ultrafine particles in this system frequently grew to amplified sizes greater than 1.8 μm , significantly larger than the desired 1.0- μm size required for the virtual impactor used in their first experiment (Demokritou et al. 2002).

Conceptual Implementation of In-line Bioaerosol Amplification Device

A conceptual device used to achieve the condensational phenomenon comprises two essential components: a humidification section, in which the bioaerosols are introduced into a saturated water vapor atmosphere, and a condensation section, in which the atmosphere becomes supersaturated with vapor and leads to condensation on the biological nuclei. Alcohol and other low-vapor-pressure liquids are often selected to be used as the vapor for the condensational amplification process of inert particles. Achieving high supersaturation levels is easier for low-vapor-pressure liquids with low molecular diffusivity (Hering and Stolzenburg 2005). If the molecular diffusivity is significantly slower than the thermal diffusivity, then the temperature in

the condenser drops much faster than the saturation level, leading to high supersaturation levels. Achieving high supersaturation levels is more difficult when water is used as the condensing vapor because its high molecular diffusivity decreases the supersaturation levels quickly. However, water is the appropriate choice in this study to preserve the viability of the bioaerosols, as alcohol and other liquids can inactivate microorganisms and therefore cannot be utilized as the vapor. Figure 1-1 illustrates the conceptual design.

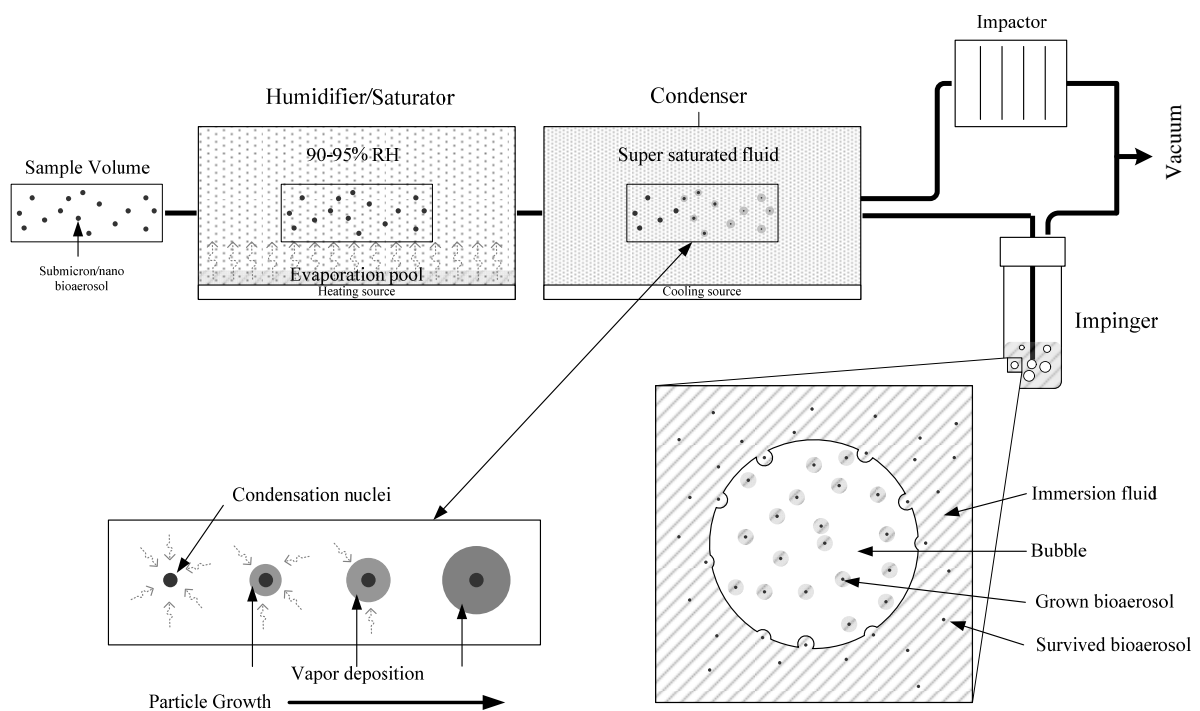


Figure 1-1. Bioaerosol amplification conceptual schematic.

Here, a bioaerosol sample flow is introduced into the humidification stage, in which a heated pool of water is used to create a virtually saturated water vapor atmosphere at a slightly elevated temperature (Hinds 1999; Friedlander 2003). After the sample volume passes through the saturator, it enters the condenser, which consists simply of a cooled environment. This section lowers the water vapor temperature enough to reach supersaturated conditions. As the

vapor becomes supersaturated, water condenses onto the bioaerosol nuclei, and the biological particle subsequently begins to amplify in diameter. The effective size of the amplified particle is now significantly larger than the actual particle size of airborne virus. The grown sample exits the BAU and can be collected using common bioaerosol collection methods such as impingement or impaction.

Reaerosolization

Besides size and hydrophobicity, reaerosolization is another factor that can affect the collection efficiency. Although the BAU can minimize the limitations of airborne virus sampling due to size, the nature of impingers allows for significant potential for reaerosolization (Willeke et al. 1995; Lin et al. 1997). Although impingers are currently the established method for airborne virus sampling, the performance characteristics of the impinger are still lacking. Reaerosolization occurs when collected particles are re-entrained into the air stream; this leads to decreased collection efficiency and is a common concern in impinger operation (Willeke et al. 1995; Grinshpun et al. 1997). The turbulence associated with impinger operation provides enough energy for particles to become re-entrained into rising bubbles due to high operational flow rates. The particles re-entrained in the rising bubbles are then reaerosolized (Grinshpun et al. 1997).

Theoretical models for aerosol transfer between bubbles and surrounding liquid are largely based on Fuchs' work presented in *The Mechanics of Aerosols* (1964), which describes the movement of particles from the bubble to the surrounding liquid, similar to the mass transfer used in a wet scrubber. The theory sums the contributions of mass transfer from multiple removal mechanisms, of which diffusion and inertia are the most relevant to the present research. For small, submicron particles, Brownian motion and thermophoresis are the main removal mechanisms. For larger particles, inertia and sedimentation become increasingly effective for

removal of aerosols from a bubble to the surrounding liquid (Ghiaasiann and Yao 1997). The coefficients of deposition due to diffusion (α_d) and inertia (α_i) are presented in the Equations 1-4, 1-5, 1-6, and 1-7, and a complete list of nomenclature is provided in Table 1-1.

$$\alpha_i = \frac{9U_B \tau}{2R_B^2} \quad (1-4)$$

$$\tau = \frac{2\rho_p R_p^2}{9\mu} \quad (1-5)$$

$$\alpha_d = 1.8 \left(\frac{D}{R_B^3 U_B} \right)^{1/2} \quad (1-6)$$

$$D = \frac{kT_G C_c}{6\pi\mu R_p} \quad (1-7)$$

Table 1-1. Nomenclature for mass transfer of particles between bubbles and liquid

Symbol	Title	Units
α_i	Coefficient of deposition due to inertia	1/m
α_d	Coefficient of deposition due to diffusion	1/m
U_B	Bubble velocity	m/s
τ	Relaxation time	s
R_B	Bubble radius	m
R_p	Particle size	m
ρ_p	Particle density	kg/m ³
μ	Gas viscosity	Pa-s
k	Boltzmann constant	1.3x10 ⁻²³ J/K
T_G	Temperature of gas	K
C_c	Cunningham's correction factor	Dimensionless
D	Aerosol diffusivity	m ² /s

Although his work does not specifically refer to mass transfer in a scenario such as that in the impinger, it provides some insight into what can be expected. By analyzing these theoretical expressions, it becomes apparent that inertial removal of aerosols from bubbles into a surrounding liquid clearly plays a larger role as particle size (R_p) increases and as bubble velocity (U_B) increases. Similarly, diffusive removal of particles from a bubble into a surrounding liquid

increases as the diffusivity coefficient increases as R_p decreases, as the bubble radius (R_B) decreases, and as U_B decreases, which allows more time for diffusion to occur. The overall effect of mass transfer of aerosols from a bubble to a liquid is very similar to the passage of aerosols through filters (Fuchs 1964; Pich and Schutz 1991). The deposition of aerosols from a bubble into a liquid as a function of particle size will have a clear minimum, with large aerosols collected well by inertial transfer and small particles collected well by diffusive transfer. For a scenario with a bubble velocity of 25 cm/s and bubble radius of 0.5 cm at standard conditions (20°C and 1 atm), the calculated coefficients are displayed in Figure 1-2.

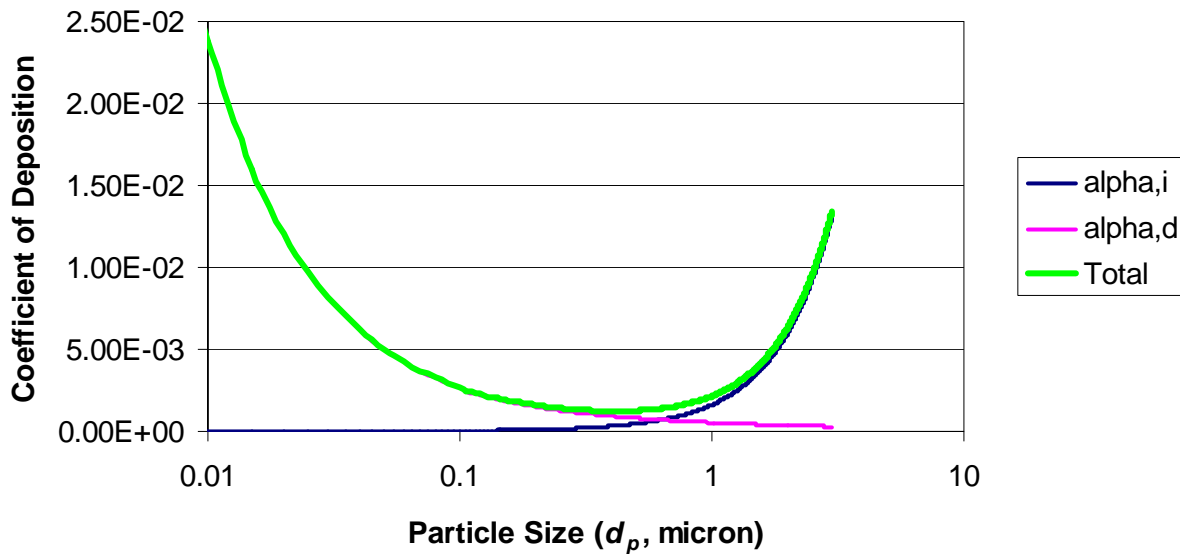


Figure 1-2. Coefficients of mass transfer due to inertia and diffusion for transfer of particles from bubbles to surrounding liquid.

Both methods of mass transfer must be examined to study the reverse effect, such that particles in the liquid are transferred from the liquid into the bubble, as is the case during reaerosolization. The case for diffusion will be a similar situation. Mass transfer from the liquid into the bubble will increase as diffusivity of the particle increases and more time is allowed for

diffusion to occur. The case for inertial mass transfer will be nearly opposite. In this scenario, the amount of inertia required to re-entrain a particle into a bubble will increase as particle size increases. Therefore, mass transfer of aerosols into the bubble due to inertia will increase as particle size decreases. The mass transfer of particles into bubbles from liquid to enable reaerosolization will be significantly larger for smaller particles because diffusion will be increased and the inertial requirement to re-entrain the particles will be smaller. Therefore, the diffusional deposition coefficient will have the same equation, while the inertial coefficient will be inverted. For a scenario with a bubble velocity of 25 cm/s and bubble radius of 0.5 cm at standard conditions (20°C and 1 atm), the calculated coefficients are displayed in Figure 1-3. Note that the α_i values are predominant, and the *Total* trend is dictated by them. The total diffusive transfer would also depend on the concentration of particles in the liquid.

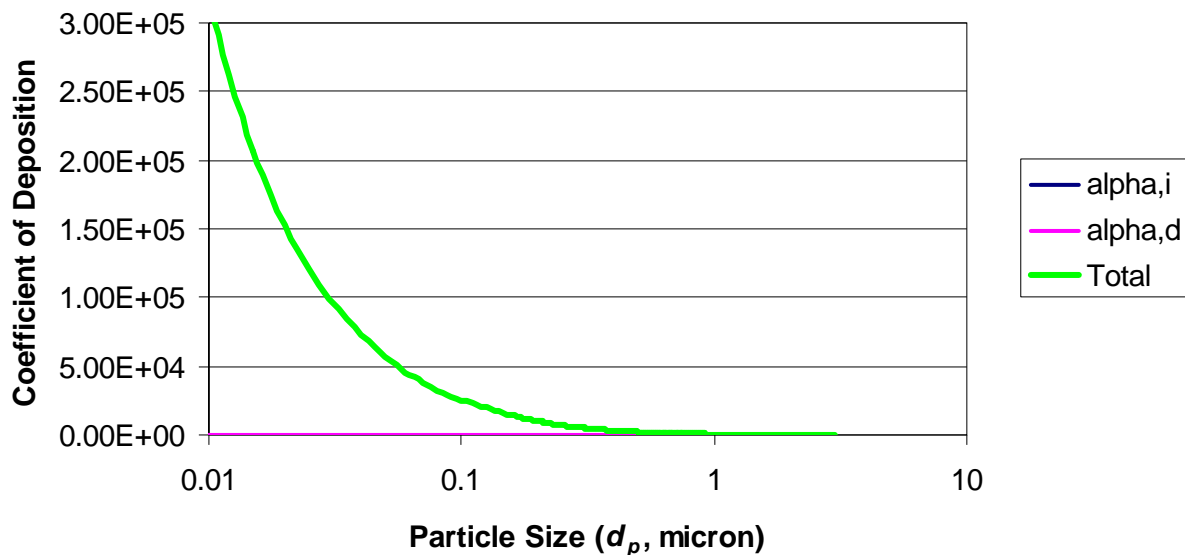


Figure 1-3. Coefficients of mass transfer due to inertia and diffusion for transfer of particles from liquid to bubbles.

A study on *Bacillus cereus* bacterial spore reaerosolization from liquid impingers by Grinshpun et al. (1997) observed that intense bubbling occurred even at 10 Lpm, although no bacterial reaerosolization was recorded. At the normal operation of 12.5 Lpm, the research group reported that several supermicrometer particles were detected downstream of the impinger outlet, and the collection efficiency decreased from 100% at 10 Lpm to 80–90% at 12.5 Lpm. A separate experiment noted that there was significantly more reaerosolization of the bacterial spore as flow rate increased from 5 to 12.5 Lpm. The observation and subsequent experiment led them to conclude that the decrease in impinger collection efficiency of the *Bacillus cereus* bacterial spore at 12.5 Lpm was due to reaerosolization. Theoretical models presented by Fuchs (1964) and Ghiaasiaan and Yao (1997) predict this observation, by theorizing that increased bubble rise velocity introduces more inertia into the system, thereby enhancing the removal of aerosols from a liquid.

Lin et al. (1997) found that reaerosolization of polystyrene latex (PSL) particles in size range of 0.51 μm to 1.60 μm increased with sampling time due to the increased concentration of collected particles in the impinger collection liquid. After approximately 30 minutes of sampling, reaerosolization started to steadily increase as collection liquid was removed from the impinger. After 60 minutes of sampling, the amount of reaerosolization significantly affected the collection efficiency of the impingers. They note that reaerosolization is much more dependent on the concentration in the collection liquid than the incoming airborne concentration. This trend can be explained with the theoretical discussions due to the fact that the concentration gradient between the liquid and bubble will increase as the concentration in the collection liquid increases, thereby increasing diffusive mass transfer into the bubble and enhancing reaerosolization. The collection of 0.51- μm particles was much more impacted by

reaerosolization than the collection of 1.02- μm or 1.60- μm particles; nearly 10% of all 0.51- μm particles were reaerosolized after 60 minutes of sampling.

This experimental observation that reaerosolization increases as particle size decreases is a physical representation of the theoretical mass transfer expressions discussed previously. As particle size decreases, diffusive mass transfer increases while the inertia required to reaerosolize the particle is less. Because of these two combined effects, total reaerosolization is expected to increase significantly as particle size decreases.

Regardless of the past work done on the subject of reaerosolization for specific particle types, it should be stressed that the extent of reaerosolization is often dependent on particle characteristics (Grinshpun et al. 1997; Lin et al. 1997; Tseng and Li 2005). Size plays a role because of increased diffusion and lower inertia required to reaerosolize small particles, as seen by the increased reaerosolization of the 0.51- μm particles in comparison with the 1.02- μm or 1.60- μm particles in the study conducted by Lin et al. (1997). Hydrophobicity is also one of the key components that will determine reaerosolization. As previously mentioned, Tseng and Li (2005) found that hydrophilic viruses were collected 10–100 times more effectively in bioaerosol samplers than were hydrophobic viruses. Although they did not differentiate between the contributing factors to the low collection of hydrophobic viruses, it is reasonable to assume that hydrophobicity affects initial collection as well as reaerosolization; hydrophobicity makes initial collection more challenging while reaerosolization occurs more easily.

Aerosolization of the collection liquid is dependent on its characteristics, especially the viscosity and surface tension (Russell and Singh 2006). Viscosity and surface tension play a crucial role in the amount of liquid that is aerosolized, and subsequently in the amount of particles that are reaerosolized (Hogan et al. 2005; Lin et al. 1999). For instance, 20 mL of water

(viscosity of 0.89 cP at 25°C) will be evaporated or aerosolized from an impinger after approximately 1.5 hours (Lin et al. 1997; Willeke et al. 1998). Similarly, 20 mL of water will be evaporated from a BioSampler after approximately 2 hours of operation, while 10 mL of glycerol (viscosity of ~930 cP at 25°C) (White 2003) in a BioSampler has negligible loss after 8 hours of sampling (Willeke et al. 1998). A decrease in surface tension or viscosity should result in higher aerosolization, while an increase in surface tension or viscosity should result in lower aerosolization. The addition of a surfactant to the collection liquid will decrease surface tension (Weissenborn 2006) and likely result in higher reaerosolization. The addition of a more viscous, insoluble liquid on the surface of the collection liquid has the potential to suppress the bubbling due to the energy addition during the normal operation of the impinger. Heavy white mineral oil has been found to support microbial viability well enough to serve as a potential collection liquid for the BioSampler (Lin et al. 1999), but higher viscosity liquids cannot be used alone with the impinger because of the formation of large bubbles that prevent the transfer of airborne particles to the bulk liquid (Willeke et al. 1998).

Reaerosolization due to aerosolization of the impinger collection liquid can be expected to reduce airborne virus collection efficiency. Analysis of reaerosolization will determine the extent to which the phenomenon competes with the improved physical collection efficiency of the new BAU.

Objective

The objective of the project was to investigate reaerosolization of viral particles from the impinger to assess the impact of this mode of loss on the capability of the new Bioaerosol Amplification Unit. The present work focuses on characterizing reaerosolization of viral particles from impingers as a function of flow rate and impinger collection liquid concentration. The impact of collection liquid surface tension and viscosity was also explored, and virus

reaerosolization from the AGI-30 impinger was compared to that from the BioSampler. The Bioaerosol Amplification Unit is introduced presently to demonstrate the motivation for the current work. Experimental methods and preliminary results for the BAU are included in Appendix A, and a full characterization study of the BAU will be addressed in future work.

CHAPTER 2

EXPERIMENTAL METHODOLOGY

Four sets of experiments were conducted to analyze reaerosolization of viral particles from the AGI-30 impinger (Ace Glass, Inc., Vineland, NJ, USA). Table 2-1 summarizes the experimental conditions and the corresponding purpose for each test.

Table 2-1. Summary of tests and corresponding purpose to characterize viral reaerosolization from impingers

Test No.	Test Name	Purpose
1	Reaerosolization with PSL particles	Determine the effect of liquid impinger concentration on reaerosolization at 12.5 Lpm
2	Reaerosolization with MS2	Determine the effect of flow rate and liquid impinger concentration on reaerosolization
3	Effect of Surface Tension and Viscosity	Determine the effect of collection liquid viscosity and surface tension on reaerosolization
4	Reaerosolization from BioSampler	Determine extent of reaerosolization from BioSampler in comparison to AGI-30 impinger

Experiments to determine reaerosolization as a function of flow rate and impinger concentration followed experimental methods similar to those used in previous work to characterize bacterial reaerosolization (Willeke et al. 1998; Lin et al. 2000; Hogan et al. 2005). Figure 2-1 shows a schematic of the experimental system. A known concentration of particles was placed in the impinger collection liquid, and the impinger was operated with sterile air. The flow rate through the system was controlled by a rotameter. The flow exiting the impinger carried any aerosolized droplets and reaerosolized particles downstream. A slip stream directed 0.6 Lpm of the impinger exhaust flow through a diffusion dryer to remove excess moisture and finally into the Scanning Mobility Particle Sizer (SMPS, Model 3936, Shoreview, Minn., USA), where reaerosolized particles were measured. A baseline test using pure deionized water (0 PFU/mL) in the impinger collection liquid was used to confirm that the experimental setup was operating properly prior to every experiment. The nebulizer in the baseline test

hypothetically produced pure water droplets, in which case the diffusion dryer removed any moisture, and the SMPS registered negligible aerosol particles. Any aerosols detected in the baseline were due to low levels of salt present in the deionized water and the total reaerosolized concentrations were accordingly adjusted.

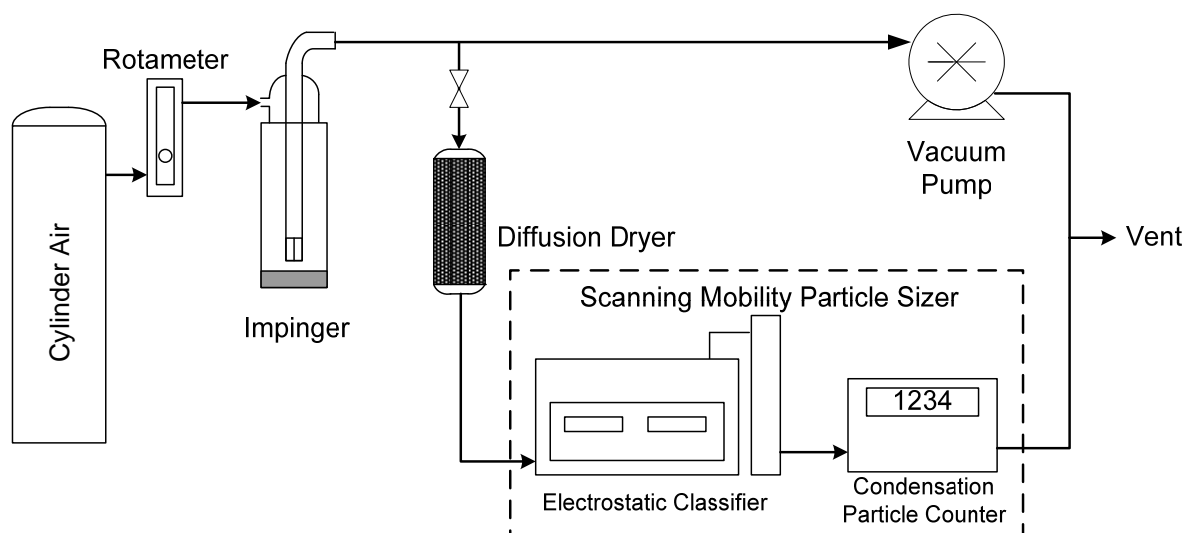


Figure 2-1. Reaerosolization experimental setup.

Reaerosolization with PSL

The first experiment utilized polystyrene latex particles (PSL, Duke Scientific, Palo Alto, Calif., 3030A, nominal 30-nm particles, density 1.05 g/cm^3) in the impinger liquid to provide a preliminary analysis of reaerosolization of viral-sized particles. Airborne virus particles are difficult to distinguish from residual solute particles caused by the liquid medium, and the liquid medium typically dictates the airborne virus particle size distribution (Hogan et al. 2005). Viruses also have inherent microbial uncertainties, including loss of viability and microbial interactions, which can influence their behavior. The use of PSL particles in deionized water eliminated these uncertainties and provided a simpler and more straightforward test. Therefore, very explicit results regarding aerosolization of viral-sized particles were obtained.

Deionized water was used to dilute the PSL particles to the desired concentrations. The test was conducted for a range of concentrations (0.1, 1.0, 10, 100 ppm by mass or volume; $\rho=1.05 \text{ g/cm}^3$) at a flow rate of 12.5 Lpm only, which is the recommended operational flow rate for the impinger (Ace Glass Inc. 2008).

Reaerosolization with MS2

Although PSL particles provided explicit information regarding the reaerosolization of virus-sized particles, the test needed to be conducted with MS2 to see if the results from PSL translated to actual virus. Thus, the reaerosolization experiment was then conducted much more thoroughly with MS2 virus (*Escherichia coli* bacteriophage ATCC[®] 15597-B1[™]) in the impinger liquid to obtain results specific to the virus.

MS2 is a bacteriophage that is often used as a surrogate pathogen for airborne virus testing and is an appropriate choice for use as a surrogate human pathogenic virus (Aranha–Creado and Brandwein 1999). The nominal size of the MS2 bacteriophage is 27.5 nm (Golmohammadi et al. 1993); thus, it will serve as a suitable challenge for the BAU in future studies because typical collection efficiencies in the impinger at this particle size are less than 10% (Hogan et al. 2005). MS2 is classified as a hydrophilic virus because of the absence of a lipid envelope surrounding the nucleocapsid (Vidaver et al. 1973; Madigan et al. 2003; Tseng and Li 2005).

To determine the effect of flow rate and impinger collection liquid concentration on reaerosolization, a matrix was used with several different flow rates and concentrations as shown in Table 2-2. Twenty-five tests were run in total for the experiment, and each is numbered separately in the matrix. A few samples were also examined at an impinger collection liquid concentration of 10^1 PFU/mL.

Preliminary infectivity tests were run during some of the initial reaerosolization tests, but the results were not sensitive enough to assess any trends to the results. Although extensive operation of the impinger can decrease the viability of MS2 after approximately 30 minutes of sampling (Hogan et al. 2005), the time span of the reaerosolization tests (<15 minutes) did not appear to be long enough to substantially affect viability. Any minor difference in the level of infectivity before and after the reaerosolization test could easily have been attributed to many other circumstances that are known to affect microbiological enumeration techniques. The infectivity component was therefore stopped because the results were not providing clear information.

Table 2-2. Experimental matrix to determine the effect of flow rate and concentration on reaerosolization

Impinger Liquid Concentration (PFU/mL)	Flow Rate (Lpm)				
	3	6	9	12.5	15
Baseline	No. 1	No. 2	No. 3	No. 4	No. 5
10 ²	No. 6	No. 7	No. 8	No. 9	No. 10
10 ⁴	No. 11	No. 12	No. 13	No. 14	No. 15
10 ⁶	No. 16	No. 17	No. 18	No. 19	No. 20
10 ⁸	No. 21	No. 22	No. 23	No. 24	No. 25

Lin et al. (1997) found that increased impinger collection liquid concentration significantly increased the amount of reaerosolization for PSL particles in bacterial size ranges. Grinshpun et al. (1997) observed that reaerosolization of bacterial spores was initiated as impinger flow rate increased. Theoretical models predict that mass transfer from the collection liquid to the bubble will increase as particle size decreases due to two reasons: (1) diffusivity will increase as particle size decreases; and (2) the inertial requirement to re-entrain particles will decrease as particle

size decreases. The models also predict that diffusive mass transfer from the collection liquid to the bubble will increase as the concentration gradient between the collection liquid and the bubble increases.

Therefore, logical hypotheses for virus particles were that reaerosolization would increase as both flow rate and accumulative impinger collection liquid concentration increased, and that reaerosolization for virus-sized particles would be greater than that for bacteria-sized particles. While operational flow rate is often established by sampling protocol, the accumulative impinger concentration increases with sampling time. The results from these experiments will be able to provide recommended sampling time limits based on accumulative impinger concentration that can be established to minimize the effects of reaerosolization. Hydrophobic viruses will have different considerations than MS2, and future work may need to address this issue.

One concern for the reaerosolization tests with MS2 was the decision to use phosphate buffered saline (PBS) or pure deionized water as the impinger liquid. Although PBS (1.8 g KH_2PO_4 , 15.2 g $\text{K}_2\text{H}_2\text{PO}_4$, and 85 g NaCl in 1L of deionized water) is often used in bioaerosol sampling to maintain bioaerosol viability, the salt aerosols formed when the liquid is aerosolized can mask the magnitude of reaerosolized virus particles. Similarly, it is difficult to distinguish aerosolized viruses from residual solute particles formed from aerosolized liquid media, and the media typically dictates the airborne virus particle size distribution (Hogan et al. 2005). The experiments attempted to minimize the effects of background media such as PBS and virus stock medium, but the issue was inherent to the task at hand regardless of these efforts. 0.02 mL of PBS was inherently included in 20 mL of virus solution in the process of the impinger liquid preparation.

Effect of Surface Tension and Viscosity on Reaerosolization

Once reaerosolization for virus-sized particles was fully characterized, experiments were conducted to analyze the effects of surface tension and viscosity, which were hypothesized to play a crucial role in the amount of liquid that is aerosolized, and subsequently the amount of particles that were reaerosolized (Lin et al. 1999; Hogan et al. 2005; Russell and Singh 2006). Two experiments were conducted to explore the effects of viscosity and surface tension for various concentrations of PSL particles (0.1, 1.0, 10, 100 ppm) at 12.5 Lpm. To determine the effect of surface tension, a surfactant (Palmolive concentrated dish liquid, Colgate–Palmolive Company, New York, N.Y.) was introduced to reduce the surface tension of the collection liquid. 0.2 mL of a diluted soap solution (composed of approximately 0.1 mL in 10 mL of deionized water) was used in each of the triplicate experiments, such that approximately 0.002 mL of the concentrated dish liquid was added to the impinger liquid. The amount was sufficient to cause significant bubbling without overwhelming the impinger with soap bubbles under normal operation. Although the condition was predicted to increase reaerosolization, the experiment was conducted to verify the effect of surfactants.

The addition of a more viscous, insoluble liquid on the surface of the collection liquid has the potential to suppress the bubbling during the normal operation of the impinger. To investigate this, a small layer (0.3 mL) of heavy white mineral oil (Mineral Oil, NDC 0003-0559-33, E.R. Squibb and Sons, Inc. Princeton, N.J.) was added to provide a more viscous layer, and the results were analyzed to determine whether reaerosolization decreased. Heavy white mineral oil was selected because it was found to maintain bacterial viability over 8 hours (Lin et al. 1999).

Reaerosolization with BioSampler

The last experiment was a test comparing reaerosolization from the AGI-30 impinger to that from the BioSampler (SKC, Inc., Eighty-Four, P.A.). Previous research indicated that the BioSampler had significantly less reaerosolization for particles in the bacterial size range due to the swirling motion during collection (Willeke et al. 1998; Lin et al. 2000). This experiment attempted to confirm that this was also the case for particles in the virus size range. Figure 2-2 shows the BioSampler and the swirling collection mechanism. Reaerosolization of 30-nm PSL particles from the BioSampler was compared to that from the AGI-30 impinger using conditions identical to the first experiment. The experimental flow rate was 12.5 Lpm, and the concentrations used were 0.1, 1.0, 10, and 100 ppm.

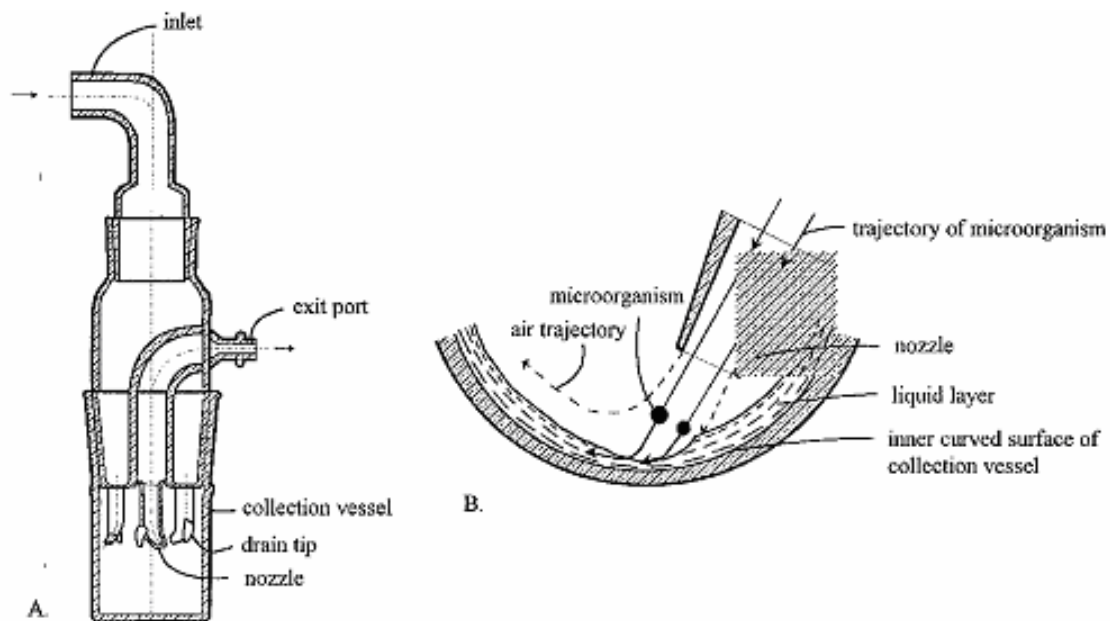


Figure 2-2. The BioSampler. A) A schematic. B) Collection mechanism. (Lin et al. 2000)

CHAPTER 3 RESULTS

Reaerosolization with PSL

Polystyrene latex (PSL) particles (30 nm) were tested at various concentrations in the impinger collection liquid at 12.5 Lpm, which is the standard operational flow rate recommended for impingers (Ace Glass, Inc. 2008). Five tests at each scenario were measured by the SMPS over a 12-minute period. Deionized water was the impinger collection liquid, and the results were appropriately adjusted for any particles measured during the baseline experiment (pure deionized water represented as 10^0 PFU/mL for graphing purposes). The measured concentrations for the subsequent tests are therefore displayed as adjusted reaerosolized concentration.

The amount of PSL particle reaerosolization continued to increase as the collection liquid concentration increased, as shown in Figure 3-1. Data sets for each of the triplicate tests are included in Appendix B. An analysis of variance (ANOVA) test shows that each increase at the higher concentrations (from 1 to 10 ppm and from 10 to 100 ppm) was deemed significant ($p < 0.05$), while the increases between the lower concentrations (from 0 ppm to 0.1 ppm and from 0.1 ppm to 1 ppm) were not as significant ($p > 0.05$). Table 3-1 displays the percentages of particles reaerosolized. Less than 1.0% of the particles contained in the impinger were reaerosolized at any concentration over the sampling period.

Table 3-1. Percent of PSL particles reaerosolized

Impinger Concentration (ppm)	% Particles Reaerosolized
0.0	N/A
0.1	0.84%
1.0	0.10%
10.0	0.03%
100.0	0.01%

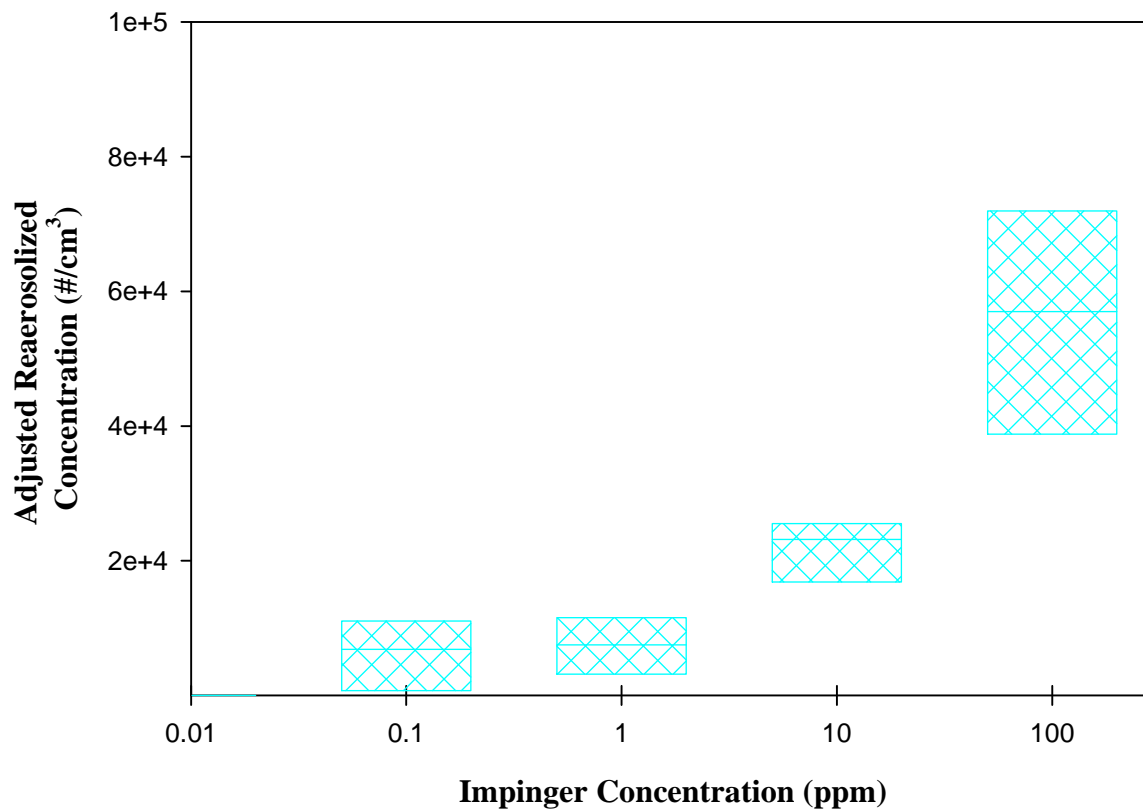


Figure 3-1. Reaerosolization as a function of impinger concentration for PSL particles at 12.5 Lpm. The lower end of the box represents the 25th percentile, the middle line represents the median, and the upper end of the box represents the 75th percentile.

Reaerosolization with MS2

The dependence of the reaerosolization of MS2 bacteriophage particles on flow rate and impinger liquid concentration was evaluated using a diffusion dryer followed by the SMPS. Five tests at each scenario were run over a 12-minute period. Results indicated that increasing the flow rate significantly increased the number of virus particles reaerosolized. A typical trend is displayed in Figure 3-2, which presents data obtained from the SMPS at a constant impinger collection liquid concentration (1×10^2 PFU/mL) and varying flow rate.

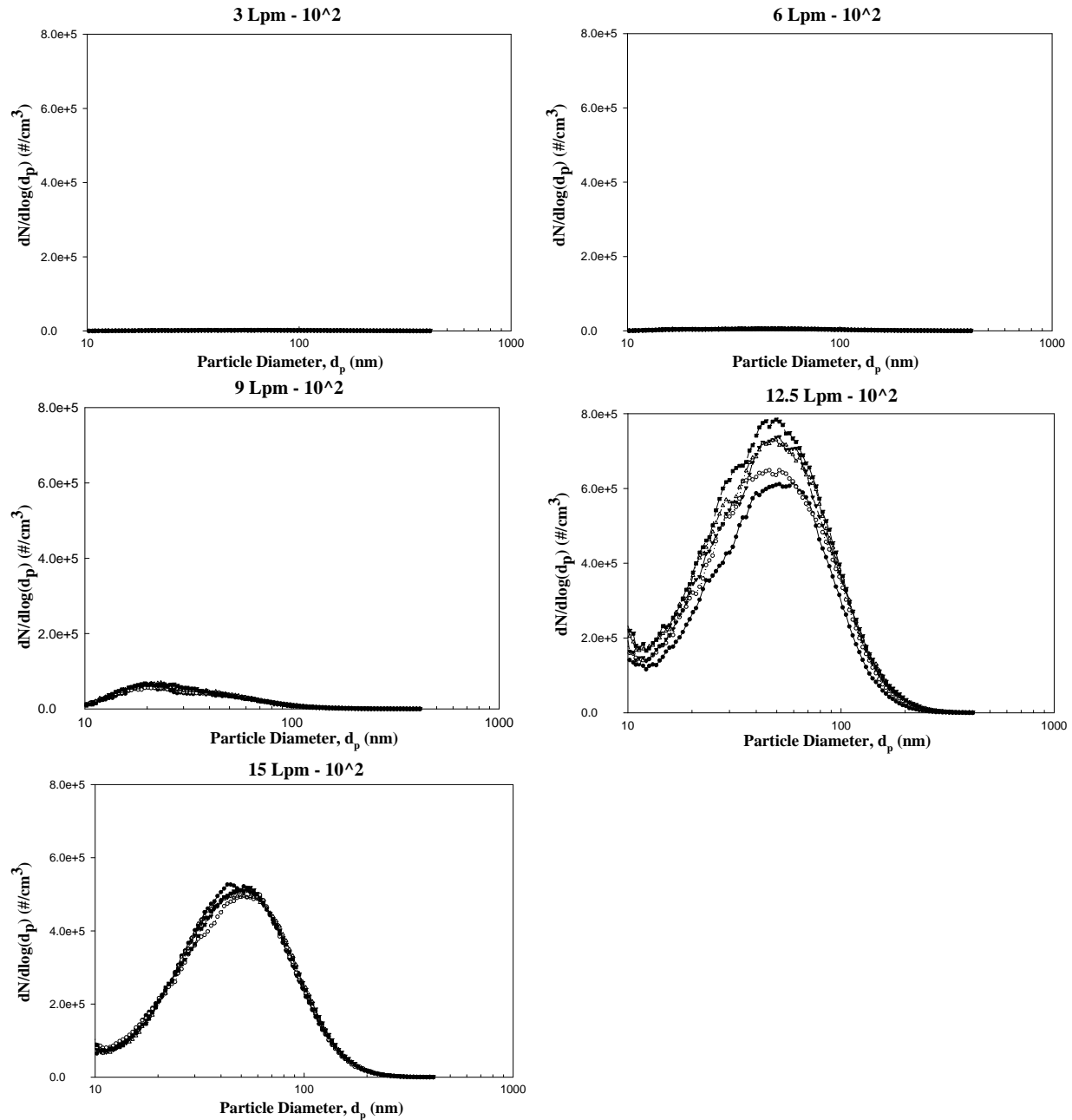


Figure 3-2. Size distribution of reaerosolized particles as a function of flow rate at an impinger collection liquid concentration of 1×10^2 PFU/mL.

Increased concentration, however, did not necessarily lead to an increase in reaerosolization for virus particles. Rather, the count of reaerosolized virus particles increased as concentration increased until it reached a concentration of approximately 10^6 PFU/mL, at which

point the reaerosolized count began to decrease. This trend is shown in Figure 3-3. These data sets maintained a constant impinger flow rate, but the concentration of MS2 in the collection liquid varied.

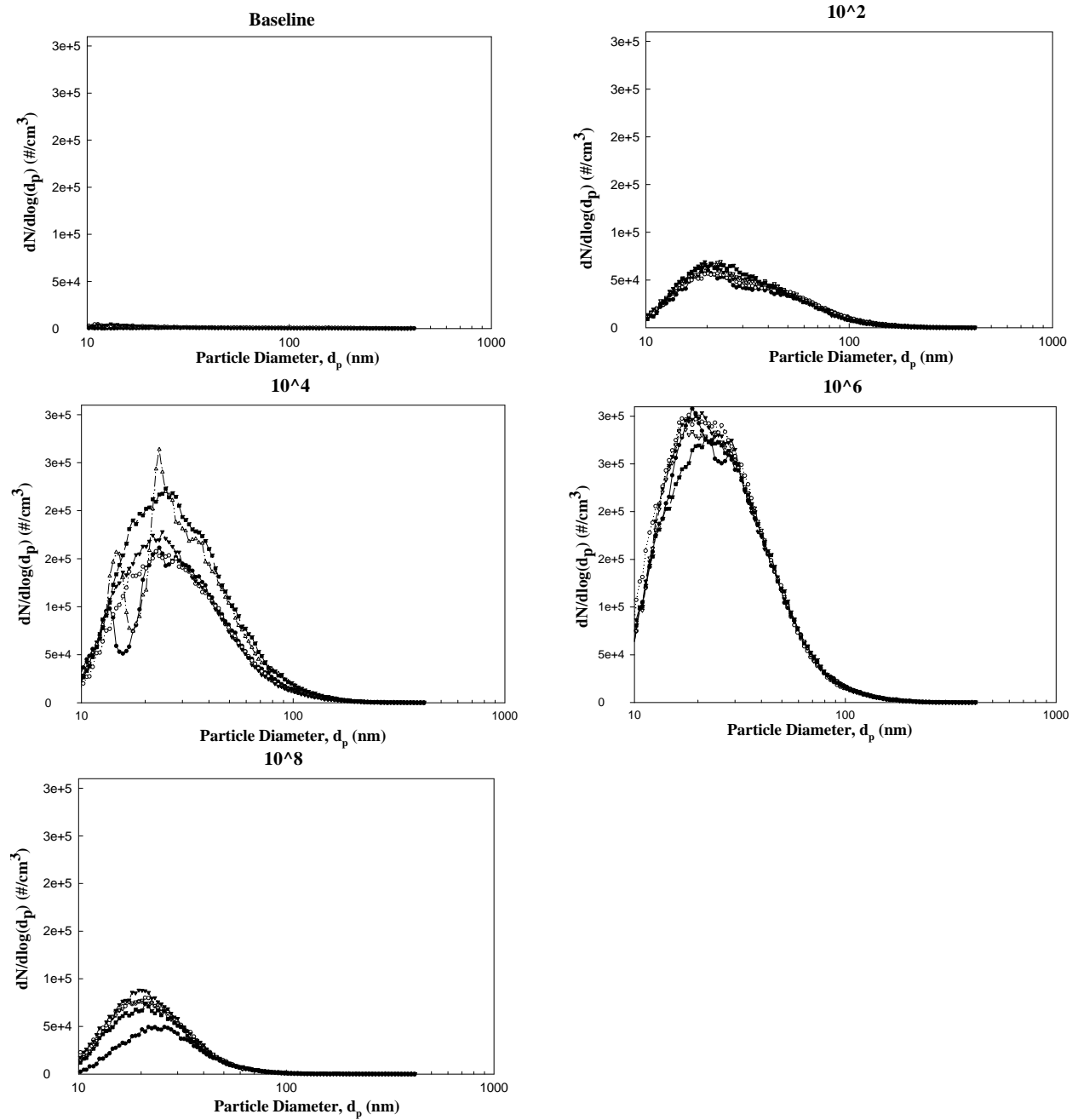


Figure 3-3. Size distribution of reaerosolized particles as a function of collection liquid concentration at a flow rate of 9 Lpm.

Results for the final reaerosolized concentration as a function of concentration for each of the five flow rates tested (3, 6, 9, 12.5, 15 Lpm) are displayed in Figure 3-4. Three experiments were conducted at each of the three higher flow rates (9, 12.5, and 15 Lpm), while only two experiments were conducted at the two lower flow rates (3 and 6 Lpm). The trends at the lower flow rates followed the same pattern, but the overall level of reaerosolization was minimal in comparison to the higher flow rates. This agrees with Fuchs' work, the application of which predicted that increasing flow rate will increase reaerosolization.

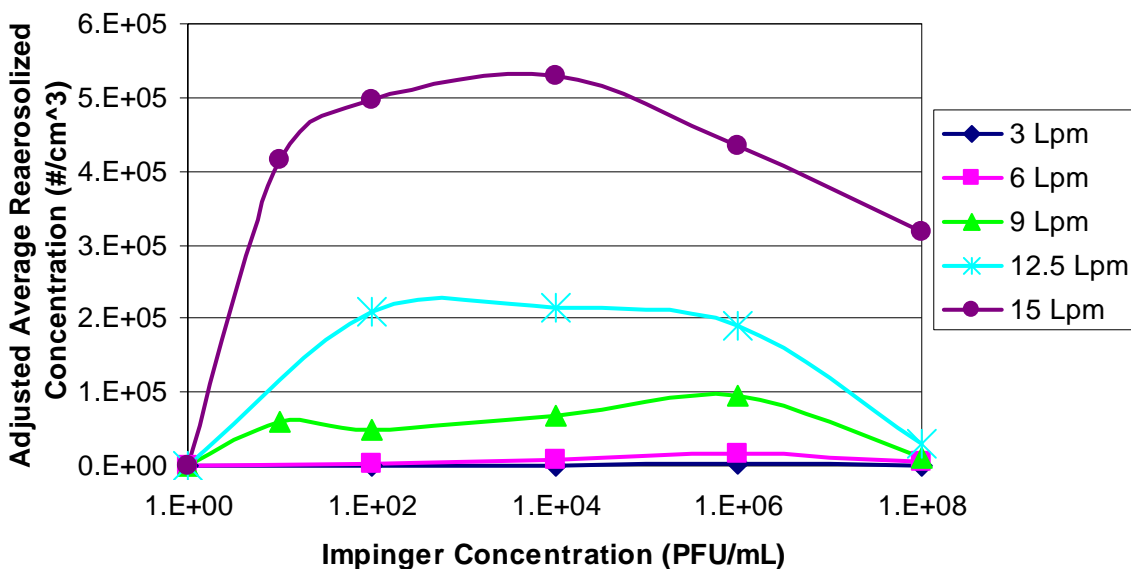


Figure 3-4. Reaerosolization as a function of flow and impinger concentration for MS2 viral particles.

Some reaerosolized particles detected were attributed to low salt concentrations in the deionized water. These salt aerosols were represented as the concentrations measured during the baseline experiments. The subsequent tests were adjusted by subtracting the baseline concentration from each. The resulting values are displayed as adjusted average reaerosolized concentration. Complete data sets for each of the presented results are included in Appendix C.

Small variations in the experimental sets displayed in Appendix C can likely be attributed to microbiological interactions, virus age, and small variations in virus stock compositions.

Statistical analysis was run on the tests using the ANOVA test. The difference between reaerosolized concentrations is generally significant ($p < 0.05$) between the baseline (10^0 PFU/mL) and the middle concentrations (10^2 , 10^4 , 10^6 PFU/mL). The three middle concentrations (10^2 , 10^4 , 10^6 PFU/mL) are generally not significantly different ($p > 0.05$). The reaerosolized amount is generally significant ($p < 0.05$) between the middle concentrations (10^2 , 10^4 , 10^6 PFU/mL) and the highest concentration (10^8 PFU/mL). The significance of the difference between the middle and highest concentrations is stronger at the higher flow rates.

As an example, at 9 Lpm, the difference between the baseline and 10^2 PFU/mL is significant ($p = 0.0008$), the difference between 10^2 PFU/mL and 10^8 PFU/mL is also significant ($p = 0.03$), but the difference between the three middle concentrations (10^2 , 10^4 , 10^6 PFU/mL) is not significant ($p = 0.42$).

In general, reaerosolization increased significantly as flow rate increased. The increasing trend agreed with the hypothesis that extra inertia would reaerosolize more particles. The unexpected result was the decrease in reaerosolization at concentrations higher than approximately 10^6 PFU/mL. For all flow rates, the highest levels of concentration resulted in a decrease in reaerosolization. Although this was not expected, the observation may be explained by changes in aggregation and surface tension due to changes in concentration of proteins and salt in the deionized water and virus stock. This will be discussed in more detail in the Discussion section.

These results make it clear that reaerosolization of viral particles from an impinger occurs and may potentially compete with the BAU if an impinger is the bioaerosol sampler in use.

Future testing should aim to establish recommended sampling time limits based on influent airborne virus concentrations. This will minimize the effects of reaerosolization by preventing the accumulative impinger concentration from reaching a certain threshold.

Effect of Surface Tension and Viscosity on Reaerosolization

Viscosity and surface tension play a crucial role in the amount of liquid that is aerosolized, and subsequently the amount of particles that are reaerosolized (Hogan et al. 2005; Lin et al. 1999; Russell and Singh 2006).

Figure 3-5 displays the results for the adjusted average reaerosolized concentration as a function of concentration for this experiment in comparison to the previous PSL experiment without soap. The percent change from without soap to with soap is also displayed for each concentration. As shown, PSL reaerosolization decreased with the soap under identical conditions within the same sampling timeframe. Complete data sets for each of the triplicate tests are included in Appendix D.

A possible solution to reduce reaerosolization would be the addition of a more viscous, insoluble collection liquid on top of the typical collection liquid. Figure 3-6 displays the results for the adjusted average reaerosolized concentration as a function of concentration for this experiment in comparison to the previous experiment without oil. The percent change from without oil to with oil is also displayed for each concentration. As expected, the addition of heavy white mineral oil led to a decrease in reaerosolized particles in comparison to PSL reaerosolization under identical conditions without the oil within the same sampling timeframe. Complete particle size distributions and reaerosolized concentrations for each of the three tests are included in Appendix E.

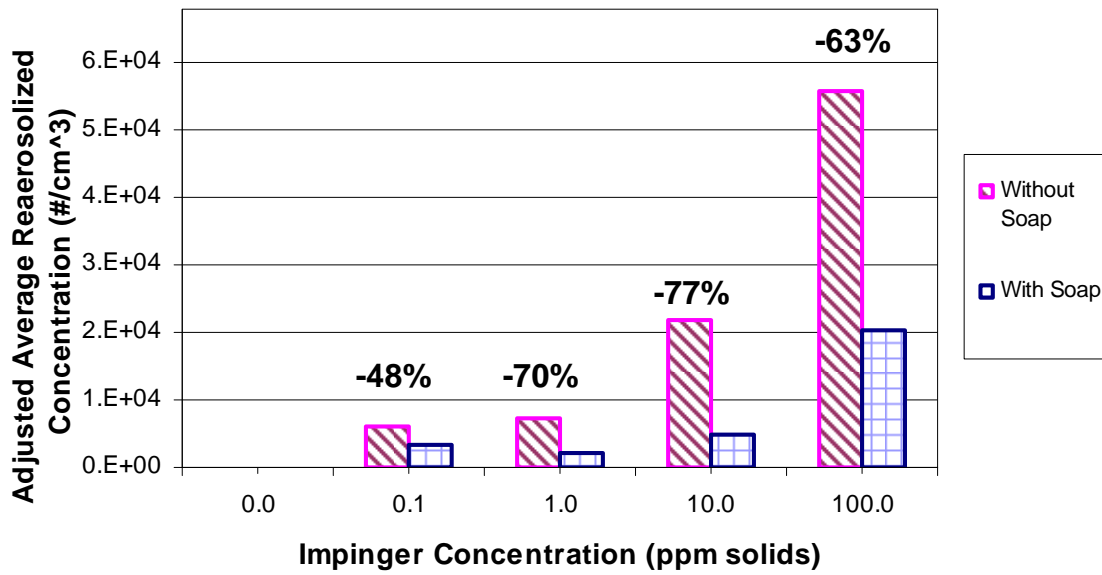


Figure 3-5. Comparison of the re-aerosolization of PSL at 12.5 Lpm with and without soap present.

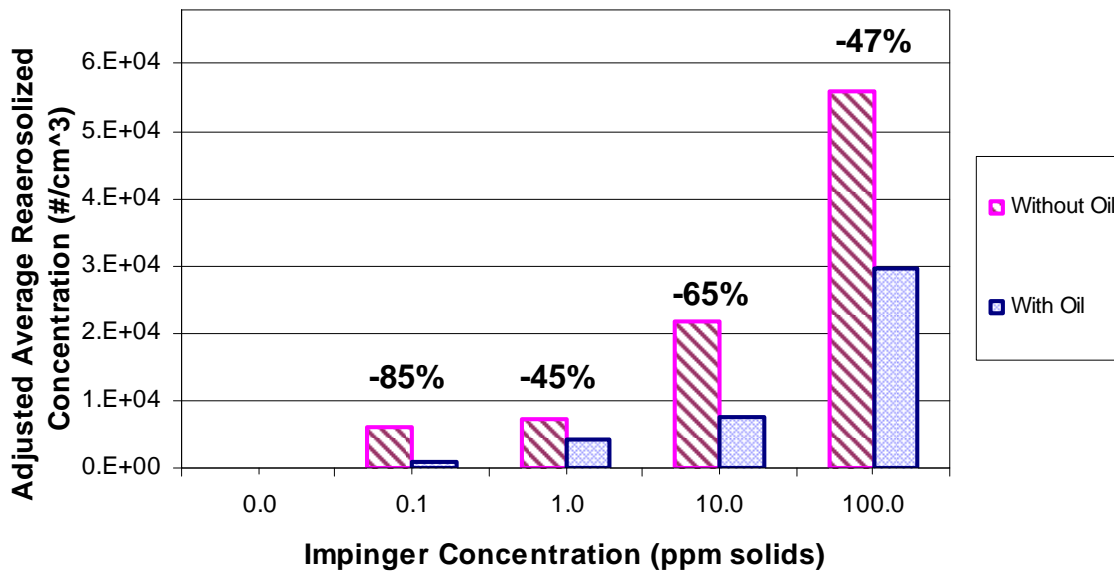


Figure 3-6. Comparison of the re-aerosolization of PSL at 12.5 Lpm with and without oil present.

The mode sizes for these tests are presented in Table 3-2. The PSL particles re-aerosolized in the test with oil were generally larger than those re-aerosolized from the pure water or water

with soap tests. As heavy white mineral oil is not as volatile as water, it is possible that a small layer of oil remained after the evaporative components of the aerosol had been evaporated. This could result in larger mode sizes.

Table 3-2. Comparison of mode sizes for PSL particles under different experimental conditions

Impinger Concentration (ppm)	Average Mode with no Additives (nm)	Average Mode with Soap (nm)	Average Mode with Oil (nm)
0.0	12	11	81
0.1	14	23	70
1.0	33	25	88
10.0	37	36	37
100.0	54	58	66

Reaerosolization with BioSampler

Reaerosolization of 30-nm polystyrene latex (PSL) particles from the BioSampler at various concentrations in the collection liquid was compared to that from the AGI-30 impinger. The flow rate was 12.5 Lpm, which is the standard operational flow rate for both the AGI-30 and the BioSampler (Ace Glass Inc. 2008; SKC, Inc. 2008). The results are shown in Figure 3-7 as adjusted average reaerosolized concentration from the three tests. Percent change from impinger to BioSampler at each concentration is also displayed. The level of reaerosolization of PSL particles from the BioSampler was significantly lower than that from the impinger. Reaerosolization from the BioSampler was generally two orders of magnitude lower than that from the impinger under identical conditions. Complete data sets for each of the three experiments are included in Appendix F.

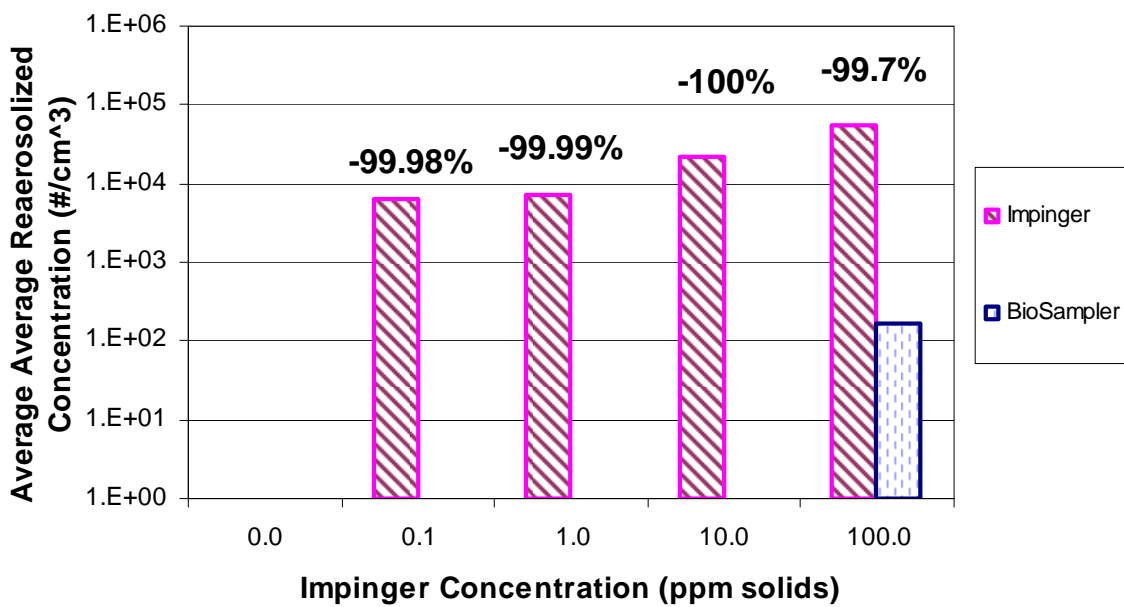


Figure 3-7. Comparison of the reaerosolization of PSL at 12.5 Lpm from impinger and BioSampler.

CHAPTER 4 DISCUSSION

Reaerosolization with PSL

Analysis of the reaerosolization of 30-nm PSL particles provided very direct documentation of viral-sized particle reaerosolization. Reaerosolization of virus particles is complicated by proteins, salts, and complex microbial interactions, all of which make it difficult to distinguish pure reaerosolized virus particles. In contrast, the results from the PSL particles in deionized water are very explicit: reaerosolization of viral-sized particles occurs and can be a mode of loss. This agrees with previous research on reaerosolization completed for particles in the bacterial size range (Grinshpun et al. 1997; Lin et al. 1997; Willeke et al. 1998).

Another benefit of conducting the experiment with PSL particles is that comparison with previous work can be made. The level of reaerosolization for virus-sized particles was compared to previous work done on reaerosolization for particles in the bacterial size range under similar conditions. Willeke et al. (1998) used 0.5- and 1.0- μm PSL particles in the AGI-30 impinger with 20 mL of deionized water, and Lin et al. (2000) used *Pseudomonas fluorescens* vegetative cells (d_a of 0.8 μm) and *Bacillus subtilis* spores (d_a of 1.0 μm) in 20 mL of deionized water. The study with PSL particles had 10^8 particles/mL in the impinger liquid and obtained peak mode concentrations of reaerosolized particles less than 60 particles/ cm^3 . The study with bacteria had 10^8 particles/mL of the respective species in the impinger liquid. The experiment with *P. fluorescens* obtained reaerosolized peak mode concentrations less than 5 particles/ cm^3 , and the experiment with *B. subtilis* obtained peak mode concentrations less than 55 particles/ cm^3 . *B. subtilis* was more hydrophobic than *P. fluorescens*, which may have caused the increased reaerosolization (Lin et al. 2000). In comparison, the present research used 10^9 particles/mL (0.1 ppm) and obtained maximum modes around 10^4 particles/ cm^3 downstream of the impinger.

A simple analysis made by “normalizing” these results for comparison shows that a 30-nm particle is much more likely to be reaerosolized than a 0.5- or 1.0- μm particle at similar number concentrations. Table 4-1 displays the comparison. Note that the simple analysis normalizes the peak mode concentration to the impinger concentration, as total reaerosolized concentrations for the previous literature were not reported. This corroborates the expectation based on Fuchs’ work (1964) that smaller particles are more likely to be reaerosolized because the energy requirements to re-entrain them are lower and their diffusivity is higher.

Table 4-1. Comparison of reaerosolization for bacteria-sized particles to that for virus-sized particles

	Current work (0.1 ppm)	Current work (100 ppm)	Willeke et al. 1998	Lin et al. 2000	Lin et al. 2000
Particle Type	PSL	PSL	PSL	<i>P. fluorescens</i>	<i>B. subtilis</i>
Particle Size (μm)	0.03	0.03	0.5, 1.0	0.8	1.0
Approximate Number Concentration in Impinger (particles/mL)	1×10^9	1×10^{12}	1×10^8	1×10^8	1×10^8
Approximate Mass Concentration in Impinger (g/mL)	1×10^{-7}	1×10^{-4}	5×10^{-5}	2×10^{-5}	5×10^{-5}
Peak Mode Concentration	8,900	120,000	60	5	55
Normalized Peak Mode Concentration	8.9×10^{-6}	1.2×10^{-7}	6.0×10^{-7}	5.0×10^{-8}	5.5×10^{-7}

While it is clear that there is more reaerosolization of the 30-nm particles for similar number concentrations, the analysis was also conducted for similar mass concentrations, assuming unit densities for the bacterial species. The 100 ppm (10^{12} particles/mL) scenario in the present research had a mass concentration similar to that in Willeke et al. 1998. Based on mass concentrations, the “normalized” reaerosolization is similar. This could potentially be explained by aggregation of the PSL particles at very high concentrations.

Although reaerosolization occurs and results in downstream total concentrations that are seemingly high, it should be noted that the amount of reaerosolization was less than 1% for all of the present work, as previously displayed in Table 3-1 in the Results section. This number cannot be compared to previous research for bacteria-sized particles because the total concentrations for those scenarios were not provided in the literature.

While the overall percentage of reaerosolization for the present work is not substantial, it is important to remember that these tests spanned only 12 minutes or less. Reaerosolization is expected to increase with sampling time (Lin et al. 1997). However, the present work indicates that reaerosolization may not be significant (<1%) over short sampling periods. Therefore, if the BAU can overcome initial physical collection limitations due to particle size, significant improvements in airborne virus sampling can be achieved.

Further analysis of the PSL reaerosolization data attempted to provide more insight into the aerosolization from the impinger. Although the impinger is not considered to be a traditional aerosol generator like the nebulizer or atomizer, it can be considered to be one due to the formation of liquid aerosols during operation. Equation 4-1 can be used to determine whether reaerosolization was volumetrically proportional to the impinger concentration (Hinds 1999).

$$V_p = V_d F_v \quad (4-1)$$

The equation states that aerosols with particle volume concentration, V_p , can be generated based on the droplet volume concentration, V_d , produced by the impinger and the volume fraction of solid material in the impinger liquid, F_v . Table 4-2 provides the volumetric analysis.

Table 4-2. Estimated droplet volume generated from impinger

Impinger Concentration (ppm)	Droplet Volume, nm ³ /cm ³			
	Experiment 1	Experiment 2	Experiment 3	Average
0.1	1.1x10 ¹⁵	1.7x10 ¹⁵	6.2x10 ¹⁴	1.1x10 ¹⁵
1.0	3.0x10 ¹⁴	2.7x10 ¹⁴	9.3x10 ¹³	2.2x10 ¹⁴
10.0	2.0x10 ¹⁴	1.8x10 ¹⁴	1.7x10 ¹⁴	1.8x10 ¹⁴
100.0	2.3x10 ¹⁴	2.5x10 ¹⁴	1.3x10 ¹⁴	2.0x10 ¹⁴

As shown, the consistency between experiments was strong. At the lowest concentration (0.1 ppm), the average droplet volume was significantly higher than the higher concentrations (1.0, 10, 100 ppm). This was likely due to the stronger effect of the residual concentration in the deionized water on the lowest concentration. The higher concentrations showed strong consistency, with approximately 2x10¹⁴ nm³/cm³ of liquid generated from the impinger at 12.5 Lpm. This confirms the hypothesis that the impinger was essentially operating as an aerosol generator and was able to consistently generating a specific droplet volume.

Reaerosolization with MS2

The results from the reaerosolization of MS2 convey the extent to which this phenomenon is a concern for bioaerosol samplers, especially in the submicrometer size range. The increase in reaerosolization as a function of flow rate is not surprising; the result is in agreement with previous work for bacteria by Grinshpun et al. (1997) as well as theoretical models based on Fuchs' (1964) work on aerosol transfer between bubbles and surrounding liquid, which indicates

that increased bubble rise velocity introduces more inertia into the system, thereby causing reaerosolization.

In contrast, the trends observed as concentration increased were unexpected. The initial increase in reaerosolization with increased concentration seems logical, but the final decrease in reaerosolization was unexpected based on the literature review. Most bioaerosols in natural systems do not generally exist in very high concentrations, and the time limitations on impingers due to the evaporative nature of the collection liquid prevent long-term sampling (Lin et al. 1997). Thus, impinger liquid concentrations as high as 10^8 PFU/mL are unlikely in most sampling scenarios. Regardless, the phenomenon is interesting, and science compels further explanation. A possible explanation was that the viruses might have been present in an aggregated state at the highest concentrations, thereby increasing the effective particle size and making reaerosolization more difficult. Another possibility was that the addition of virus stock media to the collection liquid affected the surface tension or viscosity of the liquid.

Investigation into the subject of viral aggregation provides information about the frequent state of aggregation based on viral and external factors. In aqueous scenarios, it is common for viruses to aggregate at high concentrations (Floyd and Sharp 1977; Grant 1994). External factors, such as salt concentration and pH, can also affect the level of aggregation (Floyd and Sharp 1977; Floyd and Sharp 1978). Generally, aggregation is dependent on the virus concentration, ionic strength, and pH of the liquid.

Virus concentration in an aqueous solution contributes to the level of aggregation. Aggregation occurred when Floyd and Sharp (1977) prepared reovirus and poliovirus suspensions with 1:10 dilutions in deionized water from stock solutions of 7×10^{11} and 2×10^{12} particles/mL, respectively, as physically counted by electron microscopy. Any further dilution

(1:100 or 1:1000) resulted in dispersed viruses. The concentration of viruses in natural water is typically very low, but this is not always the case in laboratory scenarios, including the concentrations used in the present work. The 10^8 PFU/mL impinger liquid concentrations possibly had total particle concentration sufficient to cause aggregation.

Literature suggests that an increase in salt concentration can significantly decrease aggregation. Floyd and Sharp (1977) found that the level of ionic strength required for their version of PBS to prevent aggregation was approximately 10 mM for poliovirus; they concluded that aggregation could occur even with appreciable salts present. As only a very small amount of PBS was added (0.01 mL 10X PBS) in the present study, there probably was not sufficient salt concentration to prevent viral aggregation.

Hydrophobic interactions between proteins from neighboring viruses also lead to the formation of aggregates. Although MS2 is labeled a hydrophilic virus because of the absence of a lipid envelope surrounding the nucleocapsid, it can still experience these hydrophobic interactions in aqueous solutions (Thomas et al. 1998; Hogan et al. 2004). In fact, Shields and Farrah (2002) found that MS2 experienced strong hydrophobic interactions during adsorption to solids, even though the absence of the lipid envelope indicates general hydrophilic behavior. The hydrophobic tendencies of the MS2 might be especially manifested at high concentrations.

The effect of pH on aggregation is based on the isoelectric point of the virus. Generally, pH values below the isoelectric point result in aggregation, while pH values above generally do not (Floyd and Sharp 1977; van Voorthuizen et al. 2001). The isoelectric point of MS2 bacteriophage is 3.9 (van Voorthuizen et al. 2001), and the pH of the impinger liquid was close to neutral. Thus, the pH in this scenario probably did not contribute to potential aggregation of viral particles as much as the other factors.

As previously discussed in the Introduction, solution viscosity and surface tension can affect the amount of liquid aerosolized during impinger operation (Hogan et al. 2005; Lin et al. 1999). Therefore, viscosity and surface tension also affect the number of particles reaerosolized. The addition of salts to a solution often results in an increase in surface tension and viscosity (Weissenborn 2006). The addition of salts required for preservation of the virus stock solution at the highest concentrations could have increased the surface tension or viscosity of the solution, thereby reducing aerosolization of the liquid.

In summary, the high concentration of MS2, the limited salt, and the tendency for MS2 to initiate hydrophobic interactions with one another indicates that viral aggregation in the impinger liquid is a plausible reason to explain the phenomenon of decreased reaerosolization at high ($>10^6$ PFU/mL) impinger liquid concentrations. Another possible reason is that the components of the virus stock solution could have affected the surface tension or viscosity of the solution and decreased reaerosolization at high ($>10^6$ PFU/mL) impinger liquid concentrations.

Although reaerosolization was observed throughout the duration of these tests, reaerosolization is expected to increase with sampling time. This is due to an increase in accumulative concentration in the impinger collection liquid as operation time increases and the amount of collection liquid decreases because of evaporation and aerosolization (Lin et al. 1997). This places yet another constraint to the use of the AGI-30 impinger for airborne virus sampling. The likelihood of reaching very high impinger concentrations ($>10^5$ PFU/mL) is also unlikely before all of the 20 mL of initial collection liquid evaporates. Thus, reaerosolization of MS2 may not be as significant a contributing factor in poor airborne virus sampling as the effect due to virus particle size.

Effect of Surface Tension and Viscosity on Reaerosolization

Although the surfactant did not directly result in an increase of reaerosolized particles as predicted by the literature review, there was more bubbling within the impinger collection liquid. One possible reason the observed increase in bubbling did not translate to an increase in reaerosolized particles was that the presence of thin layers of soap film formed prevented the transfer of particles. The thin layers of soap moved through the impinger vessel towards the exhaust, similar to the movement of soap through a bubble meter. These thin layers of soap film would trap reaerosolized particles.

Although the impinger cannot be successfully operated with only higher viscosity liquids as the collection liquid (Willeke et al. 1998), the addition of an insoluble, more viscous layer was thought to potentially be able to suppress bubbling. Unexpectedly, the high energy and turbulence associated with the traditional impinger resulted in the emulsification of the heavy white mineral oil shortly after impinger operation ensued. Although the addition of the more viscous layer might have decreased reaerosolization, the background concentration increased significantly at higher particle sizes and resulted in a bimodal distribution. This trend is displayed in Figure 4-1. The larger distribution is likely due to the aerosolization of the non-volatile oil, which could not be dried by the diffusion dryer prior to entering the SMPS for measurement. However, this distribution is completely overwhelmed when high concentrations of PSL particles are present, as displayed in Appendix D.

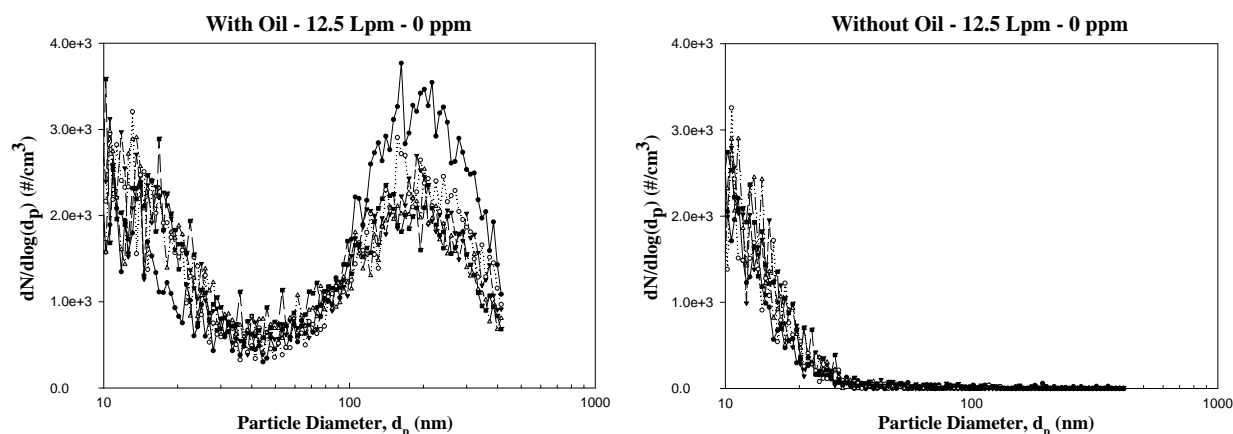


Figure 4-1. Baseline at 12.5 Lpm from impinger with oil and without oil present.

Reaerosolization with BioSampler

The significant decrease in reaerosolization for 30-nm PSL particles from a BioSampler in comparison to an AGI-30 impinger corroborated past work done on the subject for bacterial size particles. Willeke et al. (1998) used 0.5- and 1.0 μm PSL particles in 20 mL of deionized water in both the AGI-30 impinger and the BioSampler to compare reaerosolization from the two methods of liquid impingement. The BioSampler performed significantly better, with a peak mode concentration of reaerosolized particles lower than 5 particles/ cm^3 . In comparison, the AGI-30 had a peak mode concentration nearly 60 particles/ cm^3 . Similarly, Lin et al. (2000) used *Pseudomonas fluorescens* vegetative cells (d_a of 0.8 μm) and *Bacillus subtilis* spores (d_a of 1.0 μm) in 20 mL of deionized water to compare reaerosolization between the BioSampler and the AGI-30. For both bacterial cells, the peak mode concentration from the BioSampler was about 20% of that from the AGI-30. Table 4-3 displays results from the current work as well as the previous work using bacteria-sized particles.

The improved performance in reduced reaerosolization by the BioSampler is attributed to the swirling motion in which the air travels, as shown in Figure 2-2. The entrance of the air in

the AGI-30 is perpendicular to the base of the collection vessel, which allows for much more bubbling and aerosolization of the collection liquid (Willeke et al. 1998).

Table 4-3. Comparison of present work to past research on reaerosolization from AGI-30 Impinger and BioSampler

	Current work	Willeke et al. 1998	Lin et al. 2000	Lin et al. 2000
Particle Type	PSL	PSL	<i>P. fluorescens</i>	<i>B. subtilis</i>
Particle Size (µm)	0.03	1.0	0.8	1.0
Impinger Concentration (particles/mL)	1x10 ¹²	1x10 ⁸	1x10 ⁸	1x10 ⁸
Peak Mode Concentration from AGI-30 (particles/cm ³)	120,000	60	5	55
Peak Mode Concentration from BioSampler (particles/cm ³)	1,600	4	1	10
Ratio of Peak Mode Concentrations from BioSampler to AGI-30	0.013	0.067	0.200	0.182

Although Hogan et al. (2005) noted that even the BioSampler cannot exceed 10% physical collection in the 20–300 nm size range, the use of a BioSampler minimizes reaerosolization of virus-sized particles. Thus the low physical collection efficiency for virus particles seen in the BioSampler is likely due to insufficient initial physical collection rather than reaerosolization. This is likely due to the ability of nanosized particles to tolerate the centrifugal collection motion and escape collection. Particles greater than 0.5 µm are collected well (>80% collection efficiency) with the BioSampler (Willeke et al. 1998). However, Willeke et al. (1998) confirmed that physical collection efficiency of 0.3-µm particles was higher for the AGI-30 than for the

BioSampler, indicating that the AGI-30 impinger has better physical collection of the smaller particles. Thus, the low physical collection of the AGI-30 impinger shown by Hogan et al. (2005) can apparently be attributed to both poor physical collection and higher amounts of reaerosolization. Based on this information, the use of the BAU in conjunction with the BioSampler should significantly improve airborne virus sampling by increasing physical collection and minimizing reaerosolization issues, respectively.

CHAPTER 5 CONCLUSION

Reaerosolization occurs for virus-sized particles and is more of a concern for viral-sized particles than for bacterial-sized particles, as demonstrated explicitly by the use of 30-nm PSL particles. Reaerosolization increases as flow rate increases, due to the additional energy introduced to the system. However, increased concentration does not necessarily lead to an increase in reaerosolization for virus particles. Rather, reaerosolization increases as concentration increases until it reaches a concentration of approximately 10^6 PFU/mL, at which point reaerosolization begins to decrease. Although such high concentrations are unlikely due to typical airborne virus concentrations and liquid impingement sampling limitations, science compels further exploration. The observed phenomenon likely results from the aggregation of viral particles or the increase of surface tension or viscosity at high concentrations. Further investigation into the effects of surface tension and viscosity on reaerosolization indicates that both properties affect aerosolization from the impinger. While the addition of soap as a surfactant increases bubbling, it decreases reaerosolization over the time frame studied, possibly due to the formation of thin soap films that prevents reaerosolization. The addition of heavy white mineral oil to provide a viscous surface decreases reaerosolization. Further work to verify the effects of the soap and oil on virus viability needs to be conducted.

In summary, airborne virus sampling is limited by primary particle size, hydrophobicity, and reaerosolization. While hydrophobicity is not specifically addressed in this work, sampling limitations caused by particle size and reaerosolization are addressed in this research. The use of the Bioaerosol Amplification Unit has the potential to minimize the issue related to size by amplifying the particle size. Reaerosolization of virus-sized particles does not appear to be a

significant mode of loss during 15 minutes of sampling for most typical sampling scenarios, and it can be minimized by preventing high impinger concentrations and using the BioSampler.

Recommendations to improve airborne virus sampling based on the present work include the use of the BAU in conjunction with a BioSampler. Based on previous work, it is recommended that sampling last no more than approximately 30 minutes. Although much more work is required to drastically improve airborne virus sampling, the current work provides a solid base for the future of the field by characterizing reaerosolization.

APPENDIX A

BIOAEROSOL AMPLIFICATION UNIT INFORMATION

The Bioaerosol Amplification Unit (BAU) serves as the main motivation for the entire project. Reaerosolization needed to be characterized to understand how it will affect the BAU; because of this, reaerosolization therefore served as the primary focus this paper. However, significant work has also been completed on the design, construction, and preliminary evaluation of the BAU and is provided here to give more details about the motivation and future of the project.

Bioaerosol Amplification Unit Design

A prototype of the aforementioned Bioaerosol Amplification Unit was developed with the intention of its evaluation in subsequent studies. The prototype design consists of two parallel aluminum square tubes, 1 inch in diameter and 3.01 ft in length. The length of the tubes was determined by ensuring that sufficient cooling occurred to decrease a 12-Lpm air stream from 40°C to 25°C if the condensation tube surface was 10°C. The saturator tube and the condenser tube are heated and cooled, respectively, using twelve 8-W Peltier thermoelectric heat pumps. The base temperature is monitored by thermocouples in both the hot and cold bases, and the tube surface is considered to be equal to the base temperature. By varying the amount of voltage and current supplied to the Peltier array, the temperature differences between the humidification and condensation chambers can be controlled.

A schematic diagram of the first prototype BAU is shown in Figure A-1. The air sample enters the saturation chamber, where water vapor is transferred to the air stream from the water chamber via a porous hydrophilic evaporative material produced by Porex, Inc. The saturation chamber is designed to achieve a relative humidity of approximately 90% to sufficiently prepare it for the condensation chamber. Humidity is measured before and after the saturation chamber

to ensure this goal was achieved. As the air sample passes into the condensation chamber, the temperature drop decreases the vapor pressure and induces supersaturation conditions. Once supersaturation is achieved, the water vapor preferentially condenses onto the bioaerosols, which serve as condensation nuclei. The particles are subsequently amplified system and can be collected more effectively by the preferred bioaerosol sampling method.

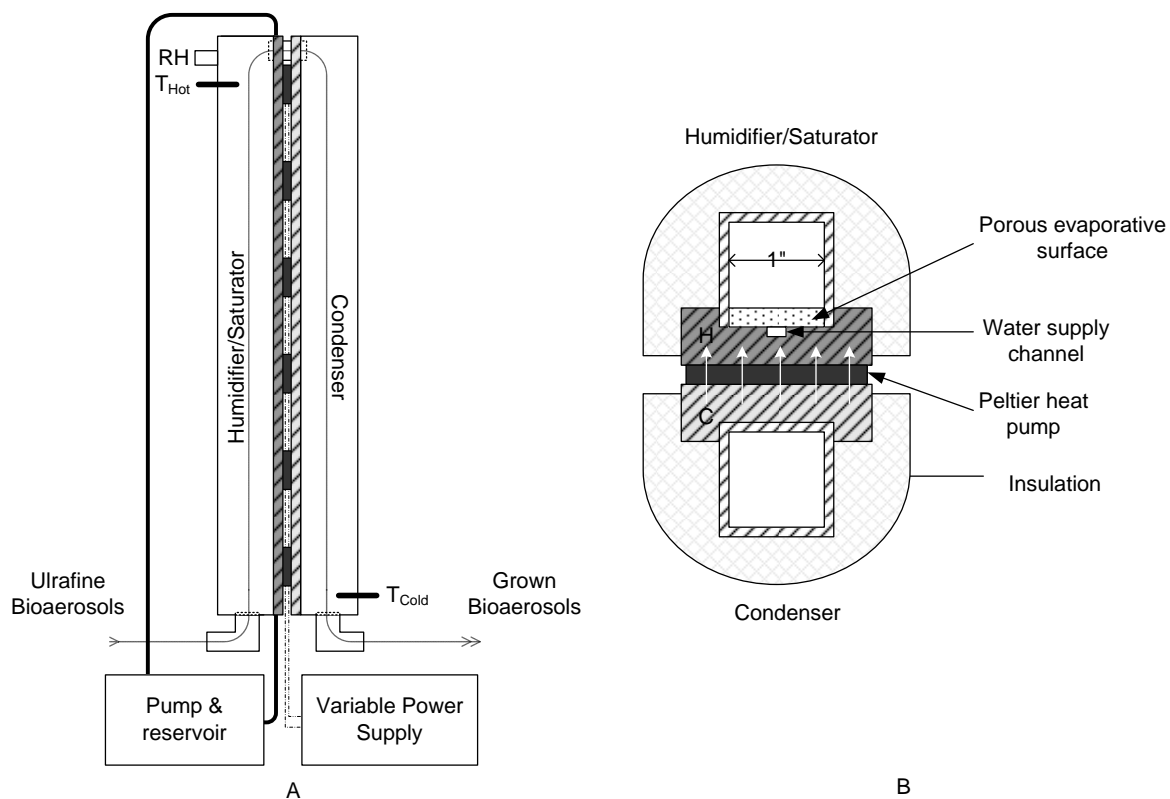


Figure A-1. BAU prototype schematic. A) Overview of system. B) Cross-sectional view of humidification and condensation chambers.

Experimental Methodology

Three experiments will be conducted to evaluate the BAU. The tests will evaluate the success of the BAU and provide insight into how this novel unit can be applied for future research and public health uses. Table A-1 summarizes the experimental conditions and the corresponding purpose for each test.

Table A-1. Summary of tests and corresponding purpose to evaluate BAU

Test No.	Test Name	Purpose
1	Inert Particle Amplification	Confirm successful design and construction
2	Physical Collection Challenge	Confirm improved physical collection efficiency
3	Viable Collection Challenge	Evaluate airborne virus sampling

Inert Particle Amplification

Firstly, the amplification of inert aerosols in the BAU will be evaluated. PSL and sodium chloride aerosols will be used as challenge aerosols to confirm that the design and construction of the system was properly completed. By using inert particles, the viability issue associated with bioaerosols will be eliminated. The experimental setup is displayed in Figure A-2.

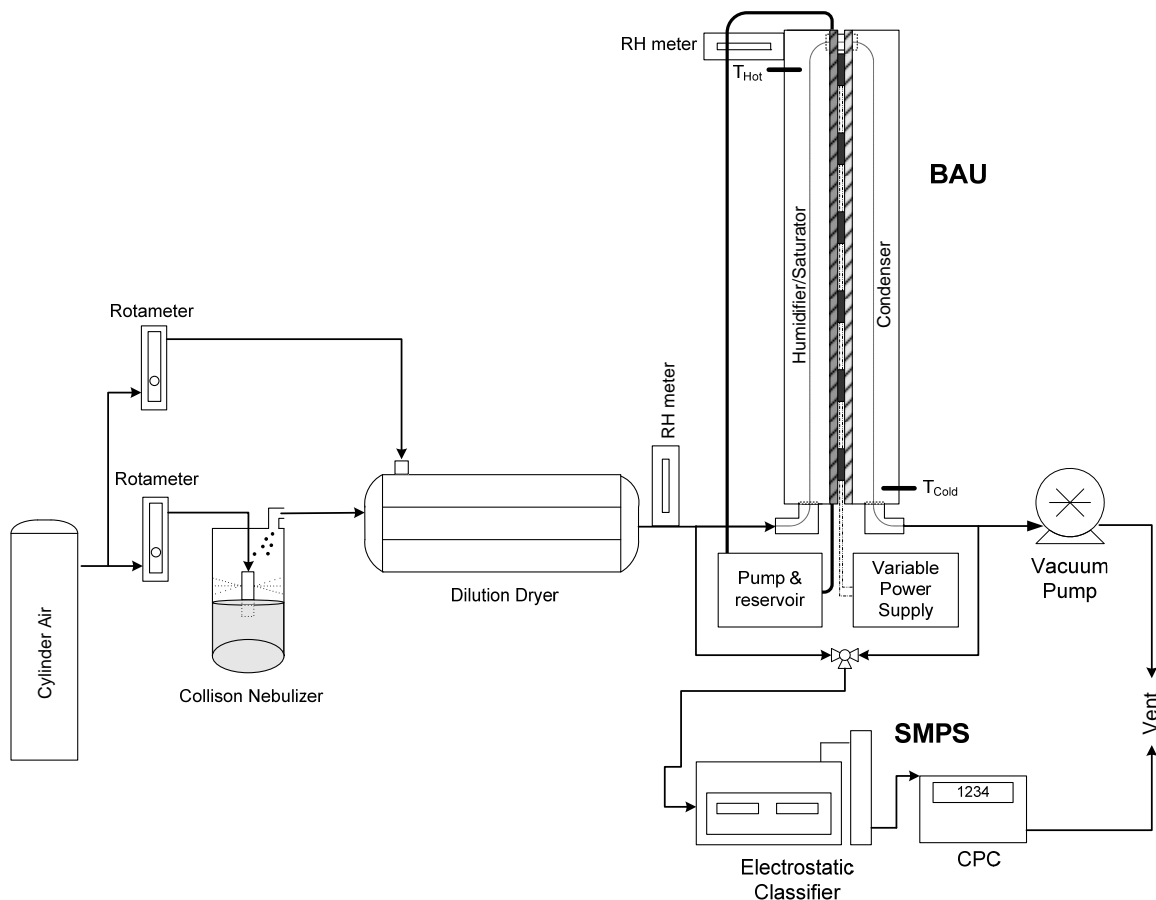


Figure A-2. Experimental setup for inert particle amplification.

A six-jet Collison nebulizer (Model # CN25, BGI, Inc.) with a flow rate of 5.5 Lpm will generate the inert aerosols that will serve as the challenge aerosols. The aerosol sizes will be measured before and after the BAU by the scanning mobility particle sizer (SMPS, Model 3936, Shoreview, Minn., USA) to determine the degree of amplification. Given that the limits of the SMPS configuration are in the submicron range, a different particle sizer may be required if the particles grow to supermicron sizes. A control will be run to measure particle sizes with the BAU in line but not in operation.

Three PSL particle sizes will be used to evaluate the success of the system at multiple sizes: 30-nm, 64-nm, and 100-nm particles. The sodium chloride aerosols will also challenge the system at similar sizes. The sodium chloride aerosols will be generated by nebulizing a sodium chloride solution. The droplets of nebulized solution will be dried in the diffusion dryer and will form sodium chloride aerosols. Equation A-1 will be used to estimate the concentration of sodium chloride required in solution to produce the desired aerosol size (Hinds 1999).

$$d_p = d_d (F_v)^{1/3} \quad (\text{A-1})$$

The equation states that aerosols with diameter, d_p , can be generated based on the droplet diameter, d_d , produced by the nebulizer and the volume fraction of solid material in solution, F_v . The six-jet Collison nebulizer operating at a flow rate of 5.5 Lpm will generate an aerosol approximately 2.1–3 μm in size (Hinds 1999). For example, to obtain a sodium chloride aerosol approximately 350 nm in size, 3.5 g/L of sodium chloride will be dissolved in the nebulizer solution to achieve an F_v of approximately 0.0035.

The Inert Particle Amplification test will determine the amplification capability of the BAU. Since the PSL particles are hydrophobic and the NaCl aerosols are hydrophilic, the experiment will also provide insight into the effect of hydrophobicity on the process.

Physical Collection Challenge

Once the amplification process has been deemed successful in the Inert Particle Amplification test, the next test will evaluate the improved physical collection efficiency of the BAU. Figure A-3 displays the experimental setup for the Physical Collection Challenge. The same challenge aerosols (PSL and sodium chloride) will be used, but an impinger will sample the aerosols downstream of the BAU, and physical collection efficiency will be determined.

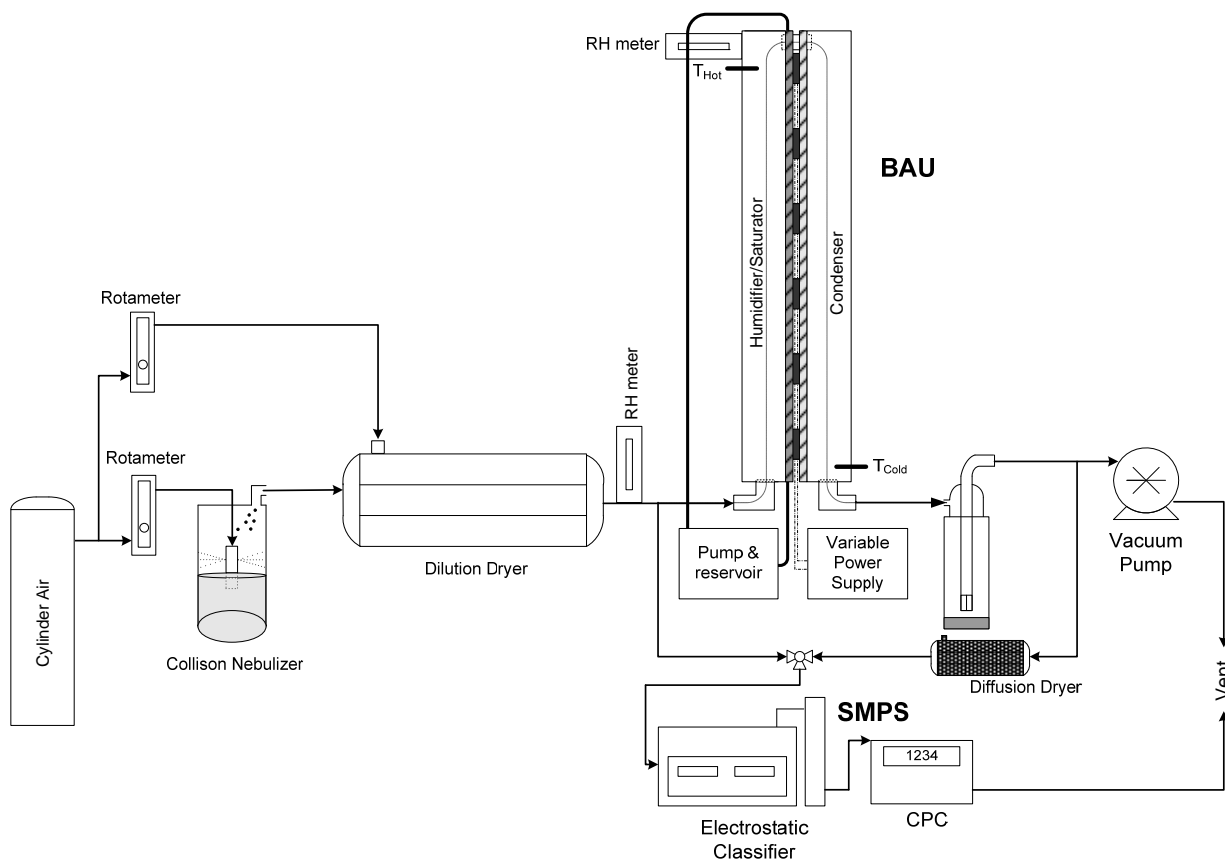


Figure A-3. Experimental setup for physical collection efficiency testing.

For the PSL particles, physical collection efficiency will be determined by using the SMPS to measure particle concentration upstream of the BAU, C_{UP} , and downstream of the impinger,

C_{DOWN} . The physical collection efficiency for the PSL particles, E_C , will be calculated with Equation A-2 (Willeke et al. 1998).

$$E_C = \frac{C_{UP} - C_{DOWN}}{C_{UP}} = 1 - \frac{C_{DOWN}}{C_{UP}} \quad (A-2)$$

The physical collection efficiency of the sodium chloride aerosols will be determined by using an ion chromatograph (ICS-1500, Dionex Corporation) to measure the concentration of sodium in the impinger collection liquid.

The control for each test aerosol will follow the same experimental procedure but will not utilize the BAU, such that the flow will still go through the unit although it will not be in operation. The improved physical collection efficiency of as a result of the BAU will be evaluated by comparing the control results with the aerosol challenge results

Viable Collection Challenge

Once improved physical collection efficiency is confirmed, the next step will be to use bioaerosols as the challenge aerosol and introduce the variability associated with microorganisms into the system. Using the same experimental setup as the physical collection efficiency test shown in Figure A-3, MS2 virus (*Escherichia coli* bacteriophage ATCC® 15597-B1™) will serve as the challenge aerosol viruses. Physical collection efficiency will be determined by SMPS measurements of the inlet and outlet streams (Equation A-2), and viral enumeration of the impinger collection liquid will determine viable collection efficiency. The improved viable collection efficiency of the BAU will be evaluated as collection enrichment. Collection enrichment, CE , will be calculated with Equation A-3, which compares the viable collection of the BAU (PFU_{BAU}) to that of the control ($PFU_{Control}$).

$$CE = \frac{PFU_{BAU}}{PFU_{Control}} \quad (A-3)$$

MS2 is a bacteriophage that is often used as a surrogate pathogen for airborne virus testing and is an appropriate choice for use as a surrogate human pathogenic virus (Aranha–Creado and Brandwein 1999). The size of the MS2 bacteriophage at 27.5 nm (Golmohammadi et al. 1993) is a suitable challenge for the BAU because typical collection efficiencies in the impinger at this particle size are less than 10% (Hogan et al. 2005). The virus stock suspension is obtained by combining freeze-dried MS2 bacteriophage with approximately 10 mL of filtered deionized water to reach a stock concentration of 10^8 – 10^9 PFU/mL. Approximately 0.1–0.2 mL of the virus stock suspension will be added to 50 mL of sterile deionized water, which has an approximate concentration of 10^5 – 10^6 PFU/mL. This solution will be placed in the Collison nebulizer and will be used to generate the airborne virus for the experiments.

The MS2 medium for the viral enumeration analysis will be prepared by gently mixing 1.0 g tryptone, 0.1 g yeast extract, 0.1 g D-glucose, 0.8 g NaCl, and 0.022 g CaCl_2 into 100 mL of distilled water in a 250-mL flask. The medium will be autoclaved at 121°C for 30 minutes to ensure sterility. The MS2 agar will be prepared by gently mixing 3.0 g tryptone, 0.3 g yeast extract, 0.3 g glucose, 2.4 g NaCl, 0.066 g CaCl_2 , and 0.3 g of Bacto-agar into 300 mL of distilled water in a 500-mL flask. The mixed agar is autoclaved at 121°C for 30 minutes to achieve sterility.

Preliminary Results

Although only recently initiated, preliminary results from the evaluation of the BAU are displayed in Table A-2, which displays viable collection efficiency. Samples were collected in an AGI-30 impinger operated at 12.5 Lpm. When the BAU was in operation, the temperature difference was 20°C between the saturator tube surface (approximately 40°C) and the condenser tube surface (approximately 20°C). Residence time was approximately 2.8 seconds in each

segment. For the nebulizer solution, 0.2 mL of MS2 virus stock (1×10^{10} PFU/mL) was added to 100 mL of sterile deionized water. Therefore, the nebulizer solution was approximately 2×10^7 PFU/mL. Relative humidity of the system at the time is unknown due to technical difficulties with the RH meters.

Table A-2. Preliminary results from viral aerosol sampling using BAU

Sampling time (30 min)	Bioaerosol Amplification Unit Status	Concentration (PFU)	Mean Concentration (PFU)
Control	Off	76,000	78,000
Control	Off	80,000	
Experiment	On	166,000	146,000
Experiment	On	131,000	
Experiment	On	143,000	

The preliminary results from the airborne MS2 virus sampling with the BAU in operation are promising, nearly doubling the viable collection efficiency with an 87% increase. Future experiments will continue to address all phases of the evaluation process explained previously.

APPENDIX B REAEROSOLIZATION WITH PSL DATA SETS

Test 1: 03/07/2008a

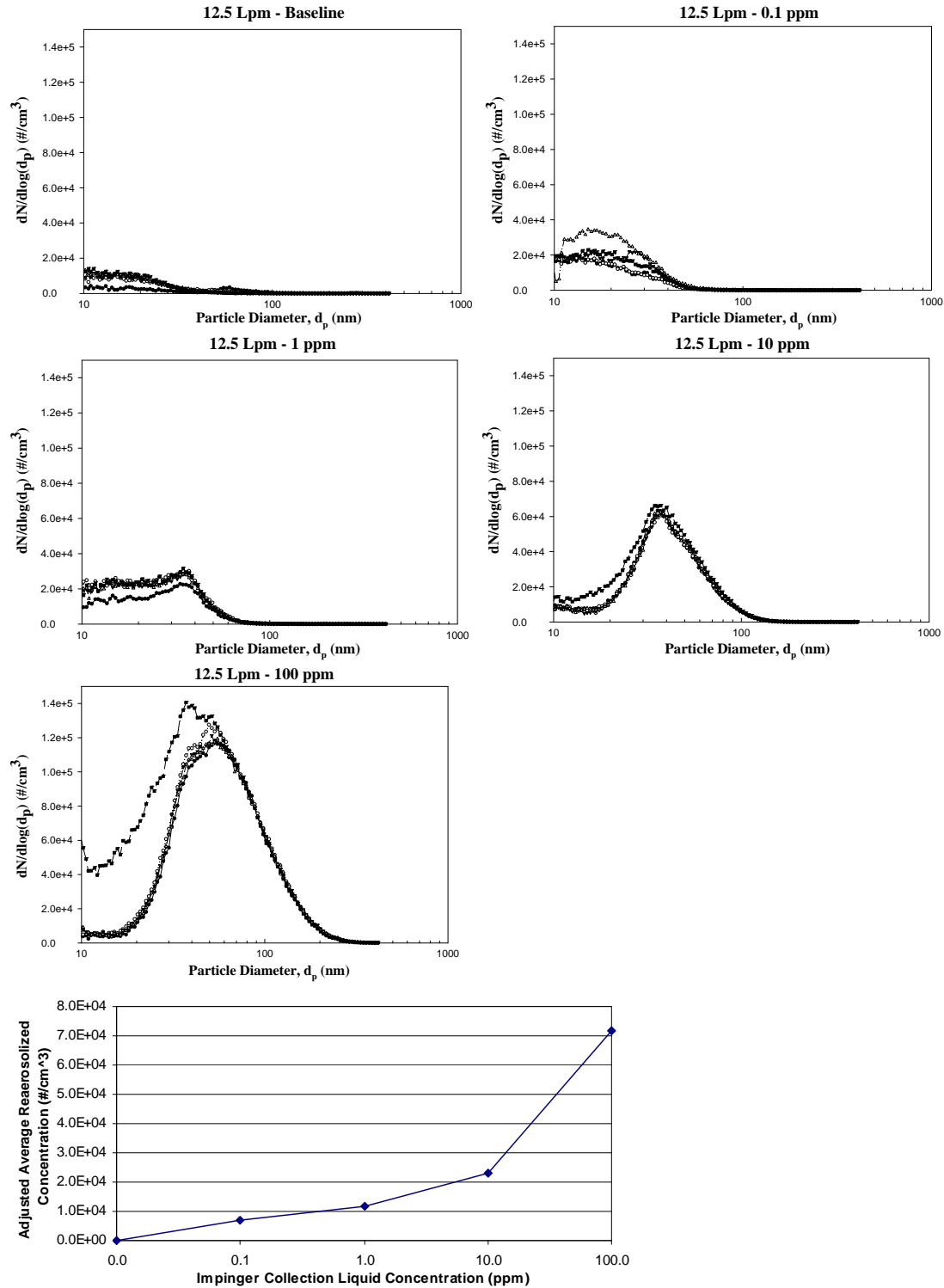


Figure B-1. Size distribution and average concentration of PSL at 12.5 Lpm (03/07/08a).

Test 2: 03/07/2008b

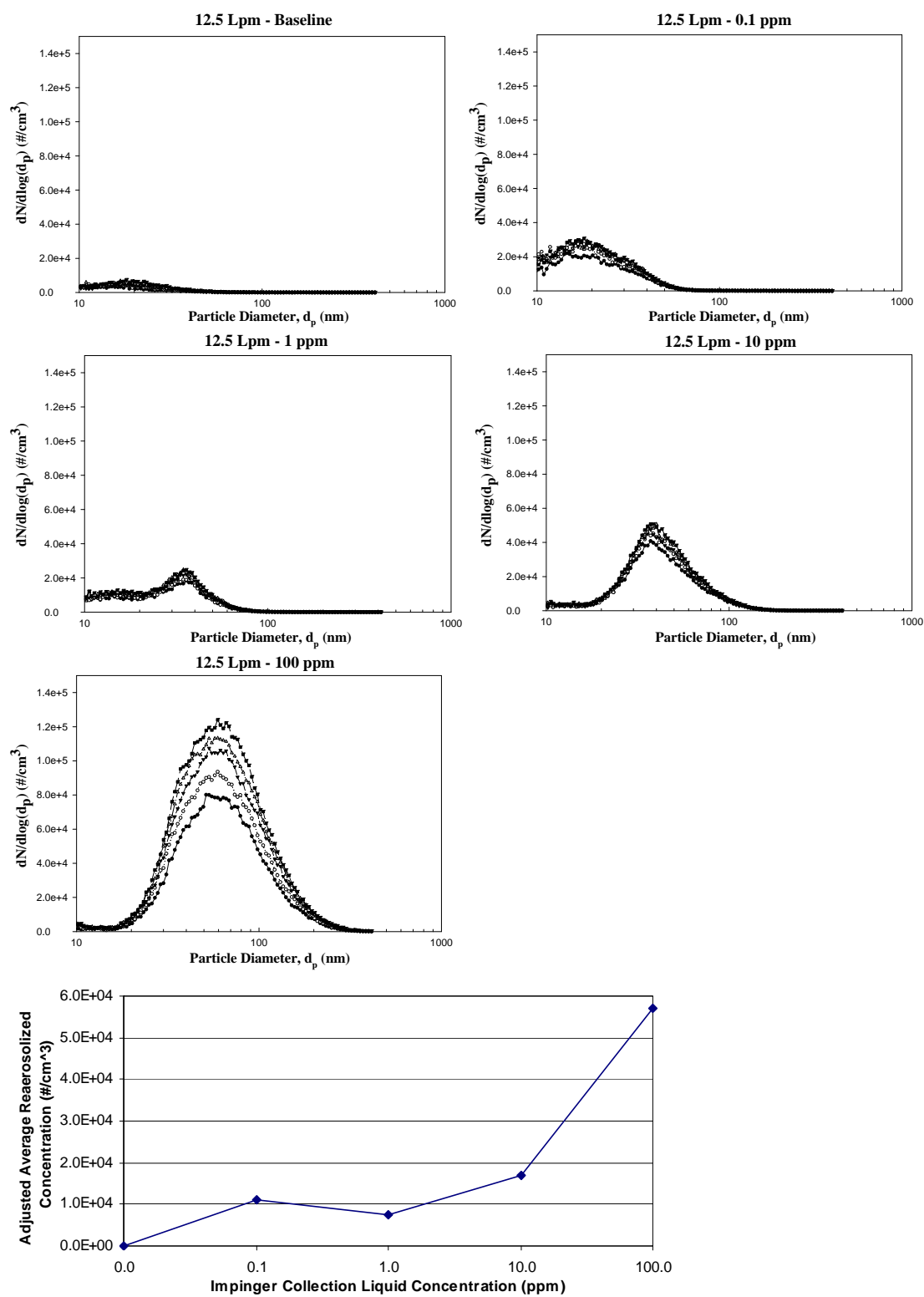


Figure B-2. Size distribution and average concentration of PSL at 12.5 Lpm (03/07/08b).

Test 3: 04/02/2008

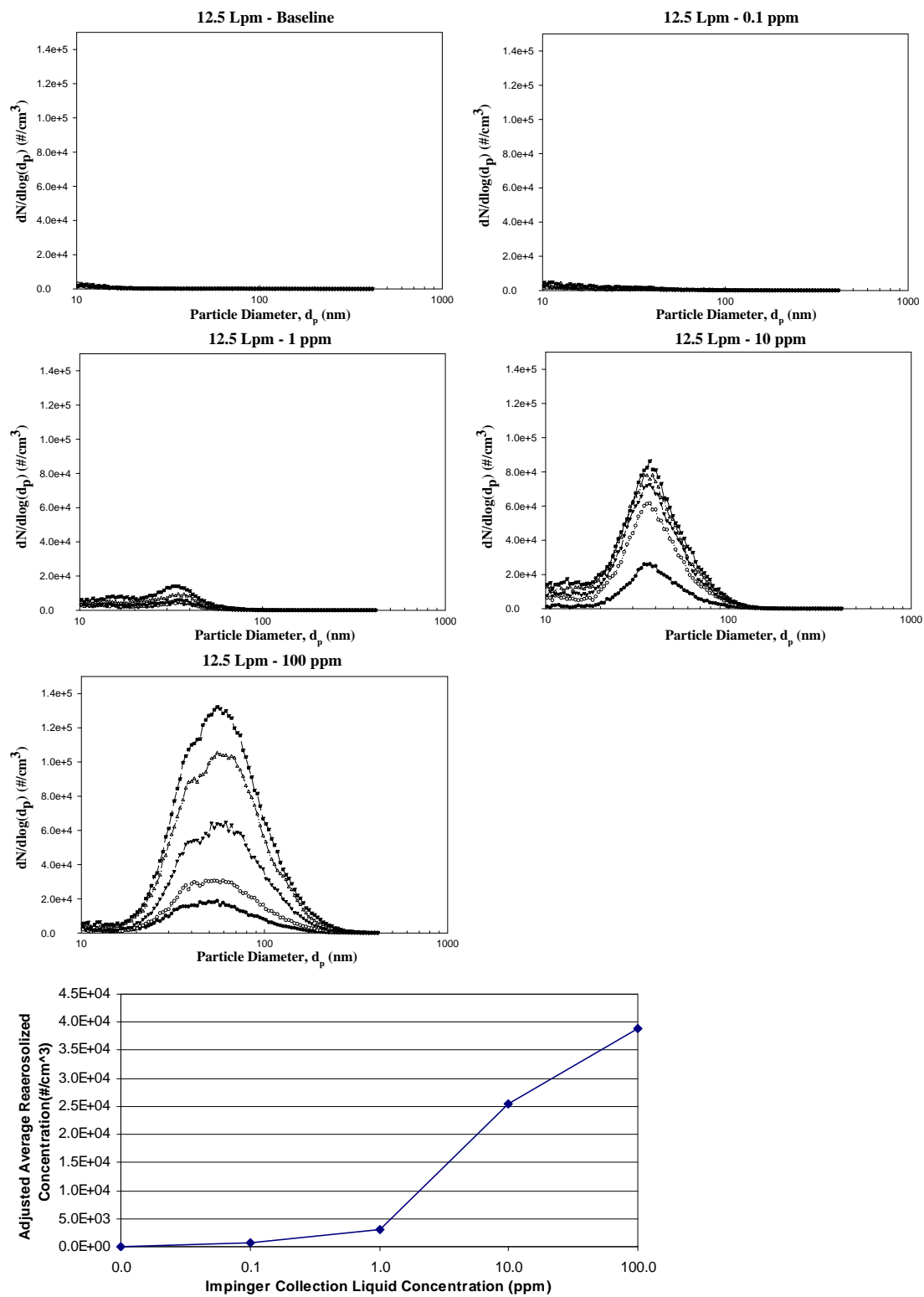


Figure B-3. Size distribution and average concentration of PSL at 12.5 Lpm (04/02/08).

APPENDIX C REAEROSOLIZATION WITH MS2 DATA SETS

Flow Rate: 3 Lpm

Test 1: 03/15/2007a

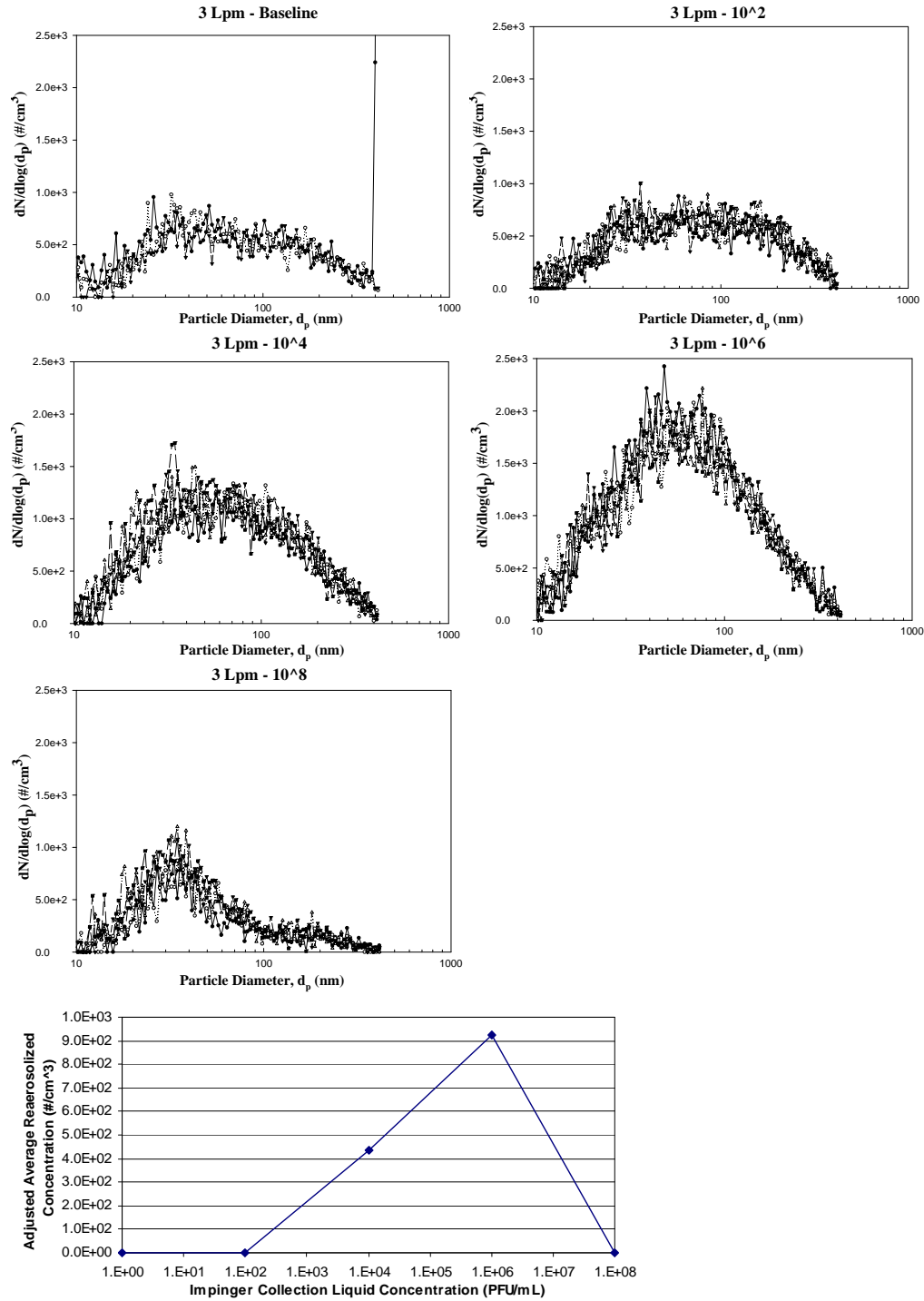


Figure C-1. Size distribution and adjusted avg concentration of MS2 at 3 Lpm (03/15/07a).

Test 2: 03/15/2007b

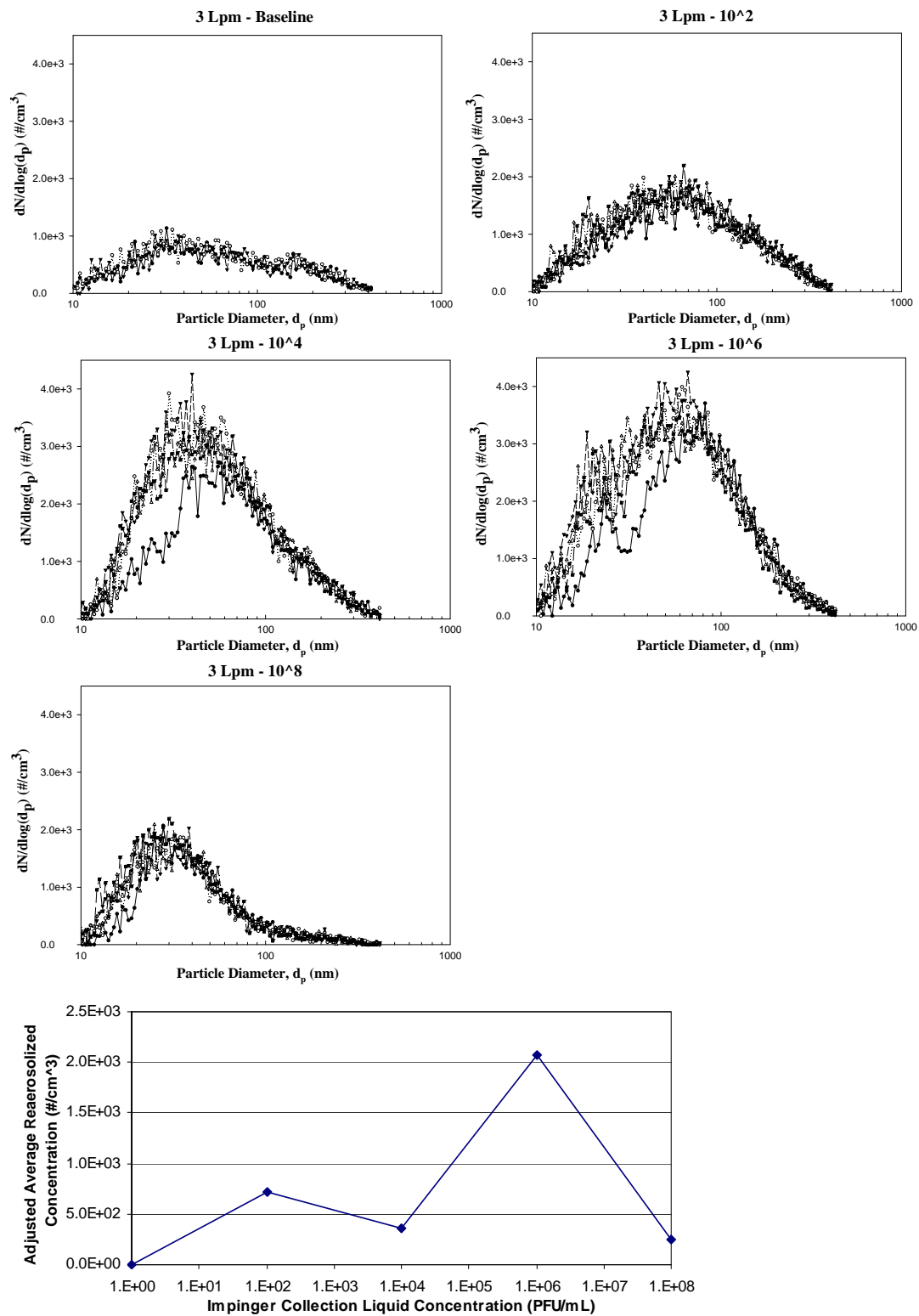


Figure C-2. Size distribution and adjusted avg concentration of MS2 at 3 Lpm (03/15/07b).

Summary of 3 Lpm

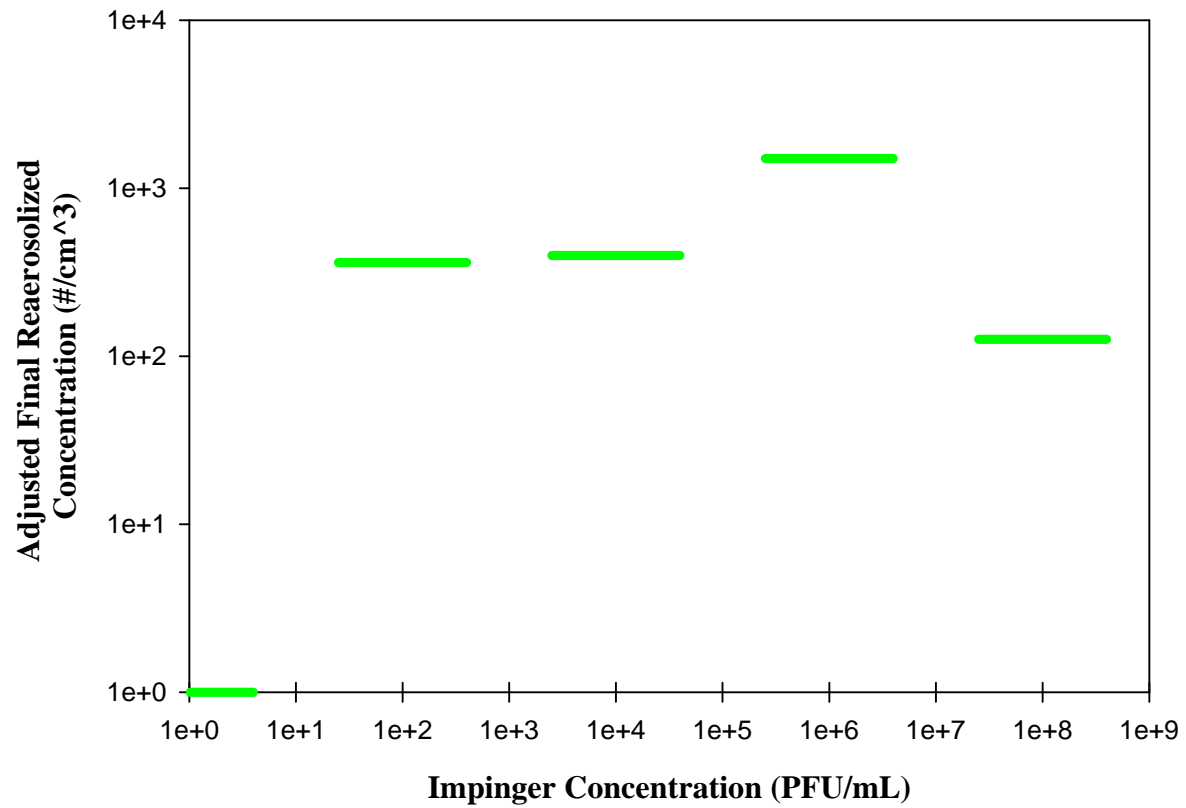


Figure C-3. Summary of adjusted average concentration of MS2 at 3 Lpm.

Flow Rate: 6 Lpm

Test 1: 03/15/2007

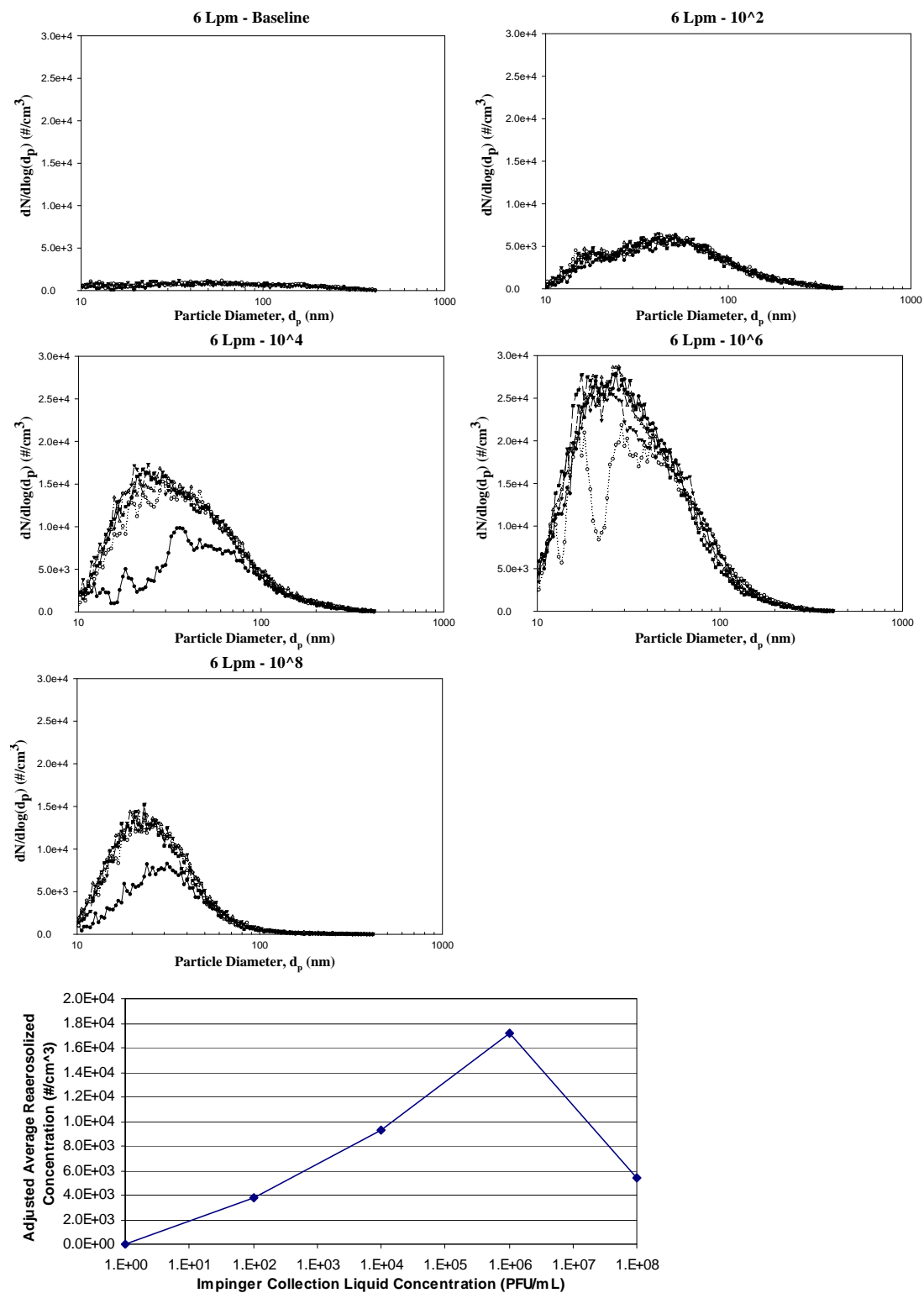


Figure C-4. Size distribution and adjusted avg concentration of MS2 at 6 Lpm (03/15/07).

Summary of 6 Lpm

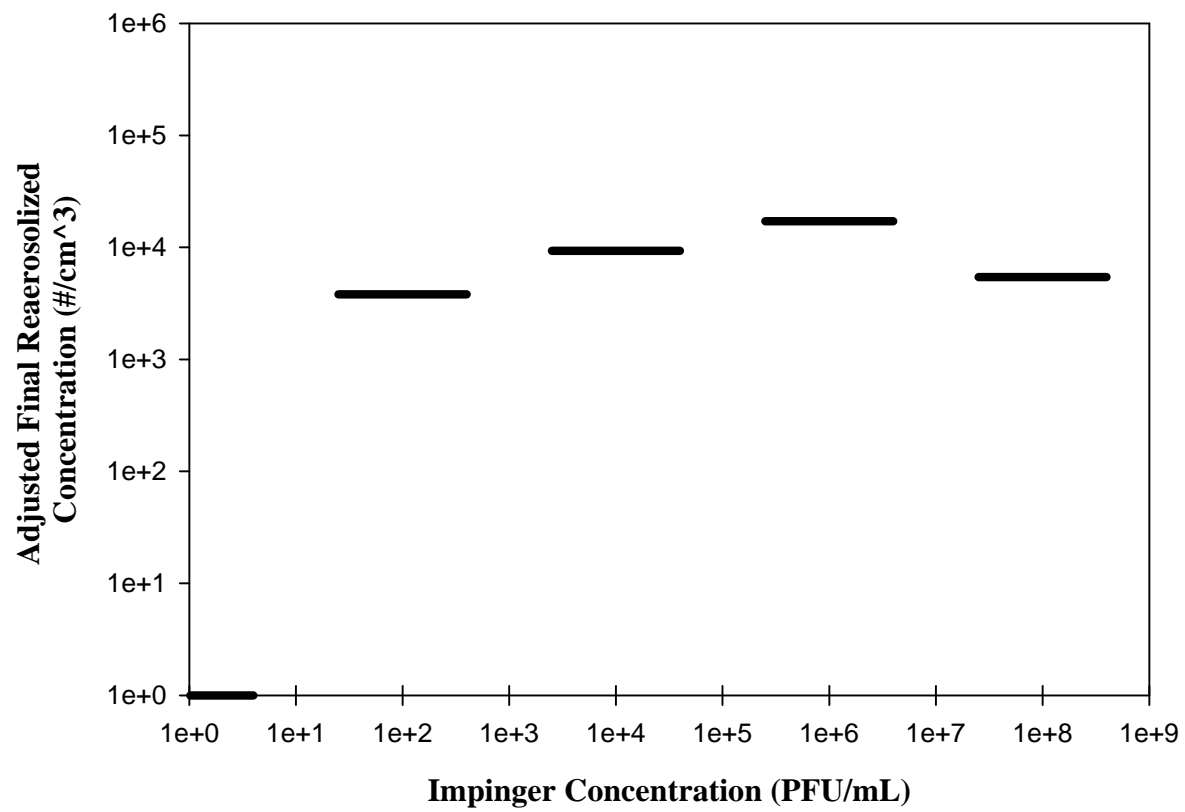


Figure C-5. Summary of adjusted average concentration of MS2 at 6 Lpm.

Flow Rate: 9 Lpm

Test 1: 02/14/2008a

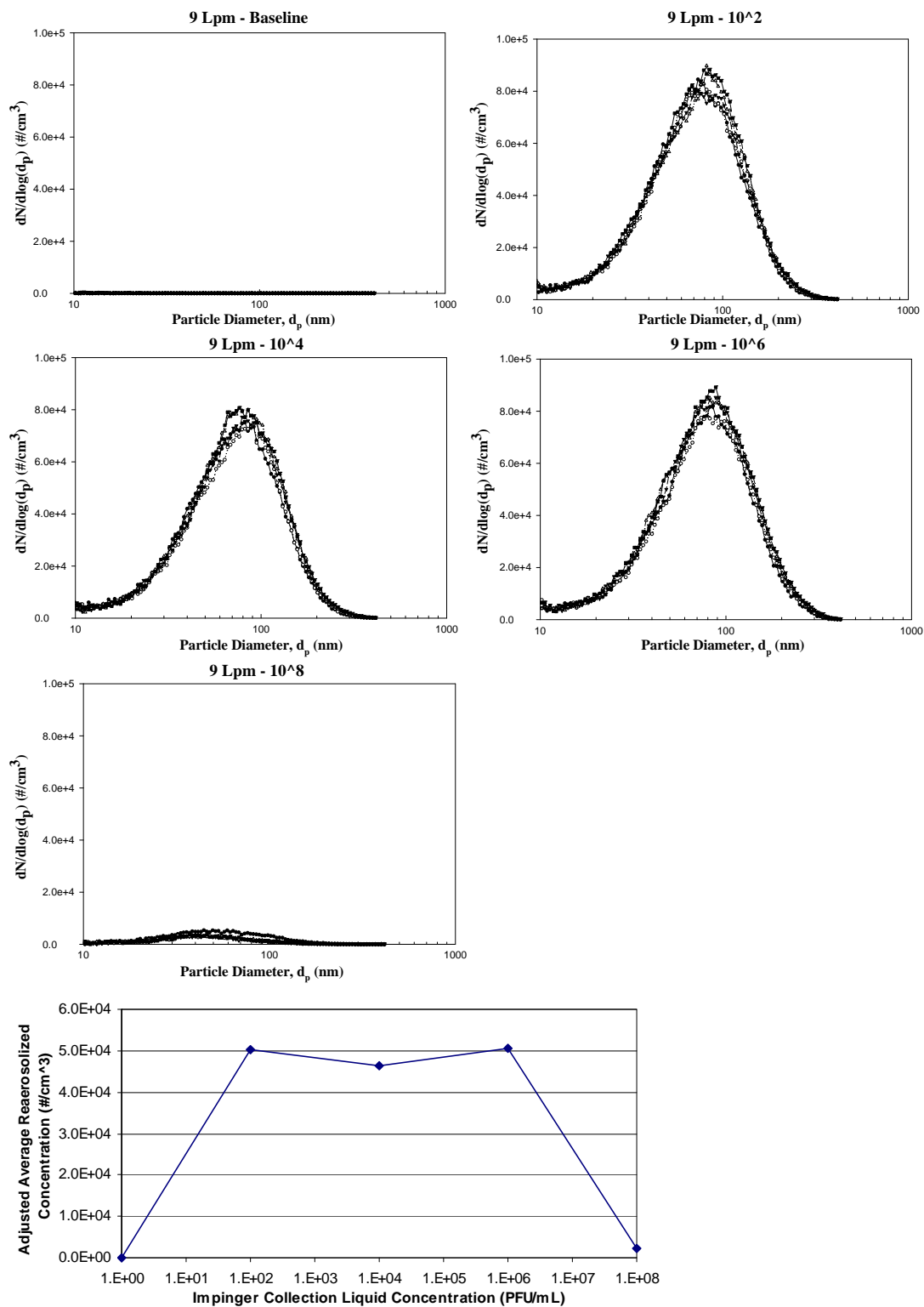


Figure C-6. Size distribution and adjusted avg concentration of MS2 at 9 Lpm (02/14/08a).

Test 2: 02/14/2008b

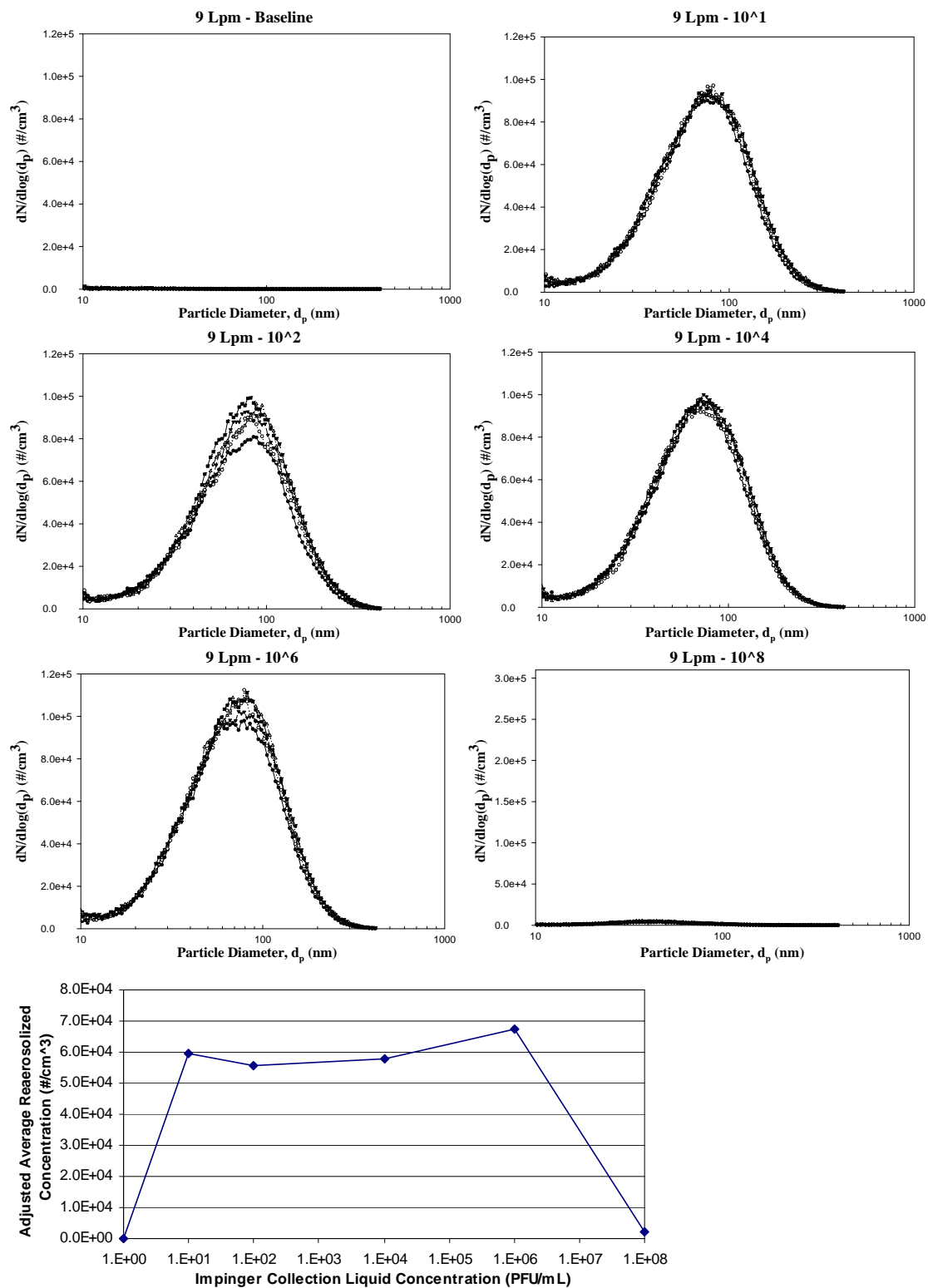


Figure C-7. Size distribution and adjusted avg concentration of MS2 at 9 Lpm (02/14/08b).

Test 3: 03/15/2007

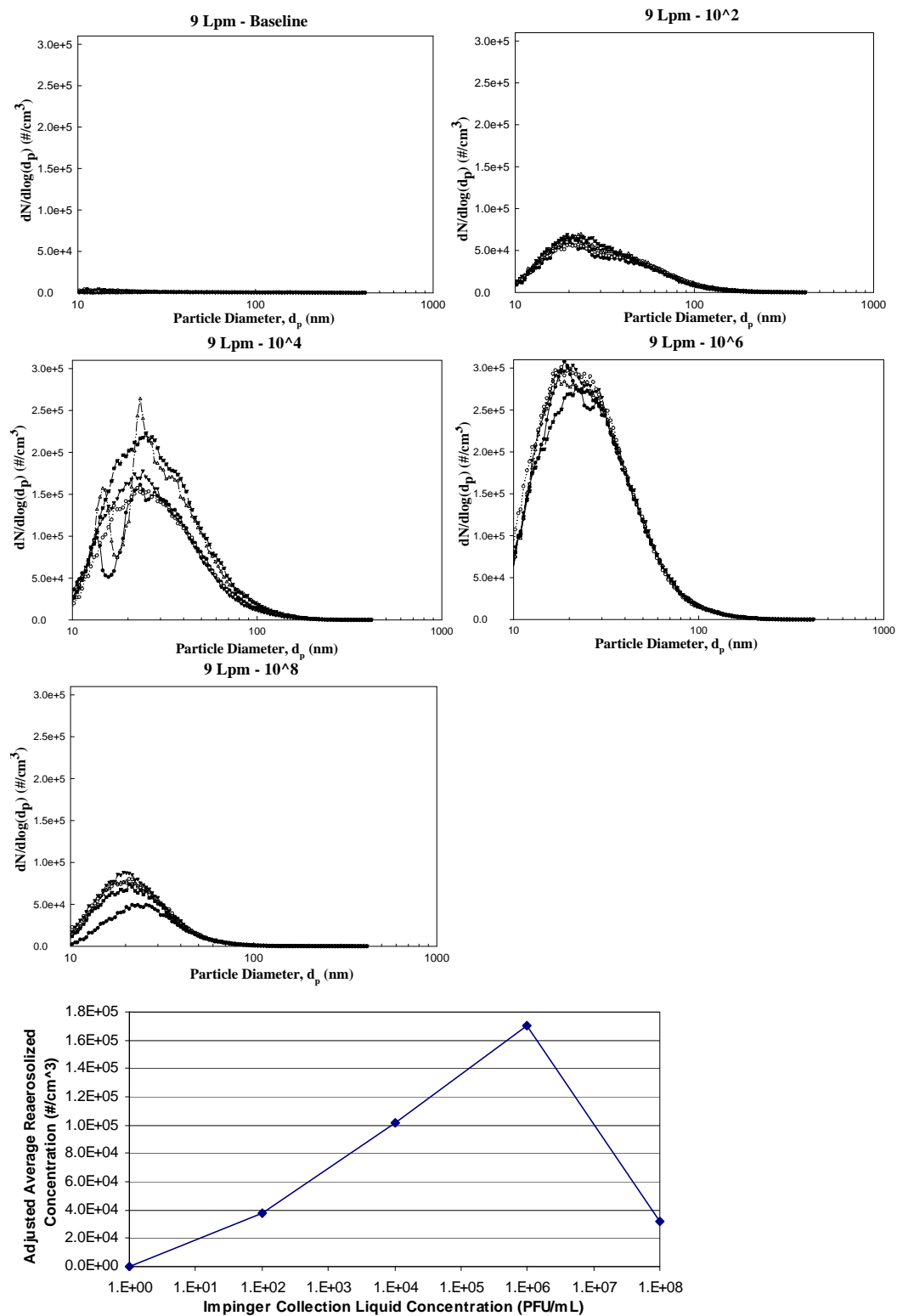


Figure C-8. Size distribution and adjusted avg concentration of MS2 at 9 Lpm (03/15/07).

Summary of 9 Lpm

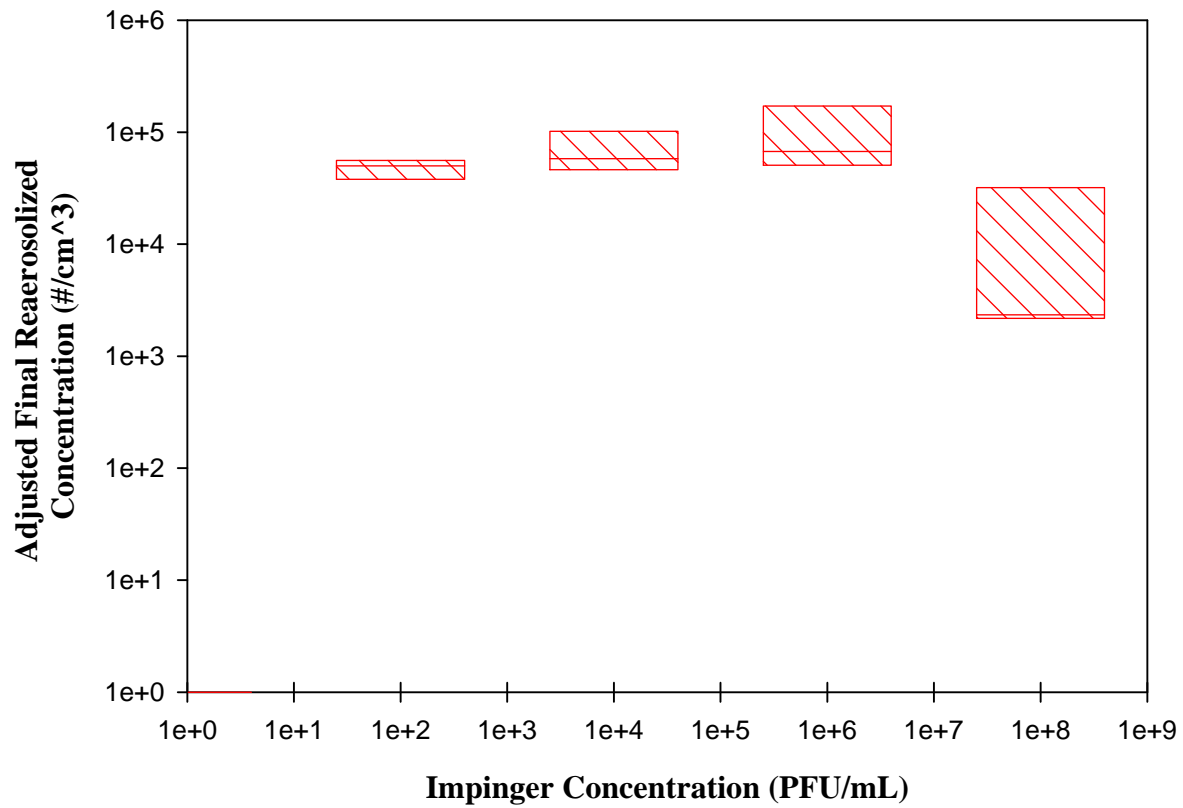


Figure C-9. Summary of adjusted average concentration of MS2 at 9 Lpm. The lower end of the box represents the 25th percentile, the middle line represents the median, and the upper end of the box represents the 75th percentile.

Flow Rate: 12.5 Lpm

Test 1: 01/24/2008

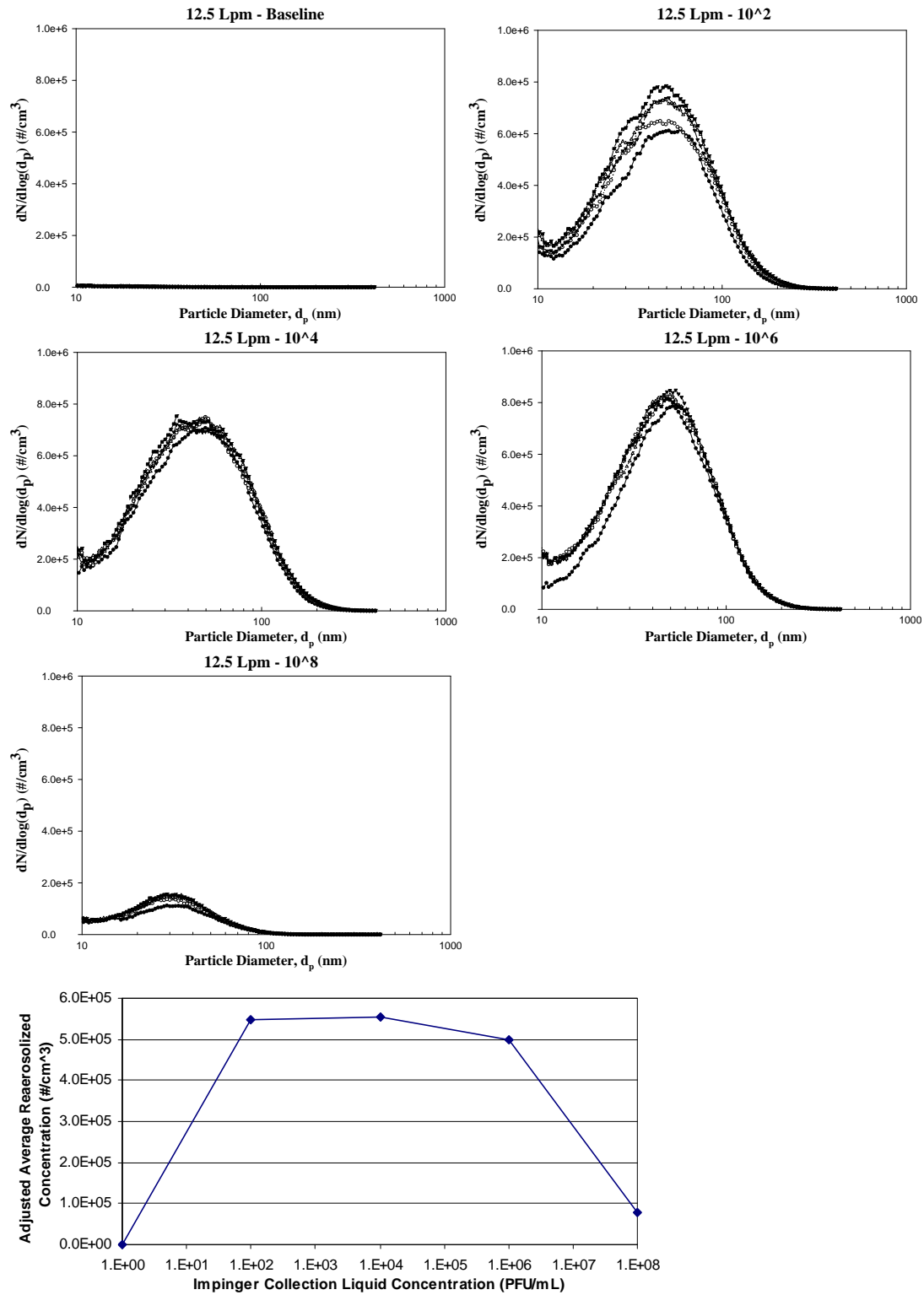


Figure C-10. Size distribution and adjusted avg concentration of MS2 at 12.5 Lpm (01/24/07).

Test 2: 01/28/2008

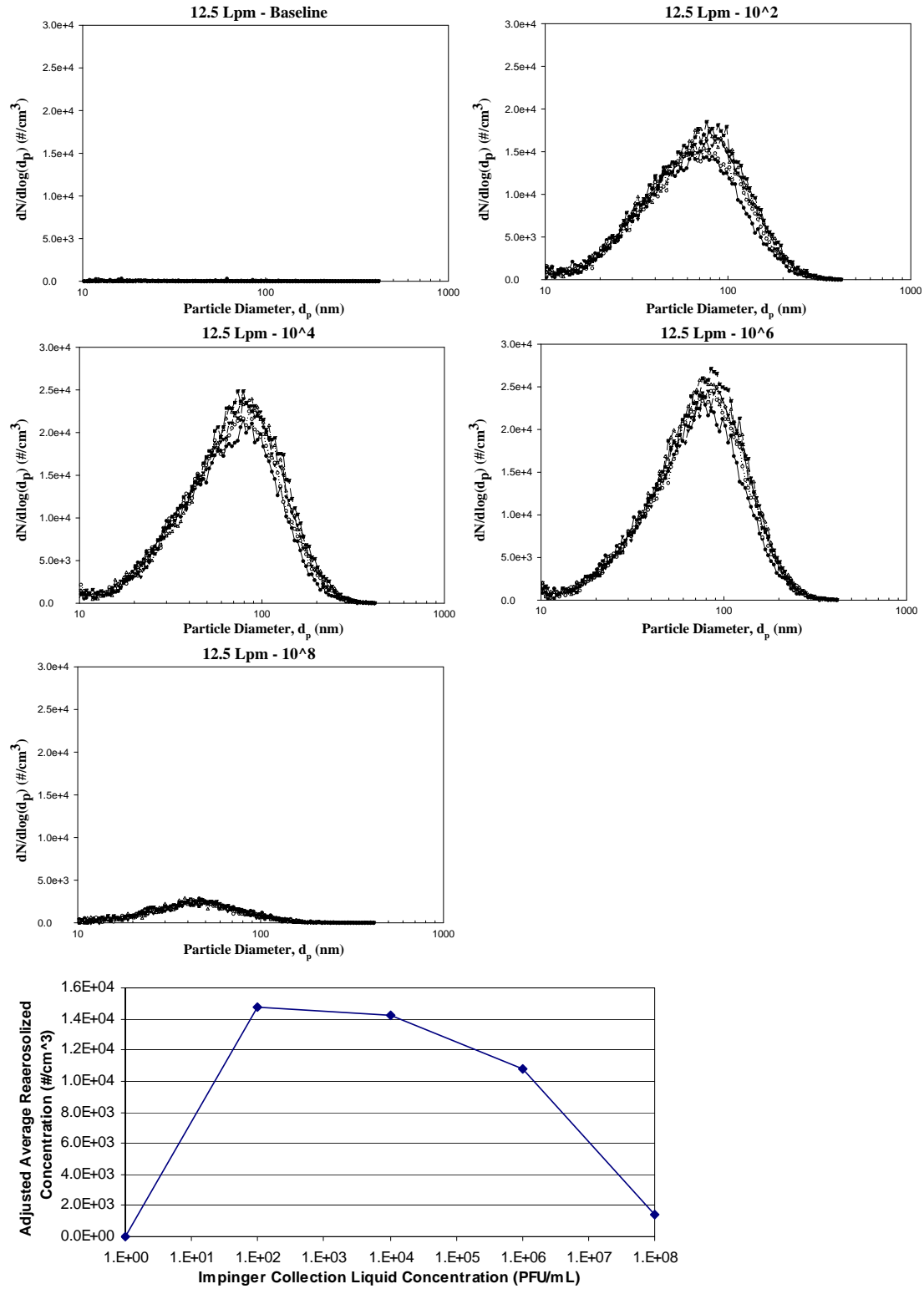


Figure C-11. Size distribution and adjusted avg concentration of MS2 at 12.5 Lpm (01/28/07).

Test 3: 02/09/2008

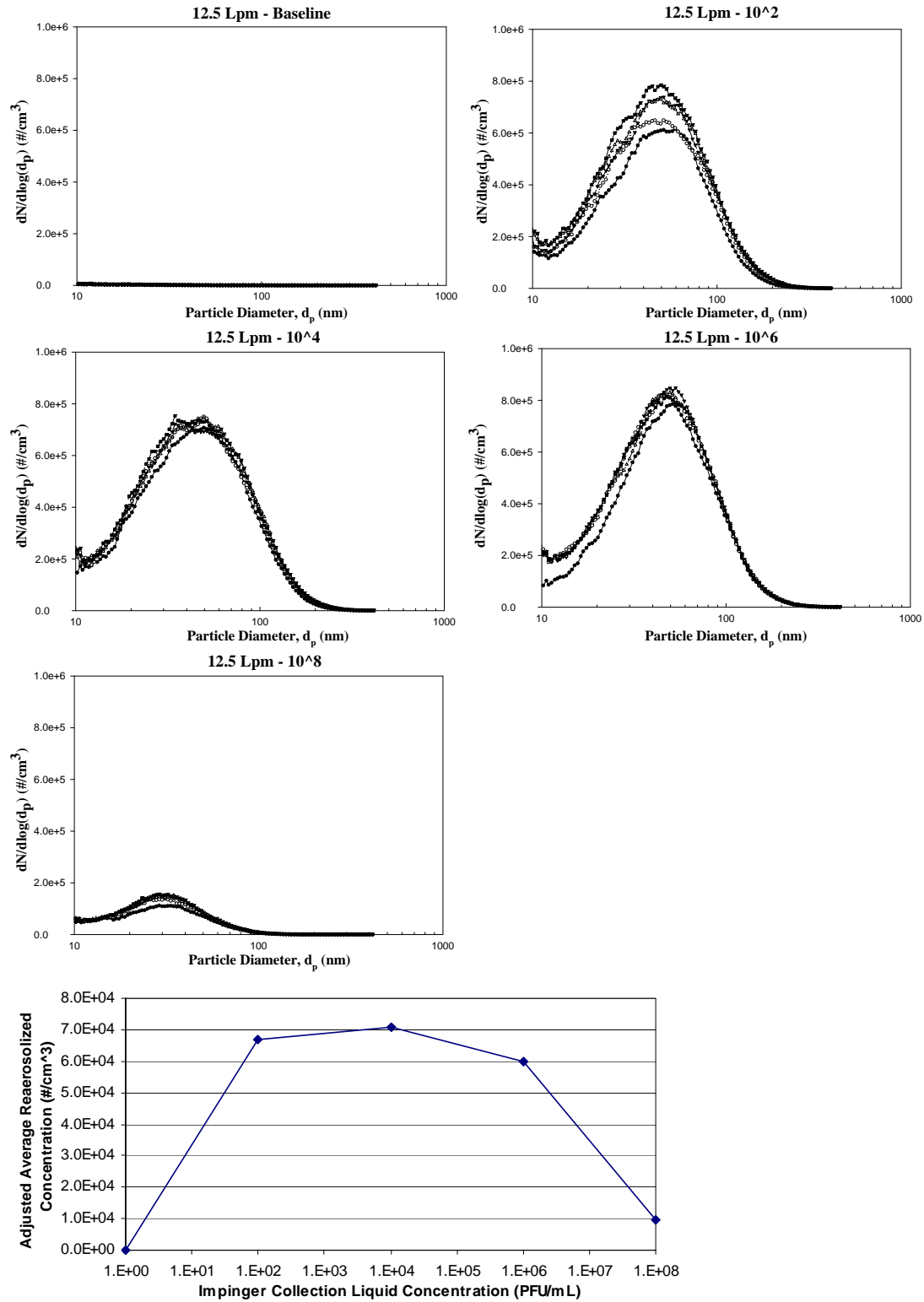


Figure C-12. Size distribution and adjusted avg concentration of MS2 at 12.5 Lpm (02/09/07).

Summary of 12.5 Lpm

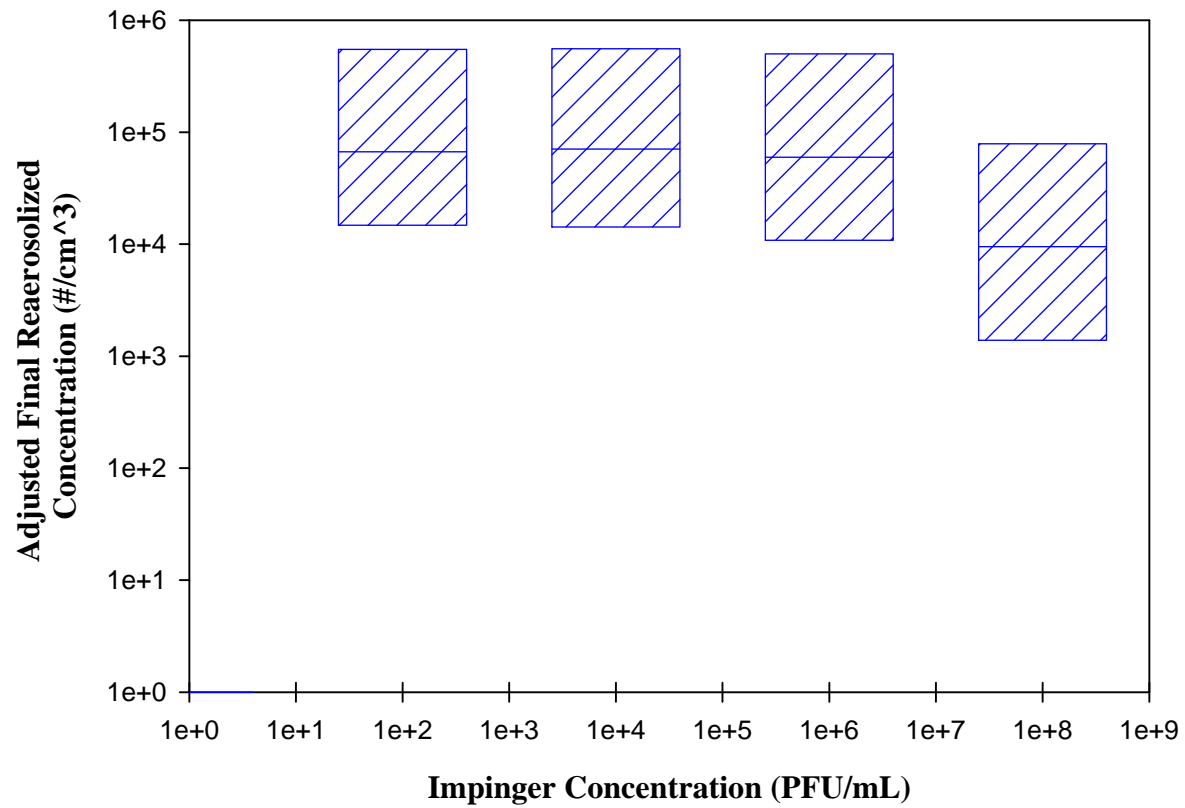


Figure C-13. Summary of adjusted average concentration of MS2 at 12.5 Lpm. The lower end of the box represents the 25th percentile, the middle line represents the median, and the upper end of the box represents the 75th percentile.

Flow Rate: 15 Lpm

Test 1: 02/17/2008a

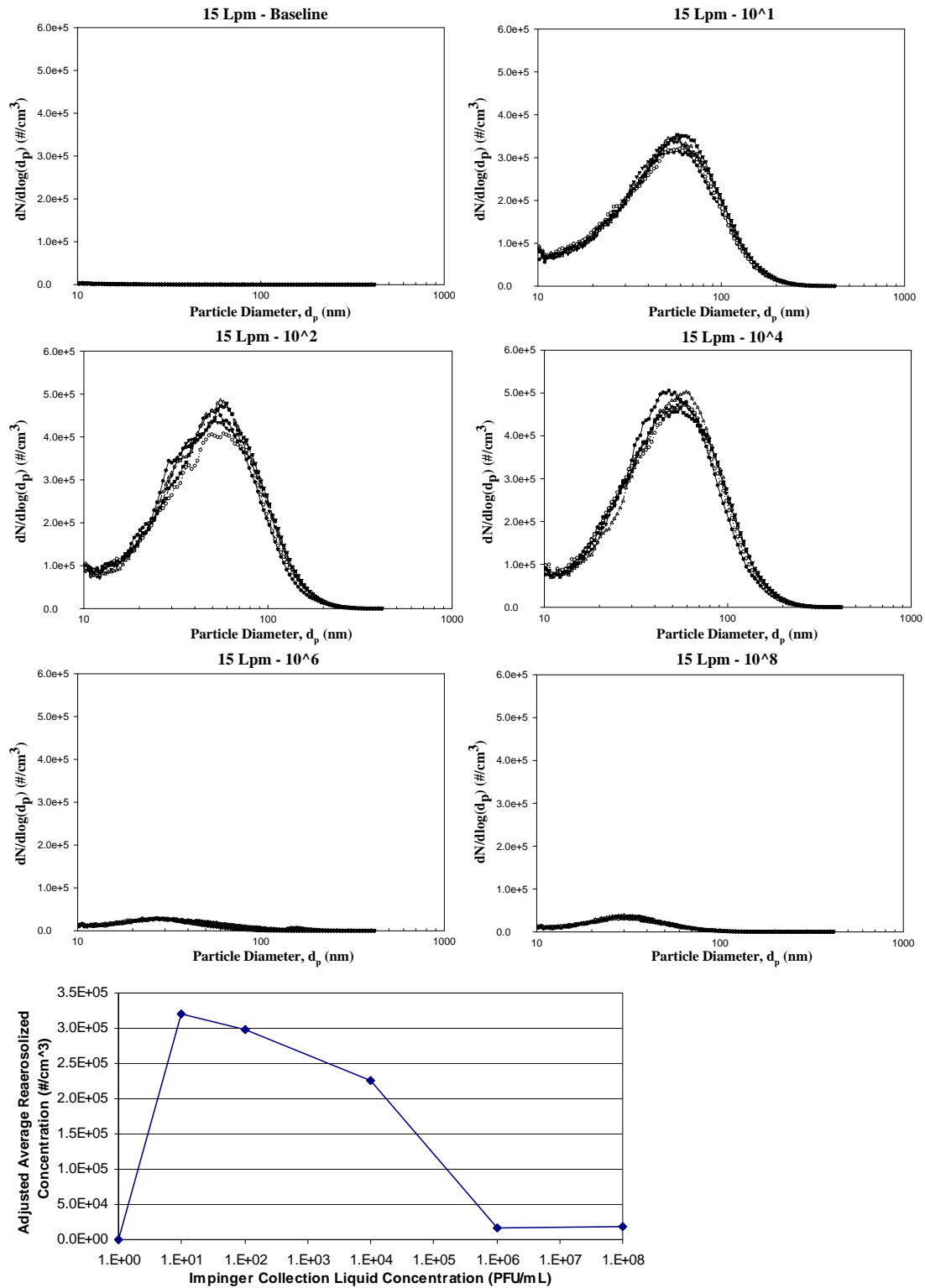


Figure C-14. Size distribution and adjusted avg concentration of MS2 at 15 Lpm (02/17/08a).

Test 2: 02/17/2008b

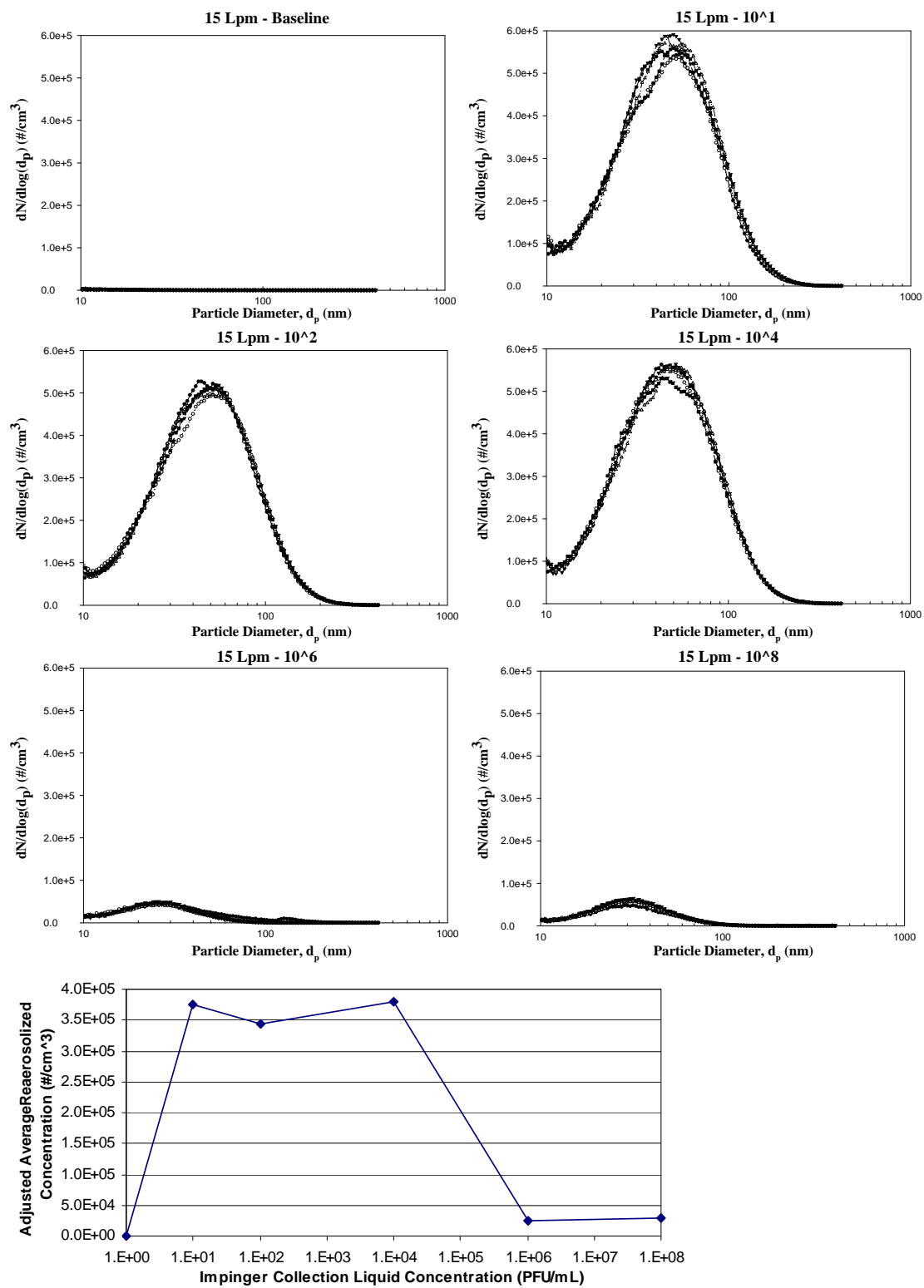


Figure C-15. Size distribution and adjusted avg concentration of MS2 at 15 Lpm (02/17/08b).

Summary of 15 Lpm

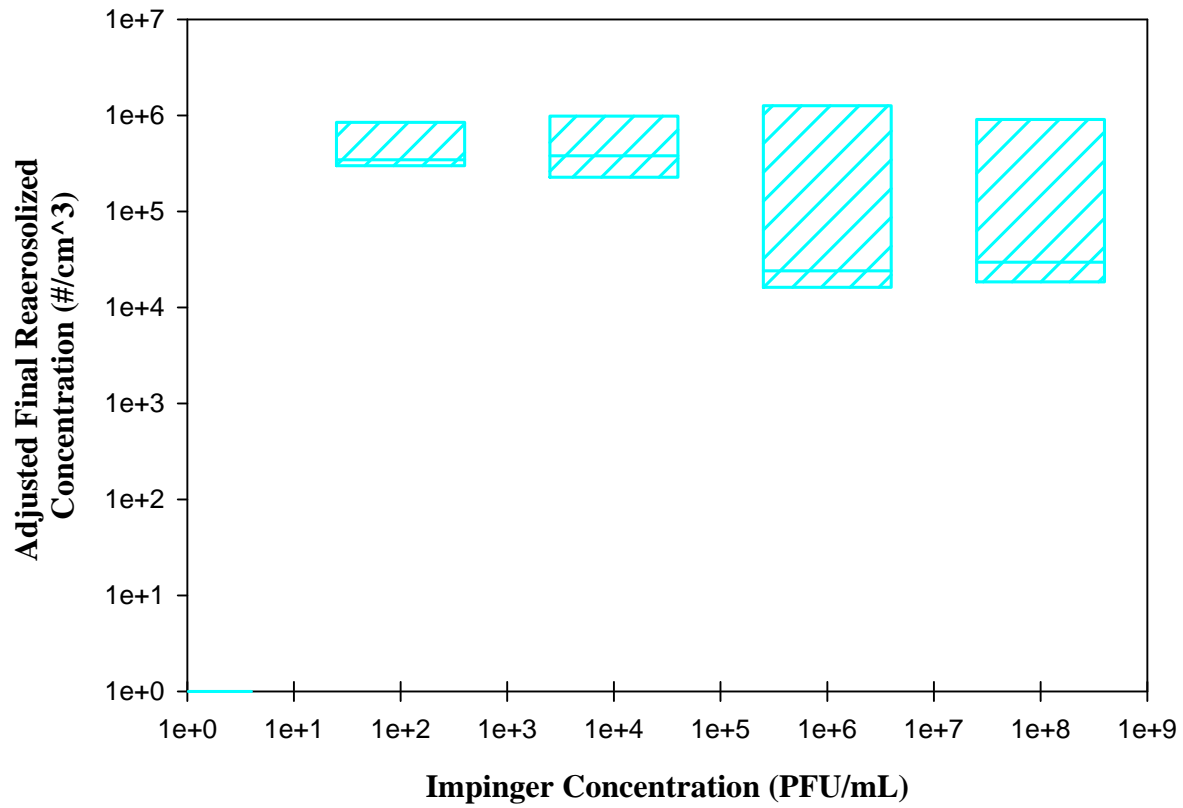


Figure C-16. Summary of adjusted average concentration of MS2 at 15 Lpm. The lower end of the box represents the 25th percentile, the middle line represents the median, and the upper end of the box represents the 75th percentile.

Mode Size of MS2 Experiments

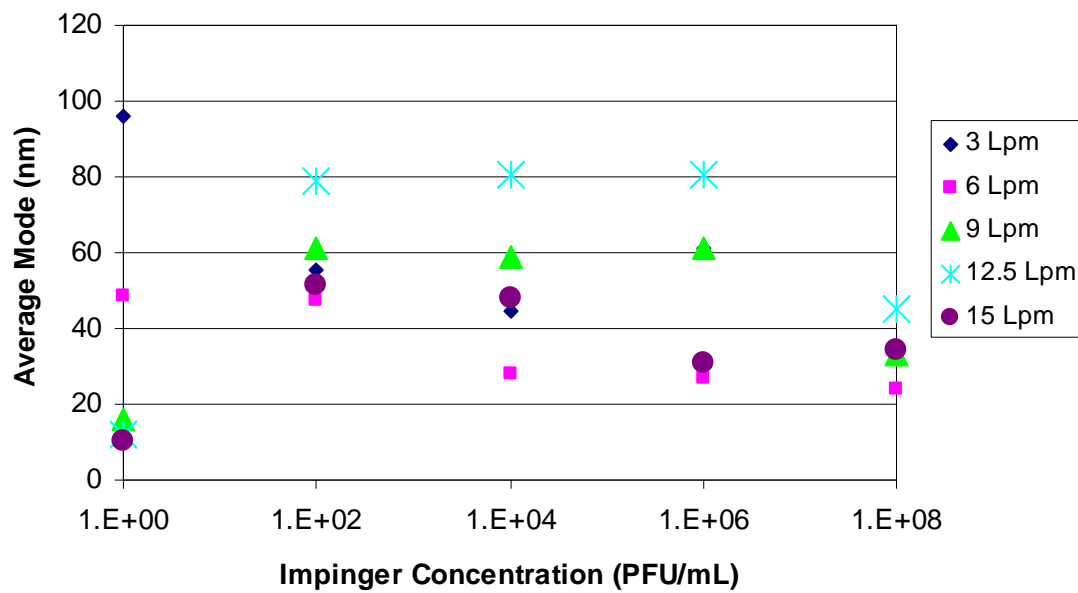


Figure C-17. Average mode size as a function of flow and impinger concentration for MS2 viral particles.

APPENDIX D
EFFECT OF SURFACE TENSION AND VISCOSITY DATA SETS

Effect of Surface Tension

Test 1: 03/21/2008a

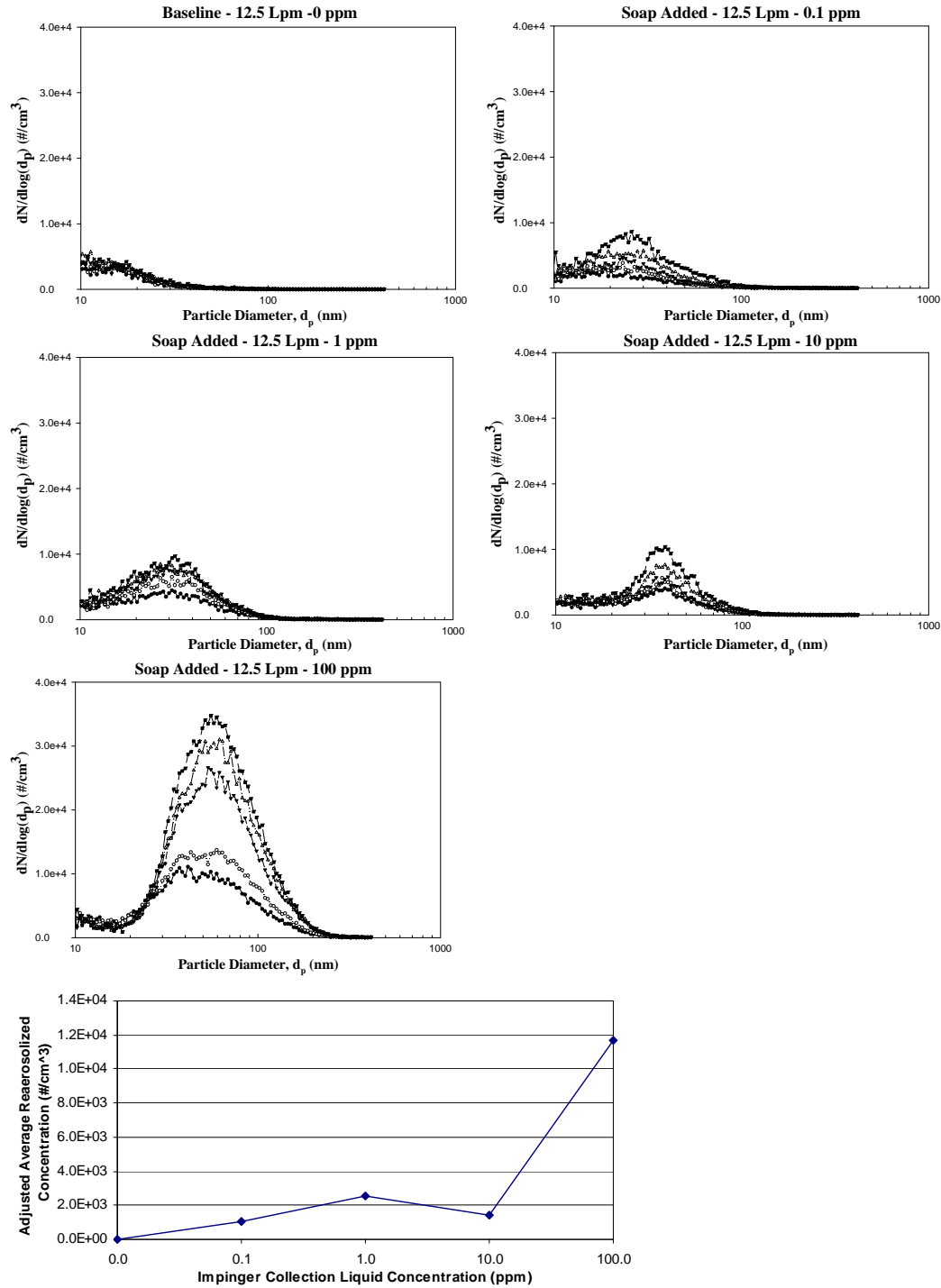


Figure D-1. Size distribution and adjusted avg concentration of PSL at 12.5 Lpm (03/21/08a).

Test 2: 03/21/2008b

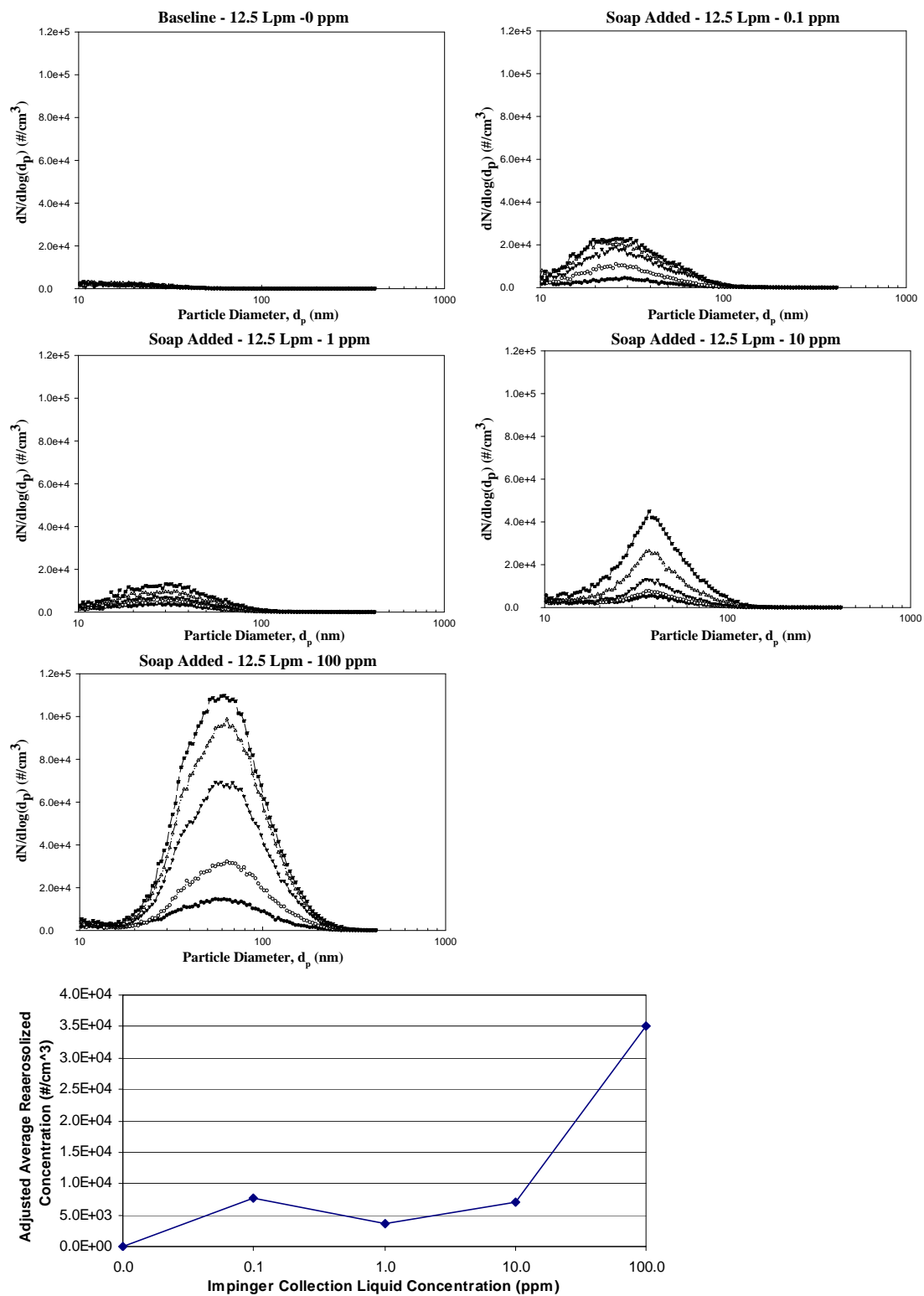


Figure D-2. Size distribution and adjusted avg concentration of PSL at 12.5 Lpm (03/21/08b).

Test 3: 03/24/2008

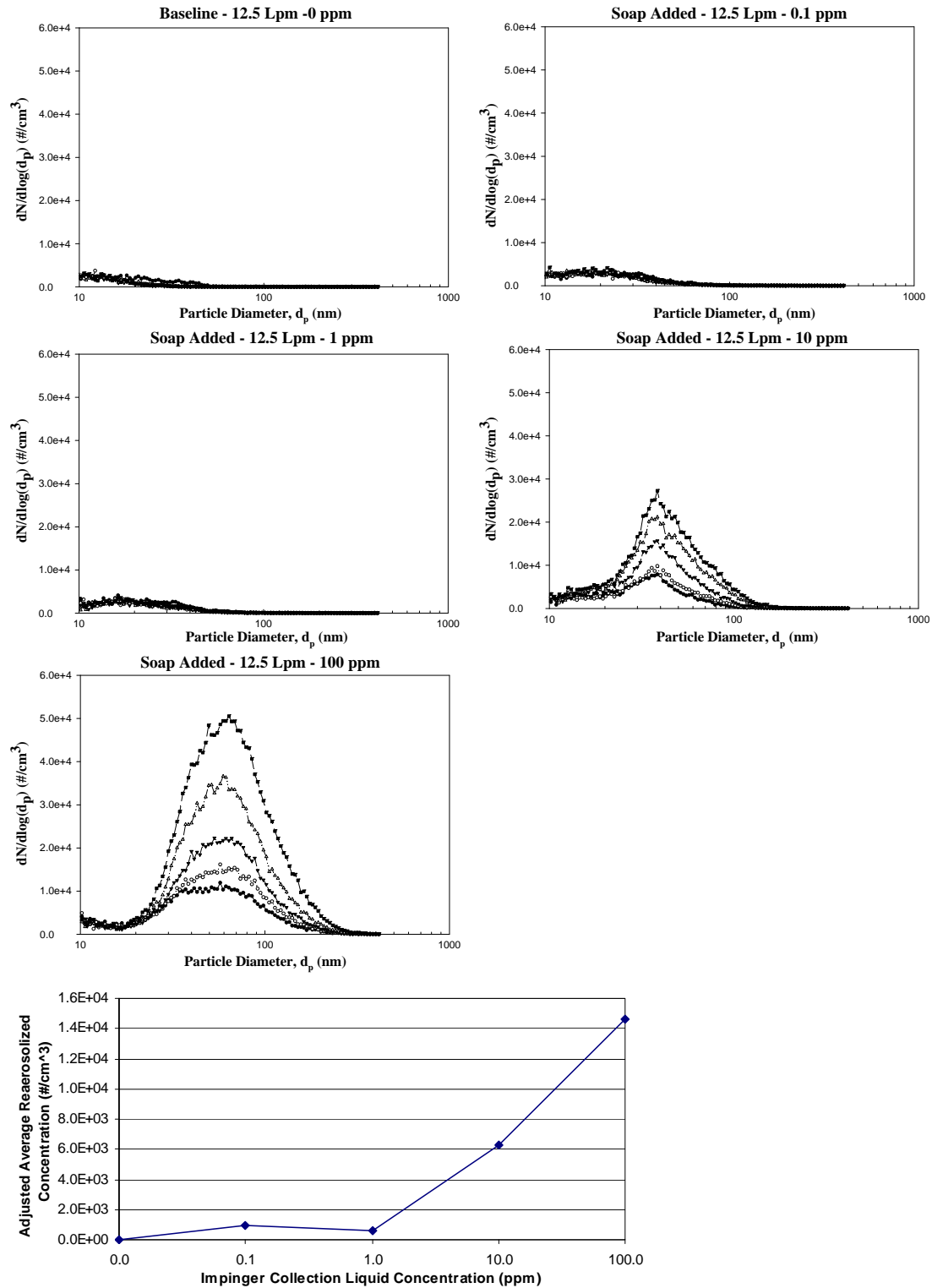


Figure D-3. Size distribution and adjusted avg concentration of PSL at 12.5 Lpm (03/21/08b).

Summary of Surface Tension

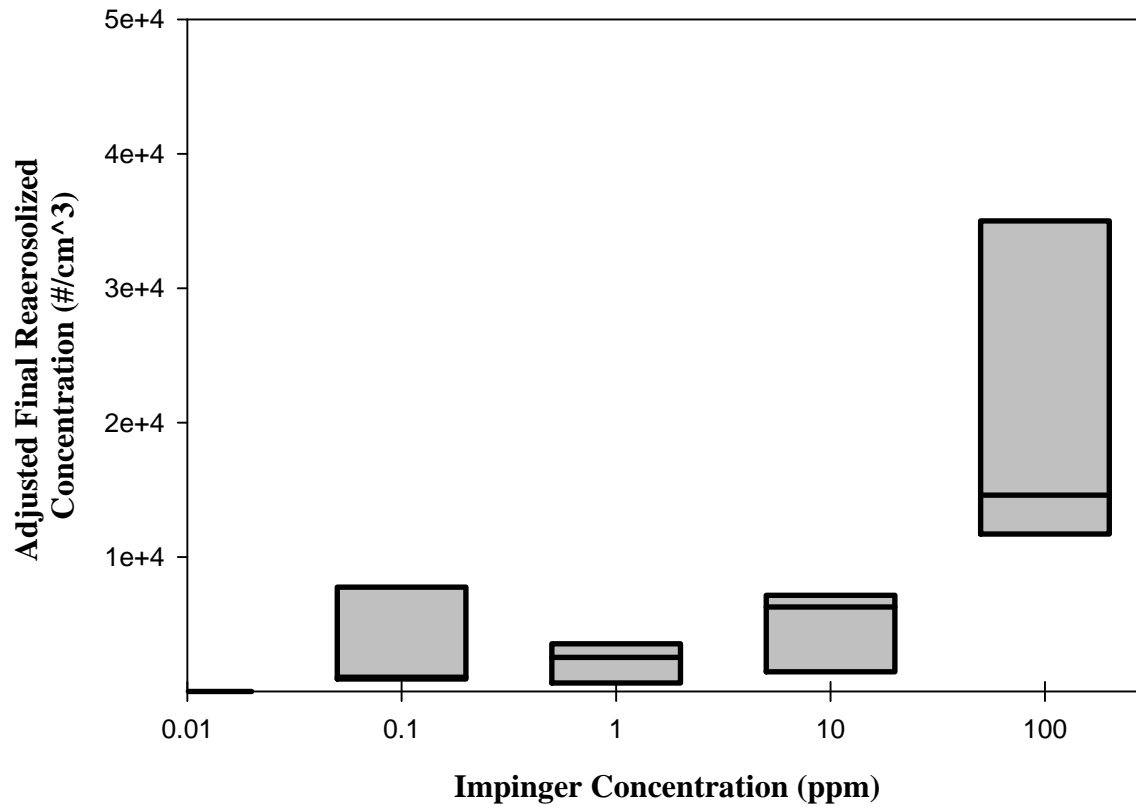


Figure D-4. Summary of adjusted average concentration of PSL at 12.5 Lpm. The lower end of the box represents the 25th percentile, the middle line represents the median, and the upper end of the box represents the 75th percentile.

Effect of Viscosity

Test 1: 03/31/2008

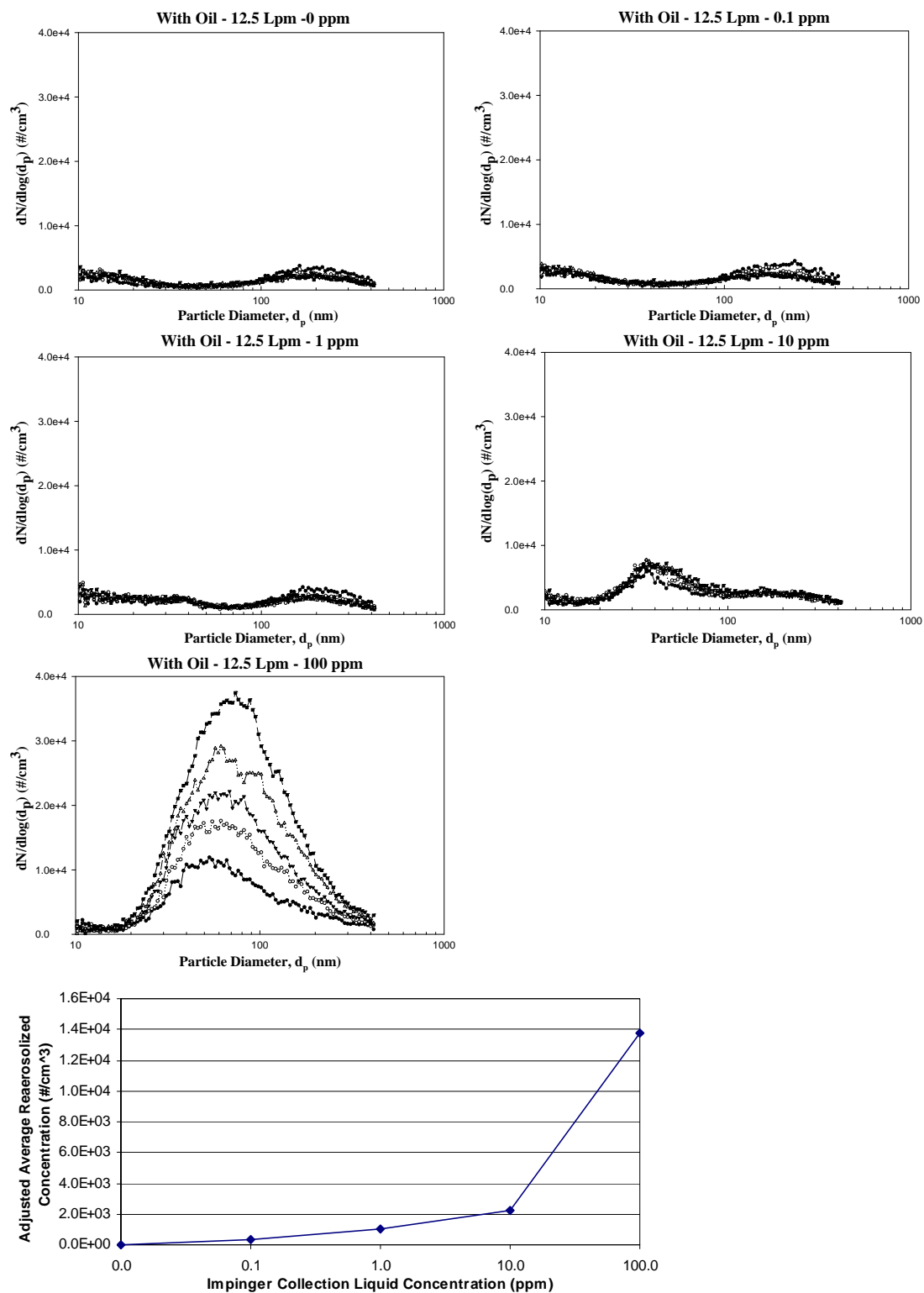


Figure D-5. Size distribution and adjusted avg concentration of PSL at 12.5 Lpm (03/31/08).

Test 2: 04/02/2008a

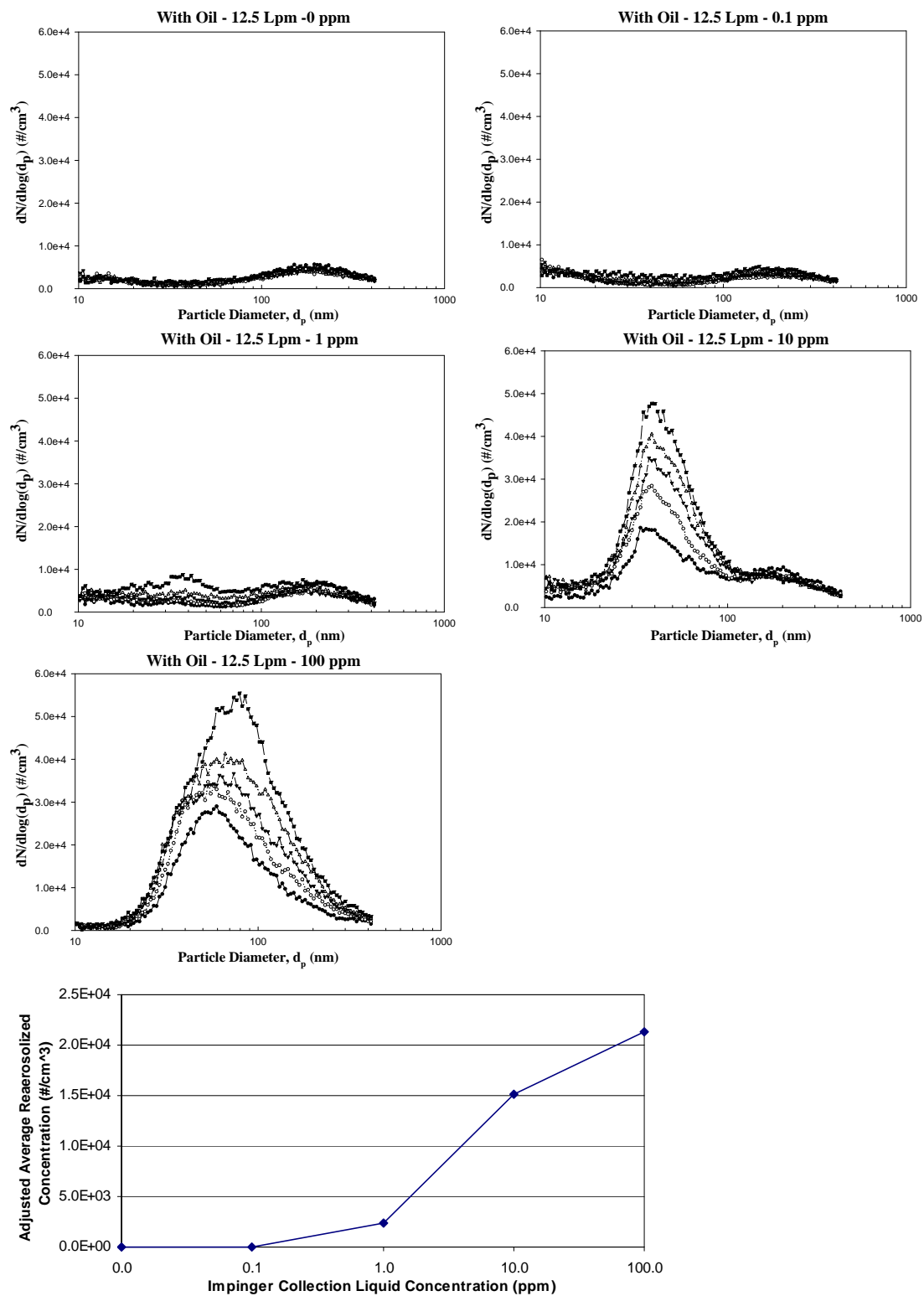


Figure D-6. Size distribution and adjusted avg concentration of PSL at 12.5 Lpm (04/02/08a).

Test 3: 04/02/2008b

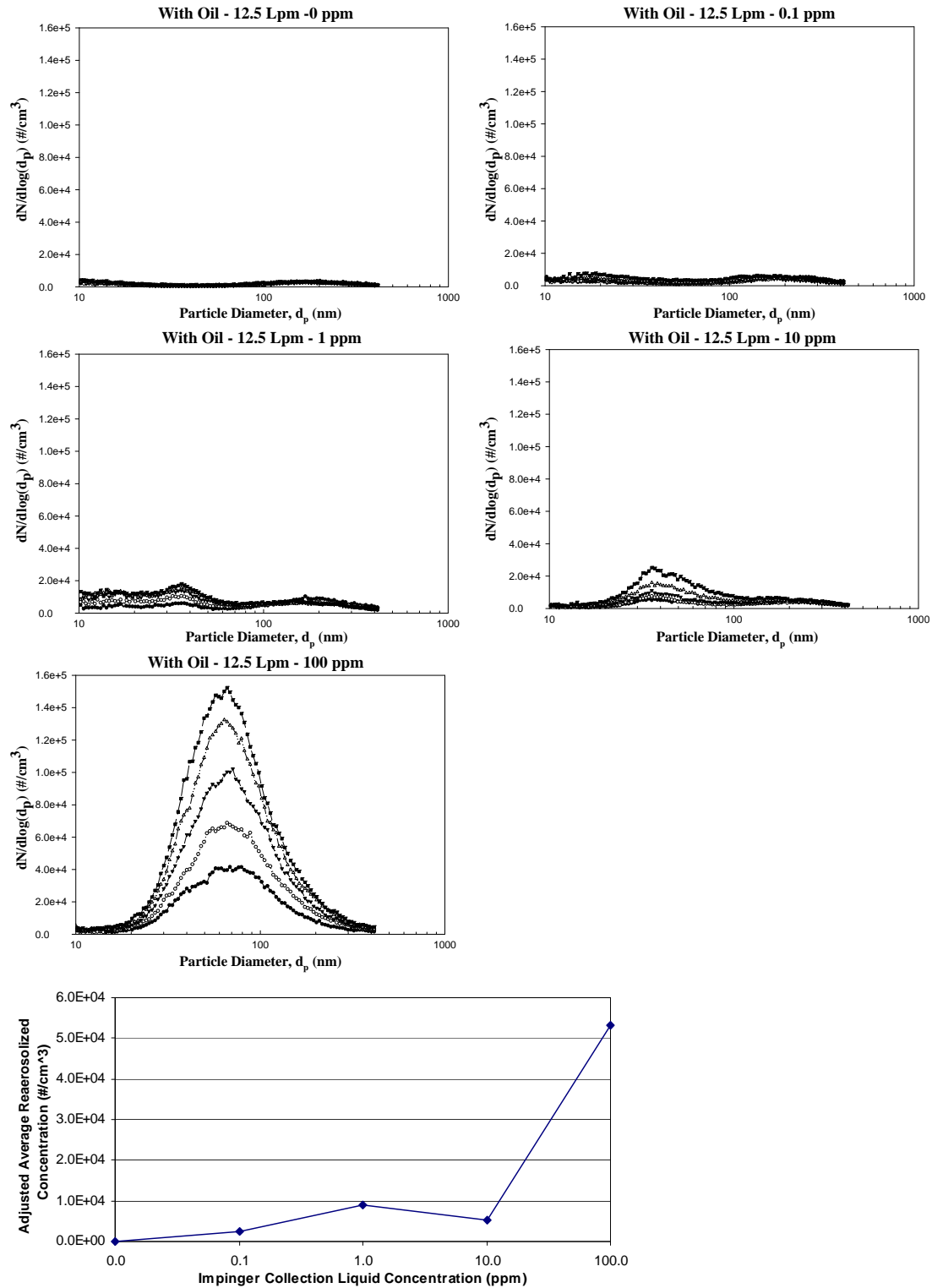


Figure D-7. Size distribution and adjusted avg concentration of PSL at 12.5 Lpm (04/02/08b).

Summary of Viscosity

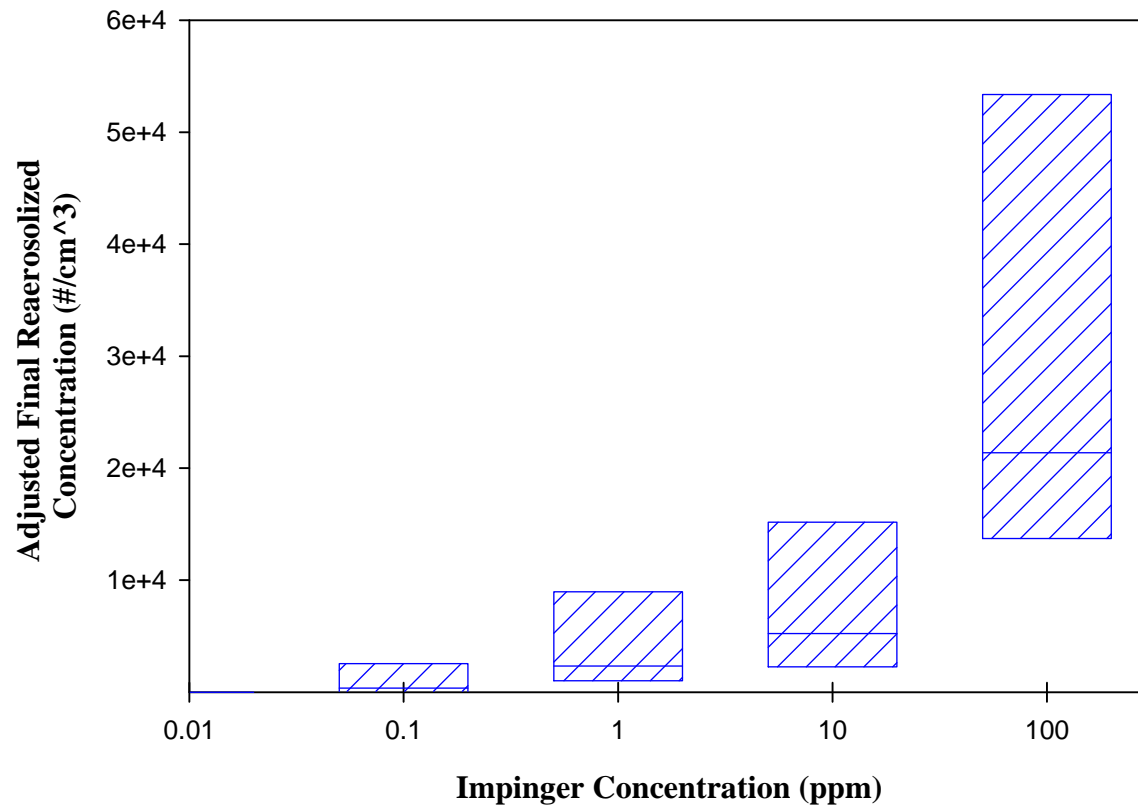


Figure D-8. Summary of adjusted average concentration of PSL at 12.5 Lpm. The lower end of the box represents the 25th percentile, the middle line represents the median, and the upper end of the box represents the 75th percentile.

APPENDIX E REAEROSOLIZATION WITH BIOSAMPLER DATA SETS

Test 1: 03/15/2008

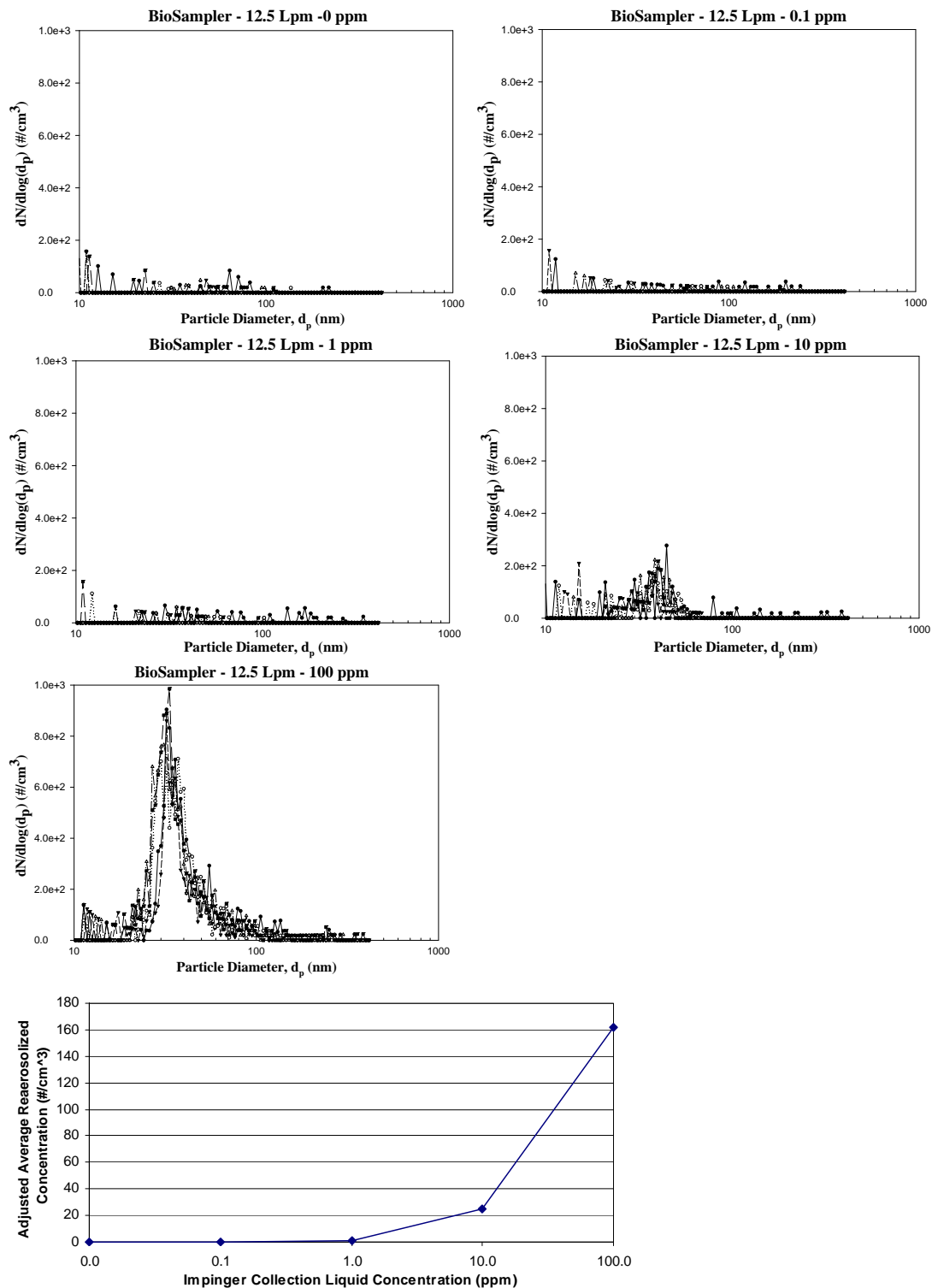


Figure E-1. Size distribution and adjusted avg concentration of PSL at 12.5 Lpm (03/15/08).

Test 2: 03/19/2008a

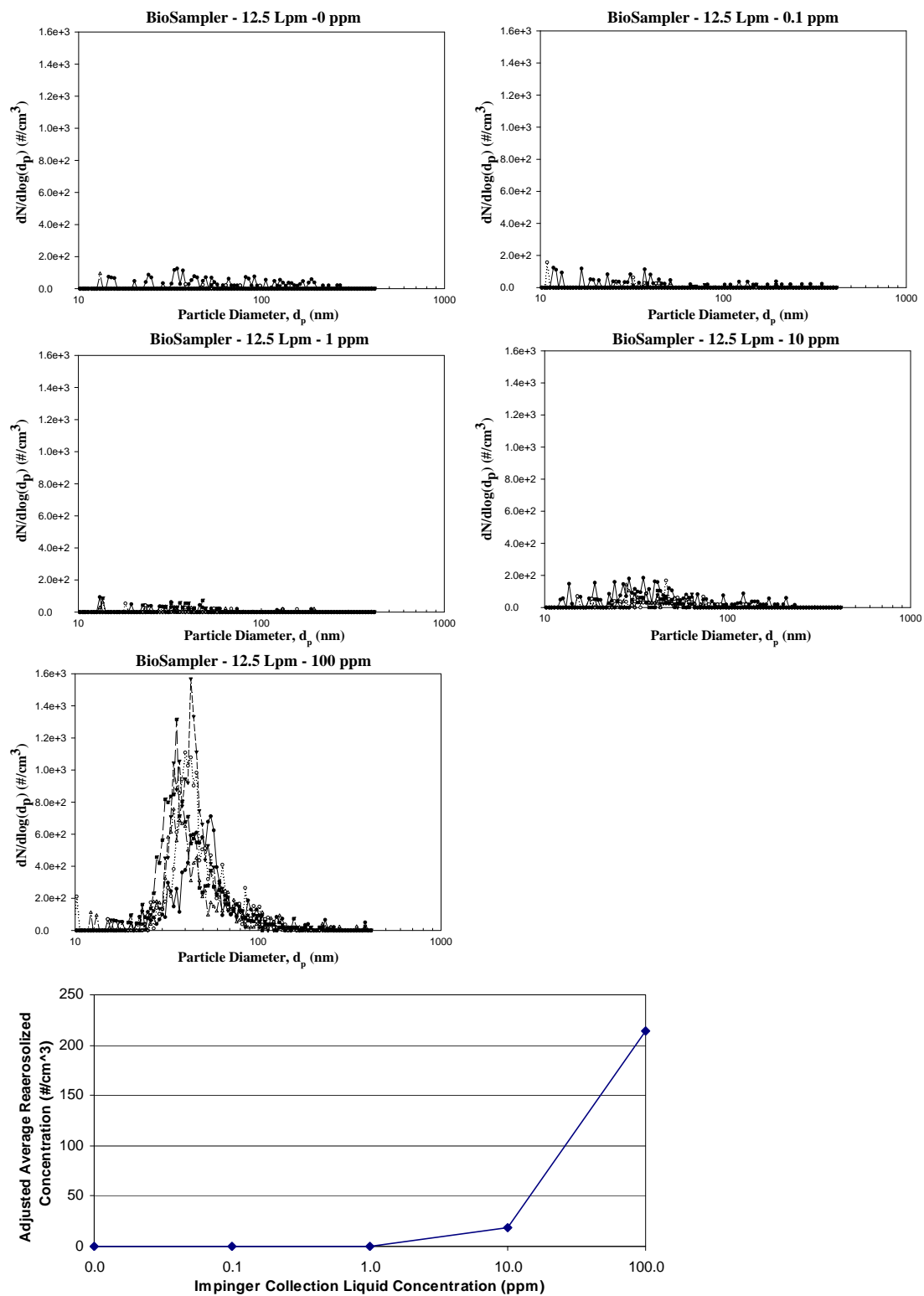


Figure E-2. Size distribution and adjusted avg concentration of PSL at 12.5 Lpm (03/19/08a).

Test 3: 03/19/2008b

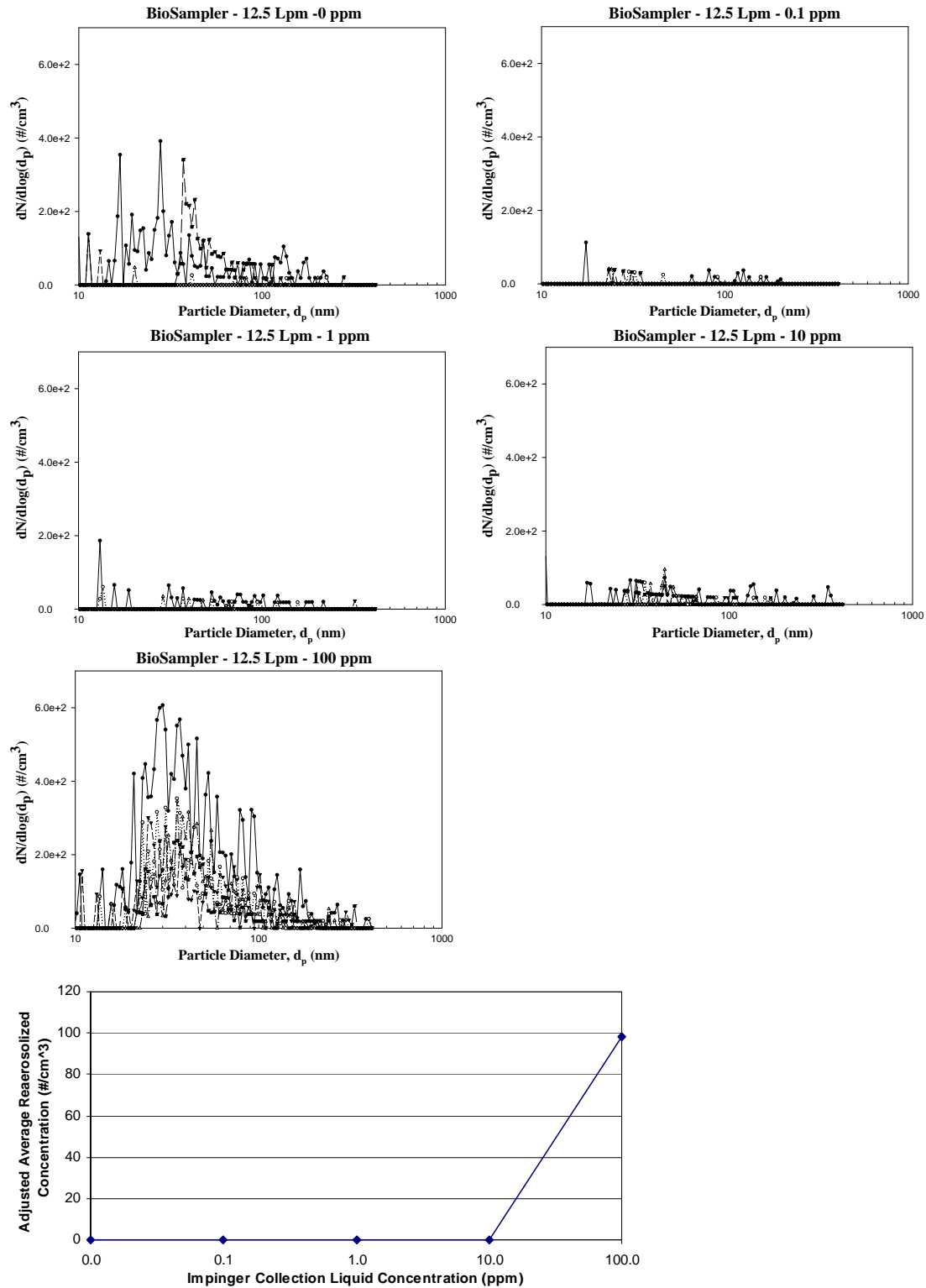


Figure E-3. Size distribution and adjusted avg concentration of PSL at 12.5 Lpm (03/19/08b).

Summary of BioSampler

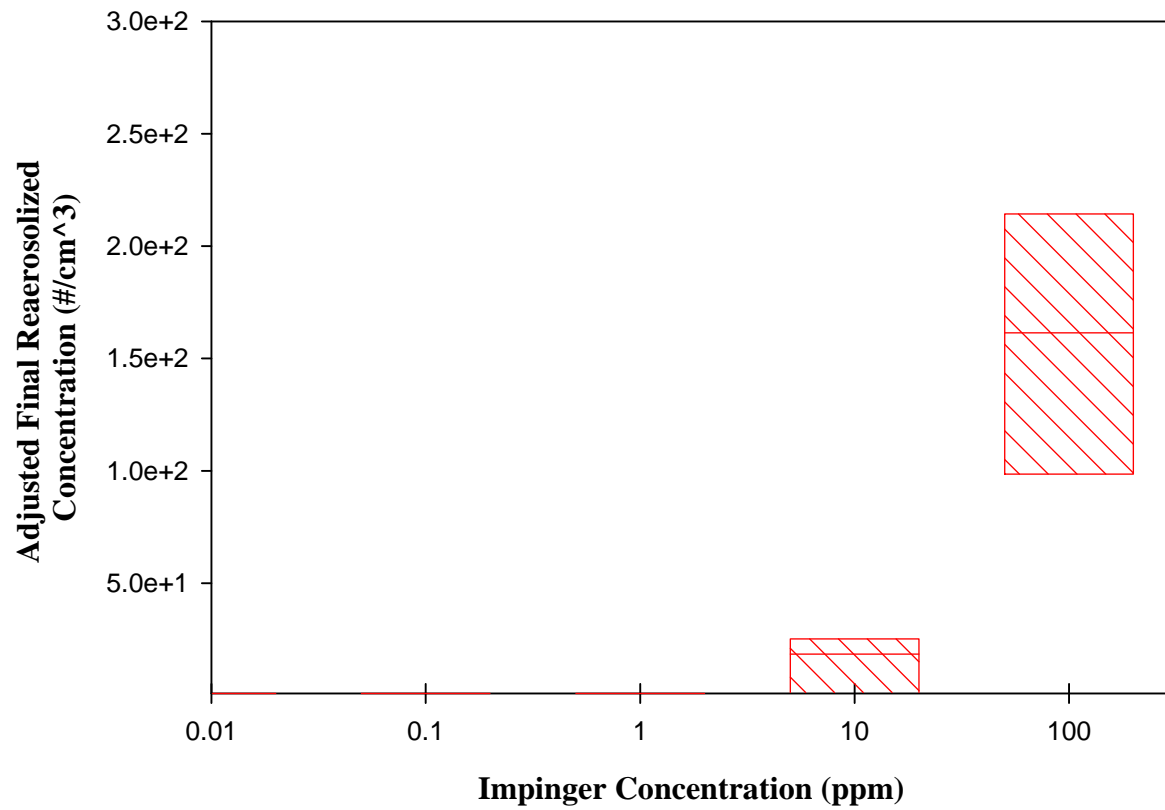


Figure E-4. Summary of adjusted average concentration of PSL at 12.5 Lpm. The lower end of the box represents the 25th percentile, the middle line represents the median, and the upper end of the box represents the 75th percentile.

LIST OF REFERENCES

- Ace Glass Inc. (2008). "7540 Impinger." *Ace Glass Catalog*, 212.
- Aranha-Creado, H., and Brandwein, H. (1999). "Application of Bacteriophages as Surrogates for Mammalian Viruses: A Case for Use in Filter Validation Based on Precedents and Current Practices in Medical and Environmental Virology." *PDA J. Pharm. Sci. Tech.*, 53(2), 75-82.
- Demokritou, P., Gupta, T., and Koutrakis, P. (2002). "A High Volume Apparatus for the Condensational Growth of Ultrafine Particles for Inhalation Toxicological Studies." *Aerosol Sci. Tech.*, 36(11), 1061-1072.
- Floyd, R., and Sharp, D. G. (1978). "Viral Aggregation: Effects of Salts on the Aggregation of Poliovirus and Reovirus at Low pH." *Appl. Environ. Microb.*, 35(6), 1084-1094.
- Floyd, R., and Sharp, D. G. (1977). "Aggregation of Poliovirus and Reovirus by Dilution in Water." *Appl. Environ. Microb.*, 33(1), 159-167.
- Friedlander, S. K. (2003). "Gas-to-Particle Conversion." *Smoke Dust and Haze*, Oxford University, 275-305.
- Fuchs, N. A. (1964). "Absorption of Aerosols by Bubbling." *The Mechanics of Aerosols*, Pergamon, New York, 240-245.
- Ghiaasiaan, S. M., and Yao, G. F. (1997). "A Theoretical Model for Deposition of Aerosols in Rising Spherical Bubbles due to Diffusion, Convection, and Inertia." *Aerosol Sci. Tech.*, 26(2), 141-153.
- Golmohammadi, R., Valegard, K., Fridborg, K., and Liljas, L. (1993). "The Refined Structure of Bacteriophage-MS2 at 2.8 Angstrom Resolution." *J. Mol. Biol.*, 234(3), 620-639.
- Grant, S. (1994). "Virus Coagulation in Aqueous Environments." *Environ. Sci. Technol.*, 28(5), 928-933.
- Grinshpun, S. A., Willeke, K., Ulevicius, V., Juozaitis, A., Terzieva, S., Donnelly, J., Stelma, G. N., and Brenner, K. P. (1997). "Effect of Impaction, Bounce and Reaerosolization on the Collection Efficiency of Impingers." *Aerosol Sci. Tech.*, 26(4), 326-342.
- Hering, S., and Stolzenburg, M. (2005). "A Method for Particle Size Amplification by Water Condensation in a Laminar, Thermally Diffusive Flow." *Aerosol Sci. Tech.*, 39(5), 428-436.
- Hinds, W. C. (1999). "Condensation and Evaporation." *Aerosol Technology*, John Wiley and Sons, Inc., New York, 278-303.
- Hinds, W. C. (1999). "Production of Test Aerosols." *Aerosol Technology*, John Wiley and Sons, Inc., New York, 428-432.

- Hogan, C. J., Kettleson, E. M., Lee, M. H., Ramaswami, B., Angenent, L. T., and Biswas, P. (2005). "Sampling Methodologies and Dosage Assessment Techniques for Submicrometre and Ultrafine Virus Aerosol Particles." *J. Appl. Microbiol.*, 99(6), 1422-1434.
- Hogan, C. J., Lee, M. H., and Biswas, P. (2004). "Capture of Viral Particles in Soft X-Ray-Enhanced Corona Systems: Charge Distribution and Transport Characteristics." *Aerosol Sci. Tech.*, 38(5), 475-486.
- Lin, X., Reponen, T., Willeke, K., Grinshpun, S., Foarde, K. K., and Ensor, D. S. (1999). "Long-term Sampling of Airborne Bacteria and Fungi into a Non-evaporating Liquid." *Atmos. Environ.*, 33(26), 4291-4298.
- Lin, X., Reponen, T., Willeke, K., Wang, Z., Grinshpun, S., and Trunov, M. (2000). "Survival of Airborne Microorganisms During Swirling Aerosol Collection." *Aerosol Sci. Tech.*, 32(3), 184-196.
- Lin, X., Willeke, K., Ulevicius, V., and Grinshpun, S. (1997). "Effect of Sampling Time on the Collection Efficiency of All-Glass Impingers." *Am. Ind. Hyg. Assoc. J.*, 58(7), 480-488.
- Madigan, M. T., Martinko, J. M., and Parker, J. (2003). *Brock Biology of Microorganisms*, Prentice Hall, New Jersey, 231-260, 520-546.
- Okuyama, K., Kousaka, Y., and Motouchi, T. (1984). "Condensational Growth of Ultrafine Aerosol Particles in a New Particle Size Magnifier." *Aerosol Sci. Tech.*, 3(4), 353-366.
- Pich, J., and Schutz, W. (1991). "On the Theory of Particle Deposition in Rising Gas Bubbles: The Absorption Minimum." *J. Aerosol Sci.*, 22(3), 267-272.
- Reponen, T., Willeke, K., Grinshpun, S., and Nevalainen, A. (2001). "Biological Particle Sampling." *Aerosol Measurement: Principles, Techniques and Applications*, K. Willeke, and P. A. Baron, eds., John Wiley and Sons, Inc., New York, 471-492.
- Russell, L., and Singh, E. (2006). "Submicron Salt Production in Bubble Bursting." *Aerosol Sci. Tech.*, 40(9), 664-671.
- Shields, P. A., and Farrah, S. R. (2002). "Characterization of Virus Adsorption by Using DEAE-Sepharose and Octyl-Sepharose." *Appl. Environ. Microb.*, 68(8), 3965-3968.
- Sioutas, C., Kim, S., and Chang, M. (1999). "Development and Evaluation of a Prototype Ultrafine Particle Concentrator." *J. Aerosol Sci.*, 30(8), 1001-1017.
- Sioutas, C., and Koutrakis, P. (1996). "Inertial Separation of Ultrafine Particles Using a Condensational Growth/ Virtual Impaction System." *Aerosol Sci. Tech.*, 25(4), 424-436.
- SKC Inc. (2008). "BioSampler Operating Instructions." 1.

- Terzieva, S., Donnelly, J., Ulevicius, V., Grinshpun, S. A., Willeke, K., Stelma, G., and Brenner, K. P. (1996). "Comparison of Methods for Detection and Enumeration of Airborne Microorganisms Collected by Liquid Impingement." *Appl. Environ. Microb.*, 62(7), 2264-2272.
- Thomas, J. J., Falk, B., and Fenselau, C. (1998). "Viral Characterization by Direct Analysis of Capsid Proteins." *Anal. Chem.*, 70(18), 3863-3867.
- Tseng, C. C., and Li, C. S. (2005). "Collection Efficiencies of Aerosol Samplers for Virus-Containing Aerosols." *J. Aerosol Sci.*, 36(5-6), 593-607.
- van Voorthuizen, E. M., Ashbolt, N. J., and Schafer, A. I. (2001). "Role of Hydrophobic and Electrostatic Interactions for Initial Enteric Virus Retention by MF Membranes." *J. Membrane Sci.*, 194(1), 69-79.
- Vidaver, A. K., Koski, R. K., and Van Etten, J. L. (1973). "Bacteriophage f6: a Lipid-Containing Virus of *Pseudomonas phaseolicola*." *J. Virol.*, 11(5), 799-805.
- Vonnegut, B. (1954). "Method and Apparatus for Measuring the Concentration of Condensation Nuclei." (2,684,008).
- Weissenborn, P. K. (2006). "Surface Tension of Aqueous Electrolytes." *Encyclopedia of Surface and Colloid Science*, P. Somasundaran, ed., CRC Press, Boca Raton, FL, 6029-6032.
- White, F. (2002). *Fluid Mechanics*. McGraw-Hill, New York, NY.
- Willeke, K., Grinshpun, S. A., Ulevicius, V., Terzieva, S., Donnelly, J., Steward, S., and Juozaitis, A. (1995). "Microbial Stress, Bounce and Re-aerosolization in Bioaerosol Samplers." *J. Aerosol Sci.*, 26(1), S883-S884.
- Willeke, K., Lin, X., and Grinshpun, S. (1998). "Improved Aerosol Collection by Combined Impaction and Centrifugal Motion." *Aerosol Sci. Tech.*, 28(5), 439-456.
- Wu, C. Y., and Biswas, P. (1998). "Particle Growth by Condensation in a System with Limited Vapor." *Aerosol Sci. Tech.*, 28(1), 1-20.

BIOGRAPHICAL SKETCH

Lindsey Ann Riemenschneider was born in Augusta, GA, to David Riemenschneider and Sandra Applegate on June 30, 1983. She moved to Ukiah, CA, shortly thereafter, where she lived with her parents and two brothers, Michael and Paul, until she graduated from Ukiah High School in June 2001. She attended the University of California at Davis from 2001–2006, where she received a B.S. degree in Civil Engineering with an emphasis in environmental engineering and a minor in geology.

Following graduation from UC Davis, Lindsey enrolled in the master's degree program in the Environmental Engineering Sciences Department at the University of Florida, where she was a member of the Dr. C.Y. Wu Air Resources Research Group. There, she served as a Research Assistant and a Teaching Assistant, as well as Treasurer and President of the UF Student Chapter of the Air and Waste Management Association during the 2006–2007 and 2007–2008 academic years, respectively. She received her Master of Engineering degree in environmental engineering in August 2008 and entered the environmental engineering consulting industry with Camp Dresser McKee as an Engineer II in the Water/Wastewater Services Group.